Universitätsklinikum Hamburg-Eppendorf

Institut für Experimentelle Pharmakologie und Toxikologie
(Direktor: Prof. Dr. med. Thomas Eschenhagen)

Role of HNO-dependent oxidation of cGMP-dependent protein kinase I alpha (PKGIα) for vasorelaxation

Dissertation

zur Erlangung des Grades eines Doktors der Medizin
an der Medizinischen Fakultät der Universität Hamburg

vorgelegt von:
Mara Rebecca Götz
aus München

Hamburg, 2020

Angenommen von der
Medizinischen Fakultät der Universität Hamburg am: 02.11.2021

Veröffentlicht mit Genehmigung der Medizinischen Fakultät der Universität Hamburg.

Prüfungsausschuss, der/die Vorsitzende:	**Prof. Dr. Heimo Ehmke**
Prüfungsausschuss, zweite/r Gutachter/in:	**Prof. Dr. Friederike Cuello**
3. Gutachter:	**Prof. Dr. Robert Lukowski**

Für meine Familie

Key findings and figures of this present work have been published recently:

Donzelli S*, Goetz M*, Schmidt K, Wolters M, Stathopoulou K, Diering S, Prysyazhna O, Polat V, Scotcher J, Dees C, Subramanian H, Butt E, Kamynina A, Schobesberger S, King S, Nikolaev V, de Wit C, Leichert L, Feil, R, Eaton P, Cuello F (2017). Oxidant sensor in the cGMP-binding pocket of PKGIα regulates nitroxyl-mediated kinase activity. Scientific Reports 7, 9938. [*contributed equally to this work]

Table of contents

1 List of publications

I. Donzelli S*, **Goetz M***, Schmidt K, Wolters M, Stathopoulou K, Diering S, Prysyazhna O, Polat V, Scotcher J, Dees C, Subramanian H, Butt E, Kamynina A, Schobesberger S, King S, Nikolaev V, de Wit C, Leichert L, Feil, R, Eaton P, Cuello F (2017). Oxidant sensor in the cGMP-binding pocket of PKGIα regulates nitroxyl-mediated kinase activity. Scientific Reports 7, 9938. [*contributed equally to this work]

II. Diering S*, Stathopoulou K*, **Goetz M,** Rathjens L, Harder S, Piasecki A, Raabe J, Schulz S, Brandt M, Pflaumenbaum J, Fuchs U, Donzelli S, Sadayappan S, Nikolaev V, Flenner F, Ehler E, Cuello F (2020). Receptor-independent modulation of cAMP-dependent protein kinase and protein phosphatase signaling in cardiac myocytes by oxidizing agents. Journal of Biological Chemistry 295(45):15342-15365. [*contributed equally to this work]

III. Abstract: **Goetz M**, Donzelli S, Cuello F (2015). Nitroxyl as a positive inotropic therapy in heart failure: cMyBP-C as a target? Free Radical Biology and Medicine 87, S51. Society For Free Radical Biology And Medicine (SFRBM) 22nd Annual Meeting

IV. Abstract: **Goetz M**, Donzelli S, Prysyazhna O, Polat V, Scotcher J, Stathopoulou K, Nikolaev V, Eaton P, Cuello F (2015). Role of HNO-dependent oxidation of PKGIα in the regulation of blood pressure. Young-DZHK-Retreat Potsdam 2015

V. Abstract: **Goetz M**, Schmidt K, Donzelli S, Wolters M, Stathopoulou K, Diering S, Prysyazhna O, Polat V, Scotcher J, Dees C, Subramanian H, Butt E, Kamynina A, Schobesberger S, King S, Nikolaev V, de Wit C, Leichert L, Feil R, Eaton P, Cuello F (2017). A molecular mechanism of oxidant-induced vasorelaxation in vivo. Annual Nordic Center for Cardiovascular Research (NCCR) Retreat

VI. Abstract: **Goetz M**, Donzelli S, Schmidt K, Wolters M, Stathopoulou K, Prysyazhna O, Scotcher J, Subramanian H, Butt E, Nikolaev V, de Wit C, Leichert L, Feil R, Eaton P, Cuello F (2017). A novel oxidant sensor in the cGMP-binding pocket of PKGIα regulates second messenger-mediated kinase activity. Clin Res Cardiol 106, Suppl 1 83. Jahrestagung der Deutschen Gesellschaft für Kardiologie (DKG)

VII. Abstract: **Goetz M**, Donzelli S, Schmidt K, Wolters M, Stathopoulou K, Prysyazhna O, Scotcher J, Subramanian H, Butt E, Nikolaev V, de Wit C, Leichert L, Feil R, Eaton P, Cuello F (2017). A novel oxidant sensor in the cGMP-binding pocket of PKGIα regulates second messenger-mediated kinase activity. 34th Annual Meeting of the International society for heart research (ISHR)

VIII. Abstract: **Goetz M**, Donzelli S, Schmidt K, Wolters M, Stathopoulou K, Prysyazhna O, Scotcher J., Subramanian H, Butt E, Nikolaev V, de Wit C, Leichert L, Feil R, Eaton P, Cuello F (2017). A novel oxidant sensor in the cGMP-binding pocket of PKGIα regulates second messenger-mediated kinase activity. 2nd Dutch-German Meeting of the German Society for Microcirculation, Dutch Endothelial Biology Society and Dutch Society for Microcirculation

IX. Abstract: **Goetz M**, Donzelli S, Prysyazhna S, Polat V, Scotcher J, Stathopoulou K, Leichert L, Eaton P, Cuello F (2015). HNO-mediated VASP phosphorylation through PKGIα activation. 13th Dutch-German Joint Meeting of the Molecular Cardiology Groups

X. Abstract: **Goetz M**, Diering S, Schobesberger S, Pasch S, Piasecki A, Donzelli S, Stathopoulou K, King S, Nikolaev V, Lutz S, Eaton P, Cuello F (2016). A potential molecular mechanism of Nitroxyl-mediated regulation of positive inotropy. DGK Herztage 2016

2 List of figures

3 List of tables

4 List of abbreviations

A	Ampere
ADHF	Acute decompensated heart failure
ADP	Adenosine diphosphate
AI	Autoinhibitory
AKARIII	A-kinase activity reporter III
ANP	Atrial natriuretic peptide
APS	Ammonium persulfate
AS	Angeli's Salt
ATP	Adenosine triphosphate
ARVM	Adult rat ventricular myocyte
BH_4	Tetrahydrobiopterin
BK_{Ca}	Large conductance Ca^{2+} activated K^+ channel
BNP	Brain natriuretic peptide
BSA	Bovine serum albumin
C	Cysteine
Ca^{2+}	Calcium
cAMP	Cyclic adenosine-3',5'-monophosphate
CBS	Cystathionine beta-lyase
CFP	Cyan fluorescent protein
cGMP	Cyclic guanosine-3',5'-monophosphate
CGRP	Calcitonin gene-related peptide
CI	Cardiac index
CNB	Cyclic nucleotide binding site
DAB	Denaturing alkylation buffer
ddH_2O	Distilled water
DMEM	Dulbecco's Modified Eagle's Medium
DMSO	Dimethyl sulfoxide
DTT	Dithiothreitol
EC_{50}	Half maximal effective concentration
ECL	Enhanced chemiluminescence

EDHF	Endothelium derived hyperpolarizing factor
EDTA	Dinatrium-ethylendiamin-tetraacetat
e.g.	Exempli gratia
EGTA	Ethylene glycol tetraacetic acid
ER	Endoplasmatic reticulum
FCS	Fetal calf serum
Fe^{2+}	Ferrous iron
Fe^{3+}	Ferric iron
FRET	Förster-resonance energy transfer
GPCR	G protein coupled receptor
GSH	Glutathione
GSNO	S-Nitrosoglutathione
GSSG	Glutathione disulfide
GTP	Guanosine-5'-triphosphate
h	Hour
HEK	Human embryonic kidney
HF	Heart failure
HR	Heart rate
HRP	Horseradish peroxidase
hrs	Hours
HSP20	Heat shock protein 20
$H_2N_2O_2$	Hyponitrous acid
H_2O_2	Hydrogen peroxide
H_2S	Hydrogen sulfide
ICM	Intracellular-like medium
iNOS	Inducible NOS
IP_3	D-myo-inositol-1,4,5-trisphosphate
IP_3R	IP_3-receptor
IRAG	Inositol 1,4,5-trisphophate receptor-associated cGMP kinase substrate
IUPAC	International Union of Pure and Applied Chemistry
KI	Knock-in

KO	Knock-out
LZ	Leucine zipper
MLC	Myosin light chain
MLCK	Myosin light chain kinase
MLCP	Myosin light chain phosphatase
msec	Millisecond(s)
MYPT1	Myosin phosphatase target subunit 1
NADPH	Nicotinamide adenine dinucleotide phosphate
NCA	1-Nitrosocyclohexyl acetate
NCFA	Nitrosocyclohexyl trifluoroacetate
NCP	Nitrosocyclohexyl pivalate
NO	Nitric oxide
NO_2	Nitrogen dioxide
NOS	Nitric oxide synthase
NR	Non-reducing
N_2O	Nitrous oxide
ODQ	1H-[1,2,4]-oxadiazolo-[4,3-a]-quinoxalin-1-one
$ONOO^-$	Peroxynitrite
O_2	Oxygen
O_2^-	Superoxide anion
PAGE	Polyacrylamide gel electrophoresis
PCWP	Pulmonary capillary wedge pressure
PDE	Phosphodiesterase
PGI_2	Prostacyclin
PIP_2	Phosphatidylinositol
PKA	cAMP-dependent protein kinase
pK_a	Acid dissociation constant
PKG	cGMP-dependent protein kinase
PLC	Phospholipase C
PLB	Phospholamban
pVASP	Phosphorylated VASP
PVDF	Polyvinylidene difluoride

R	Reducing
RFP	Red fluorescent protein
RGS	Regulator of G-protein signalling
ROCK	Rho kinase
ROS	Reactive oxygen species
rpm	Rounds per minute
RSH	Thiol
RSNO	Nitrosothiol
RT	Room temperature
RyR	Ryanodine receptor
S	Serine
SDS	Sodium dodecyl sulfate
SDS-PAGE	Sodium dodecyl sulfate polyacrylamide gel electrophoresis
sec	Second(s)
SERCA	Sarcoplasmic/ endoplasmic reticulum Ca^{2+} ATPase
sGC	Soluble guanylyl cyclase
SOD	Superoxide dismutase
SOH	Sulfenic acid
SO_2H	Sulfinic acid
SO_3H	Sulfonic acid
SR	Sarcoplasmic reticulum
SVI	Stroke volume index
TEMED	Tetramethylethylenediamine
Thr	Threonine
TRPA1	Transient receptor potential ankyrin 1
Trx	Thioredoxin
tVASP	Total VASP
UKE	University Medical Center Hamburg-Eppendorf
V	Volt
VASP	Vasodilator-stimulated phosphoprotein
VSMC	Vascular smooth muscle cell
v/v	Volume per volume

WT	Wildtype
w/v	Weight per volume
XO	Xanthine oxidase
3MNCA	3-methyl-1-nitrosocyclohexyl acetate
YFP	Yellow fluorescent protein
4-AP	4-aminopyridine

5 Introduction

5.1 Importance of blood pressure regulation

Dysregulated blood pressure control leading to hypertension or hypotension is prevalent in the modern western world and is a prominent risk factor for several cardiovascular disorders. In Germany, 32.8% of men and 30.9% of women are diagnosed with hypertension with a considerable high number of unreported cases (Neuhauser et al. 2017). Untreated constant high blood pressure is the most common and most important risk factor for cardiovascular diseases including the development of organ dysfunction and subsequent failure (Oparil et al. 2018; Williams et al. 2018). Stroke and myocardial infarction are known complications and are a direct consequence of persistent high blood pressure levels (Kaplan et al. 1999). Importantly, the reduction in cardiovascular induced morbidity and mortality is largely mediated by adequate treatment-induced blood pressure reduction, suggesting an urgent need for effective and specific antihypertensive drugs (Pucci et al. 2015).

High blood pressure induces micro- and macrovascular dysfunction and damage. At the microcirculatory level, endothelial dysfunction is followed by local inflammatory processes and subsequent microvascular damage (Dharmashankar and Widlansky 2010; Schulz et al. 2011). At the macrocirculatory level, atherosclerosis is amongst the final consequences (Hollander 1976). The vessel walls lose their ability to react to the blood flow demands of the organs and the body. Thus, high blood pressure levels are positively correlated with the onset of cardiac hypertrophy and left ventricular systolic dysfunction and other organ malfunctions such as impaired renal function and chronic kidney disease. In addition, hypertension is described as the most important risk factor for carotid atherosclerotic lesions, responsible for stroke and cognitive decline in elderly patients (Irigoyen et al. 2016).

Unfortunately, the symptoms and consequences of high blood pressure are generally not apparent early onwards during the process of organ damage development (Chobanian et al. 2003). Only with the manifestations of extended cardiovascular damage, patients are able to recognise organ dysfunction or

failure, e.g. coronary artery disease. Mostly, patients suffer primarily from a reduced response to metabolic stress or report symptoms of chest pain, the so-called angina pectoris syndrome (Conti 2007). The latter reflects the need for oxygen (O_2) due to insufficient supply, potentially followed by ischemia of the heart. To relieve patients from live-threatening symptoms and to reduce the risk of myocardial ischemia, patients are supported with a variety of medications. A milestone in the acute treatment is the induction of vasorelaxation (McGregor 1983).

During situations of an angina attack, the first drug to apply clinically is nitroglycerin by inhalation (Montalescot et al. 2013). In the body, nitroglycerin is metabolised to nitric oxide (NO), inducing the classical pathway of vasorelaxation via activation of the soluble guanylyl cyclase (sGC) (Agvald et al. 2002). Activation of sGC catalyses the formation of the important intracellular second messenger 3',5'-cyclic guanosine monophosphate (cGMP) from guanosine-5'-triphosphate (GTP). Binding of cGMP to protein kinase G isoforms (cGMP-dependent protein kinase; PKG) activates the kinase, leading via phosphorylation of various cellular substrate proteins to vasorelaxation, improved oxygen supply and finally to pain relief for the patient. Unfortunately, long-term therapy with nitroglycerin rapidly promotes nitrate tolerance, represented by a lack of vasorelaxation due to inactivation of NO (Münzel et al. 2005). Pharmacological strategies in order to generate compounds that do not induce this tolerance phenomenon could represent novel treatment options for this frequently occurring disease. Therefore, interest is dedicated to nitroxyl (HNO), the one-electron reduced and protonated sibling of NO. Interestingly, studies reported the endogenous generation of HNO by the reaction between hydrogen sulfide (H_2S) and NO (Eberhardt et al. 2014). Moreover, HNO has emerged as a novel regulator of cardiovascular function with cardio- and vasoprotective properties (Paolocci et al. 2001; Mondoro et al. 2001; Paolocci et al. 2003; Paolocci et al. 2007; Favaloro and Kempharper 2007; Switzer et al. 2009; Donzelli et al. 2012). However, how exactly HNO lowers blood pressure still remains elusive and under debate. A complete understanding of the molecular mechanisms that govern HNO-mediated changes in blood pressure offers the opportunity to develop a

new and rational therapy to alleviate associated disease risks.

5.1.1 Blood pressure regulation by NO

The physiological regulation of blood pressure is achieved by changes in smooth muscle tone as a consequence of a finely tuned balance between vasoconstrictive and vasorelaxing properties. Smooth muscle relaxation causes vessels to dilate with a resulting decrease in blood pressure and an adequate maintenance of oxygen supply (Klinke et al. 2009). Active vasodilators released by the endothelium include NO, prostacycline, and endothelium-derived hyperpolarizing factor (EDHF) and they regulate three principal vasorelaxation pathways (**Figure 1**) (Bevegård and Orö 1969; Ignarro et al. 1987; Palmer et al. 1987; Chen et al. 1988; Nagao and Vanhoutte 1992). These pathways converge in a reduction of intracellular calcium (Ca^{2+}) levels in smooth muscle cells, which activate myosin light chain phosphatase (MLCP) and inhibit myosin light chain kinase (MLCK). Vascular smooth muscle cell (VSMC) tone is dependent on the phosphorylation status of the myosin light chains (MLC) and thereby on the signalling events that control MLCK and MLCP activity. The overall result is a reduction in the phosphorylation status of MLC, thereby lowering their ATPase activity, resulting in diminished contraction of smooth muscle cells due to attenuated cross-bridge cycling (Somlyo and Somlyo 1994; Hirano 2007).

Vasorelaxation is mediated by shear stress and circulating factors such as bradykinin, acetylcholine, substance P, thrombin and adenosine, which bind to and activate G-protein coupled receptors (GPCR) on the surface of endothelial cells, which line the inner vessel walls (Dudzinski et al. 2006). Activation of specific GPCR mediates the activation of phospholipase C (PLC), which cleaves phosphatidylinositol (PIP_2) to generate D-myo-inositol-1,4,5-trisphosphate (IP_3) and diacylglycerol (DAG). Binding of IP_3 to IP_3-receptors (IP3R) at the endoplasmatic reticulum (ER) induces Ca^{2+} mobilisation from inner stores and leads to an increased intracellular Ca^{2+} concentration (Little et al. 1992; Kamato et al. 2015). Ca^{2+} and calmodulin form a complex, which in turn stimulates NO-synthase (NOS) activity (Dudzinski et al. 2006). NOS oxidises L-arginine via the intermediate N-hydroxy-L-arginine to NO and its by-product L-citrulline

(Förstermann and Sessa 2011). NO released by the endothelial cells freely diffuses into smooth muscle cells, where it can bind to the heme group of sGC, stimulating the catalytic ability of the enzyme to convert GTP to the second messenger cGMP. Formed cGMP relays many of the biological effects of NO by directly binding to and stimulating the activity of PKG (Hofmann et al. 2000). The critical role of this kinase in the regulation of vascular tone was demonstrated in PKG-deficient mice, which developed hypertension within 4-6 weeks (Pfeifer et al. 1999). Importantly, three major groups of proteins bind cGMP at defined sites: PKG belongs together with cAMP-dependent protein kinase (PKA) to the cyclic nucleotide-dependent protein kinases (Francis et al. 2005). Other binding partners of cGMP are cyclic nucleotide-dependent cation channels and cGMP-hydrolysing phosphodiesterases (PDEs). Interestingly, cGMP is able to potentially interact with all these proteins in one cell. However, due to the unique properties of each binding site that interacts with cGMP and the cellular compartmentalisation of the cGMP-binding proteins, the impact of these proteins on cGMP signalling within one cell varies substantially. It depends amongst others on the relative abundance and cGMP affinity of the cGMP-binding site as well as on subcellular compartmentalisation, proximity to cyclases, PDEs and not to forget, post-translational modifications as well (Francis et al. 2005).

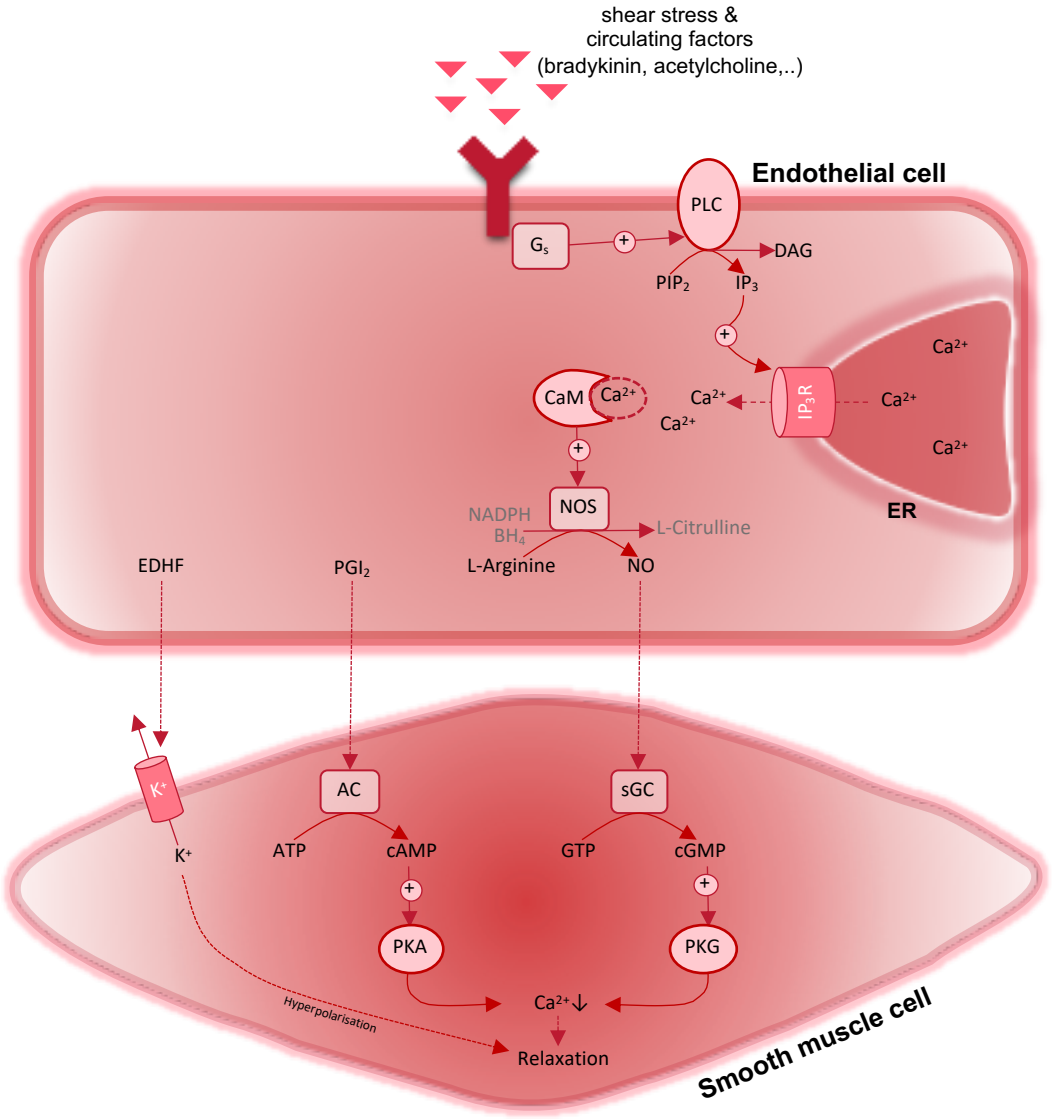

Figure 1: Vasorelaxation induced by distinct signalling pathways (adapted from Burgoyne and Eaton 2010).

5.2 Nitroxyl (HNO)

5.2.1 Chemistry of HNO

The surprising discovery of endogenous NO production in the 1980s and its involvement in many physiological signalling pathways in the cardiovascular, nervous and immune systems raised the interest in NO and its derivatives (Furchgott et al. 1984; Ignarro et al. 1987; Ignarro 1989). Primarily, oxidised NO species such as nitrogen dioxide (NO_2) and peroxynitrite ($ONOO^-$), which are reaction products of NO with molecular O_2 or superoxide anion (O_2^-), were investigated and their effects on the modification of macromolecules or immune

responses (e.g. macrophage burst) were described. However, researchers also gained interest in the reduced and protonated derivatives of NO. One-electron reduction of NO forms its anion, Nitrogen oxide or Nitroxyl (HNO, Nitrosyl hydride in IUPAC nomenclature) (Switzer et al. 2009). Although HNO is a redox derivative of NO, it possesses distinct chemical and biological properties. HNO is a weak acid with a pK_a = 11.5, leading to decomposition of HNO at a physiological pH in comparison to its corresponding base NO^- (Paolocci et al. 2007). Nevertheless, despite the high pK_a, there might be a substantial amount of NO^- released, which could contribute to the observed HNO effects and its exerted signalling properties. However, HNO and NO^- obtain different spin states, reducing the probability of proton transfer and thereby the formation of the corresponding base or acid. Furthermore, the molecules show an increased reactivity towards kinetically more convenient reactions than proton transfer and the observed effects can therefore mainly be ascribed to the original substance, HNO (Paolocci et al. 2007; Switzer et al. 2009). However, the high reactivity of HNO significantly complicates the study of its production, detection and understanding of its chemistry, especially in a biological setting (Kamynina 2017). HNO is an inherently unstable molecule due to its reaction with itself. It forms an HNO dimer (hyponitrous acid, $H_2N_2O_2$) followed by its decomposition to nitrous oxide (N_2O) and water (Fukuto et al. 2005b, 2005a; Switzer et al. 2009). As a consequence, HNO cannot be stored or concentrated and more stable donor molecules are needed to study its biochemical effects (DuMond and King 2011).

5.2.2 HNO donors

To study HNO effects *in situ*, HNO donors are needed. These donors can be divided into two groups based on their chemistry (Kamynina 2017). The first group is represented by hydroxylamine derivatives with an additional group to the nitrogen atom and includes Angeli's Salt (AS), Pyloty's acid and CXL-1020. Deprotonation of these compounds is accompanied by redox reactions that alter the oxidation state of the nitrogen atom (Huges and Wimbledon 1976; Dutton et al. 2004; Miranda et al. 2005; DuMond and King 2011). Nitroso compounds belong to the second group. These compounds undergo non-redox reactions to

release HNO. To this group belong the acyloxy nitroso compounds, such as 1-nitrosocyclohexyl acetate (NCA) (Shoman et al. 2011).

The oldest and therefore most commonly used and studied HNO donor is the short-lived Angeli's salt (AS; $Na_2N_2O_3$). AS is highly unstable at a physiological pH and releases HNO with a half-time of ~2.5 min at pH 4-8 in a „bolus dose" (Switzer et al. 2009). Therefore, only a very small amount out of a high initial concentration is available to react with biological targets. Unfortunately, AS cannot be modified to tune the release rate of HNO. Thereby, its short half-life makes it challenging to study the impact of sustained HNO levels. These might be more relevant to the cellular situation and also to evaluate the clinical implementation and versatility. Moreover, decomposition of AS yields as well NO, nitrate and nitrite to the same amount, whereas the reduction of nitrate to nitrite may cause formation of carcinogenic nitrosamines (Switzer et al. 2009). Nitrites oxidise the iron atoms in haemoglobin from ferrous iron (Fe^{2+}) to ferric iron (Fe^{3+}), rendering it unable to carry oxygen. This could lead to a generalised lack of oxygen and a methaemoglobinemia. Clinically, this is of importance and of pathophysiological relevance for example in infants, in patients with a mutation in the methaemoglobin reductase enzyme or in patients with insufficient production of stomach acid e.g. vegetarians (Colica et al. 2017). The application of AS in a clinical setting would be very limited and these additionally released molecules could be major confounders in experimental and clinical studies.

First clinical studies with HNO donors were performed with Cyanamid, which is used to date solely in the therapy of alcohol addiction. Released HNO interacts with thiol residues of the alcohol degrading enzyme alcohol dehydrogenase, leading to enzyme inhibition (DeMaster et al. 1998; Paolocci et al. 2007). The use of Cyanamid proves that it is indeed feasible that HNO donors can be used in a clinical setting.

Thus, a new group of HNO donors was generated, the acyloxy nitroso compounds (Shoman et al. 2011). The rate of hydrolysis of these compounds is dependent on the organic group and by modification of the position of the acyl

group. There is a variety of HNO donors with distinct release properties. The longer-acting HNO donor NCA belongs to these compounds and releases HNO spontaneously and slowly at neutral physiological pH with a half-life of about 800 min by spontaneous hydrolysis or esterase activity. Importantly, HNO is bound to a scaffold, 3-methyl-1-nitrosocyclohexyl acetate (3MNCA), which is released upon decomposition. Apart of this scaffold and in contrast to AS, NCA releases HNO without other side products like nitrite. The characteristic blue colour enables the control of the biochemical kinetics (Sha et al. 2006; Paolocci et al. 2007; Irvine et al. 2008). Taken together, NCA shows several important advantages for experimental studies and potential *in vivo* use. Other acyloxy nitroso compounds are nitrosocyclohexyl trifluoroacetate (NCFA), a rapid HNO-releasing donor, and nitrosocyclohexyl pivalate (NCP) with a half-life longer than 37 hrs (Shoman et al. 2011). The scaffold alone, which is the structurally similar t-butyl-ester of NCA, does not hydrolyse to HNO and failed to elicit a vasorelaxing response, suggesting that the observed actions are not due to the scaffold of NCA itself, but to the release of HNO (Donzelli et al. 2012).

CXL-1020, a Pyloty's acid derivative, is a first generation pure HNO donor compound, which has gained attention during the last years. CXL-1020 was the first HNO donor, which was tested in clinical trials as a potential therapy for patients with acute decompensated heart failure (ADHF) (clinical trials NCT01092325, NCT01096043). In patients with ADHF, CXL-1020 elicited a concentration-dependent decrease in pulmonary capillary wedge pressure (PCWP) and improved the stroke volume index (SVI) as well as the cardiac index (CI) compared to placebo (Sabbah et al. 2013). Due to infusion site toxicity, development was halted (Sabbah et al. 2013).

Bristol Myer Squibb generated a number of clinically relevant HNO donors with BMS-986231, formerly CXL-1427, being a second generation HNO donor with a half-life of 40-144 min in healthy individuals (Tita et al. 2017). It delivers HNO via a pH-dependent chemical breakdown, when exposed to the pH neutral environment of the blood stream (Cowart et al. 2019).

In healthy individuals, infusion of BMS-986231 for 24 to 48 hrs induced dose-dependent and well-tolerated reductions in systolic and diastolic blood pressure, whereas CI increased. There were no effects on heart rate (HR) or the occurrence of arrhythmias observed (Cowart et al. 2019). In an experimental canine heart failure (HF) model, BMS-986231 demonstrated beneficial inotropic, lusitropic and vasorelaxing properties with an improvement of left-ventricular ejection fraction (LVEF), decreased end-diastolic stiffness and systemic vascular resistance (Hartman et al. 2018). Results of a clinical phase IIa study already proved safety, tolerability and haemodynamic effects in response to 6 hrs BMS-986231 administration intravenously in patients hospitalised with advanced HF (Tita et al. 2017). Vasorelaxing, inotropic and lusitropic properties of BMS-986231 were confirmed together with a clinically significant improvement of dyspnea. The ongoing three related randomised clinical phase II trials StandUP-AHF (NCT03016325), StandUP-imaging (NCT03357731) and StandUP-kidney (NCT03332186) may pave the way for HNO donors into clinical practice (Felker et al. 2019).

5.2.3 Endogenous HNO production

Regarding its biochemical properties, HNO shows selectivity towards certain biological targets and it is suggested that it might be formed as an endogenous signalling molecule. Nevertheless, it is to date still unclear under which circumstances HNO is produced endogenously (Yuill et al. 2010; Kemp-Harper 2011).

Initial studies suggested that HNO production might be a consequence of nitric oxide synthase (NOS) uncoupling, due to reduced availability of substrates or cofactors such as tetrahydrobiopterin (BH_4) (Pufahl et al. 1995; Clague et al. 1997). Nevertheless, endogenous HNO production due to this mechanism could not be conclusively demonstrated.

In vitro experiments showed HNO production in response to heme-mediated oxidation of hydroxylamine involving horse radish peroxidase (HRP), myoglobin or myeloperoxidase in the presence of hydrogen peroxide (H_2O_2) (Donzelli et al.

2008). Also, studies suggested that the reduction of NO by superoxide dismutase (SOD) or xanthine oxidase (XO) may yield HNO (Niketić et al. 1999; Saleem and Ohshima 2004). As HNO is the reduced sibling of NO, reduction of NO in a physiological setting was as well evaluated. Although it seemed thermodynamically unfavourable due to its negative reduction potential at physiological pH, a couple of studies hinted to HNO as a product of the reaction of NO with physiological reductants (Shafirovich and Lymar 2002; Lymar et al. 2005). Already twenty years ago, it was shown that especially the reaction of nitrosothiols (RSNO) with other thiols (RSH) appeared to be physiologically the most relevant way to result ultimately in HNO and disulfide formation (Wong et al. 1998). Hogg et al. studied the reactions of NO and glutathione (GSH) and NO transport mechanisms and suggested that HNO might be an intermediate in the reaction of NO and GSH under anaerobic conditions, finally resulting in the formation of N_2O and glutathione disulfide (GSSG) (Hogg et al. 1996). Under aerobic conditions, NO and GSH were shown to react to S-nitrosoglutathione (GSNO) and the following reaction of GSNO and GSH might yield HNO as an intermediate. In the aerobic setting, the authors suggested that HNO might generate $ONOO^-$ as well (Hogg et al. 1996).

Recently, HNO was suggested to form endogenously as a result of the reaction of the two gasotransmitters NO and H_2S colocalised to its targets (Filipovic et al. 2013). This hypothesis was verified in isolated rat ventricular myocytes, which were exposed to H_2S and NO donors. Hereby, it was shown that the observed increase in contraction was comparable to that achieved by the HNO donor AS (Yong et al. 2010). Using an HNO-selective electrode, it was shown that HNO could indeed be produced *in vitro* by the reaction of NO donors with H_2S donors (Eberhardt et al. 2014). The same study could show as well HNO production in neurons by overexpression of inducible NOS (iNOS) together with cystathionine beta-lyase (CBS), which produces H_2S. Importantly, using the fluorescent HNO detector CuBOT, basal levels of HNO in sensory neurons were detected. In order to prove selectivity of the CuBOT sensor, depletion of cellular arginine, required for NO production, or cysteine (C), required for H_2S production, resulted in

reduced fluorescence. As a physiological consequence, activation of the transient receptor potential ankyrin 1 (TRPA1) channel via disulfide bond formation was demonstrated in response to HNO production via this mechanism. As a result, levels of calcitonin gene related peptide (CGRP), a known vasodilator, were elevated. Although these results seem to be convincing, the authors stated that other by-products could result from a reaction of NO with H_2S, which also could lead to these cellular consequences (Cortese-Krott et al. 2015). However, thus far, HNO production was only observed, when NO and H_2S were added exogenously in high concentration to cells with the producing enzymes in close proximity.

Follow-up studies using the CuBOT-sensor suggested HNO production in bovine endothelial cells after exposure with ascorbic acid (Suarez et al. 2015). Also, they could detect HNO production in RAW macrophages after stimulation with iNOS-inducing agents and treatment with ascorbate using an HNO-selective electrode (Suarez et al. 2015). These results suggested that HNO might be generated as well via the reduction of NO by aromatic or pseudoaromatic alcohols, such as hydroquinone or ascorbic acid (Hamer et al. 2015).

It is still not convincingly demonstrated, whether and importantly by which mechanism HNO is produced endogenously. However, as HNO donors show to have an impact on signalling pathways with physiological consequences and as they are under examination in clinical trials, this provides a rational for further elucidation of the mechanisms leading to these biochemical alterations.

5.2.4 Biochemistry and pharmacology of HNO

Besides of its autoreactivity, HNO is highly reactive with thiol residues or metalloproteins (Mohamed 2010). It interacts with thiol residues of receptors or ion-channels such as the ryanodine receptor 1 (RyR1) and RyR2 (Tocchetti et al. 2011). It represents a highly reactive electrophile, which preferably reacts with soft nucleophils such as cysteine thiols (Miranda et al. 2003b; Fukuto et al. 2005a, 2005b). Thus, the reaction of HNO with thiols can either lead to the reversible

production of disulfide or hydroxylamine (Doyle et al. 1988). *In silico* calculations could show that indeed the reaction of HNO with thiols would be thermodynamically favourable (Bartberger et al. 2001). The reaction rate of HNO with thiols is fast in comparison to the rate for HNO dimerization. In consequence, HNO related biochemical actions are significantly mediated by the oxidation of thiols (Miranda et al. 2005). Mechanistically, HNO interacts initially with the nitrogen atom to form N-hydroxylsulfenamide (**Figure 2**) (Doyle et al. 1988; Wong et al. 1998; Miranda et al. 2005; Fukuto and Carrington 2011). In proximity to other thiols, this leads to the formation of another disulfide and hydroxylamine. Alternatively, the absence of thiols leads to isomerisation of N-hydroxysulfenamide and to the irreversible product sulfinamide. Within the nitrogen oxide species, HNO is the only one, which is able to produce sulfinamide, which could thereby be used as a marker for the reactivity of HNO but is unfortunately only of transient character (Donzelli et al. 2006).

The described interactions with thiols, thiol residues or metalloproteins are not shown so far for NO, which might be an explanation for the disparate effects of HNO and NO. Although being the one-electron-reduced sibling of NO, HNO follows entirely its own and distinct signalling pathways (Fukuto et al. 2005a, 2005b; Fukuto and Carrington 2011). Importantly, the reaction of HNO with thiols can result in posttranslational modifications followed by a great variety of chemical and biological alterations.

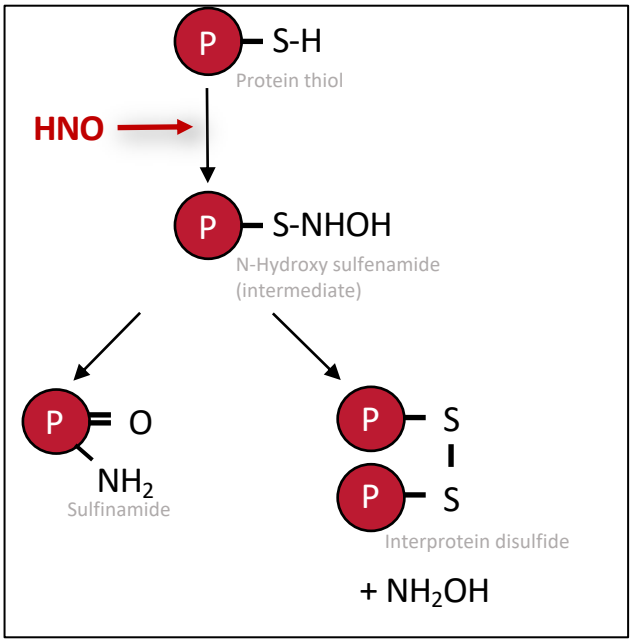

Figure 2: HNO reacts with thiol groups to form via an intermediate; either a sulfinamide group or, in presence of an additional thiol, an interprotein disulfide and hydroxylamine. P: protein, SH: protonated thiol group of cysteine (modified from Gao et al. 2012).

Another target of HNO-mediated posttranslational modifications are ferric heme proteins, as shown for metmyoglobin or methaemoglobin (Miranda et al. 2003a; Doctorovich et al. 2014). Exposure results in the formation of ferrous heme-nitrosyl complexes. One important target protein of HNO-mediated modification is sGC, as HNO interacts with the ferrous heme enzyme and induces sGC-mediated generation of cGMP, ultimately resulting in vasorelaxation. This has to be taken into account, when evaluating vasorelaxing effects in response to HNO donors which will be described in chapter 5.2.6 (Miller et al. 2009).

HNO shows a variety of effects on neuronal functions, on cardiovascular functions and has been shown to be relevant for cancer treatment as well as for the therapy of alcoholism. The following chapters will focus on its cardiovascular functions.

5.2.5 HNO and cardiac function

Application of HNO donors to the myocardium *in vivo* leads to an increase in contractile function and thereby a positive inotropic effect, and to an increase in

sarcomere relaxation, the positive lusitropic effect (Paolocci et al. 2001; Sabbah et al. 2013). Effects on cardiac function were at first studied using AS in a dog model of HF evoked by chronic tachypacing (Paolocci et al. 2001). In these studies, AS increased cardiac contractility and simultaneously cardiac preload was reduced. Importantly, HNO maintained its positive inotropic and lusitropic effects in failing hearts, despite beta-adrenergic desensitization and despite downregulation of Ca^{2+} signalling pathways (Paolocci et al. 2003). In addition, positive inotropic and lusitropic effects were independent of cardiac pre- or afterload (Paolocci et al. 2001, 2007). Increased contractility evoked by HNO exposure was not impaired by beta-blockers, suggesting modulation of cardiac function independent of beta-adrenergic signalling (Paolocci et al. 2003; El-Armouche et al. 2010). Moreover, synergistic effects concerning the positive inotropy of HNO in combination with beta-agonists such as dobutamine could be observed, whereas NO treatment rather attenuated dobutamine-dependent contractility (Paolocci et al. 2003). Therefore, a couple of groups suggested that the observed effects of HNO occurred independently of beta-adrenergic signalling and are rather associated with redox modifications of key proteins responsible for excitation-contraction coupling within the cardiomyocyte contractile machinery (Paolocci et al. 2003).

It has been proposed that posttranslational modulation of RyR2 and the sarcoplasmic/ endoplasmic reticulum Ca^{2+} ATPase (SERCA) 2a are responsible for the positive inotropic effects induced by HNO donors on the myocardium, leading to an increase in Ca^{2+} release and at the same time an increase in Ca^{2+} reuptake into the sarcoplasmic reticulum (SR). Importantly, this is not associated with an increase in total diastolic Ca^{2+} concentrations (Tocchetti et al. 2007). HNO interacts with thiol groups, as increased intracellular thiol content effectively quenched HNO action, and thereby, enhanced the open probability of the RyR2 and the intracellular Ca^{2+} release from the SR. These effects are redox sensitive as they are fully reversible under reducing conditions (Tocchetti et al. 2007). In contrast, extracellular Ca^{2+}, which enters the cardiomyocyte via L-type-Ca^{2+}-channels, has been reported to not play a role in these studies investigating the HNO donor AS. Taken together, HNO increases Ca^{2+} cycling in animal models

by its impact on Ca^{2+} release from the SR. The Ca^{2+} reuptake into the SR is increased via the modulation of the ATP-dependent Ca^{2+} transporter SERCA. Cellular HNO targets are C674 of SERCA, which induces S-guanylation of this cysteine and leads thereby to increased SERCA activity (Lancel et al. 2009). Moreover, SERCA activity may be influenced by the modulation of phospholamban (PLB). Recent studies showed that HNO enhanced PLB oligomerisation and relieved thereby the brake on SERCA activity. As a consequence, Ca^{2+} reuptake into the SR was increased, leading to faster myocardial relaxation during diastole (Froehlich et al. 2008; Sivakumaran et al. 2013). In line with the *in vivo* experiments, *in vitro* experiments showed as well an increase in sarcomere shortening and relaxation and an elevation of Ca^{2+} transient amplitude with an increase in total, but not in diastolic Ca^{2+} concentrations (Tocchetti et al. 2007; Lancel et al. 2009; Kohr et al. 2010). Importantly, these effects in response to HNO treatment were reversible after addition of a reducing agent such as dithiothreitol (DTT), further supporting the redox mechanism of action.

In addition to its effects on Ca^{2+} cycling, HNO treatment has been shown to influence Ca^{2+} sensitivity of the myofilaments (Dai et al. 2007). Studies using a mass spectrometry-based approach in combination with a biotin switch assay suggested disulfide bond formation between actin and tropomyosin and myosin heavy or light chains (Gao and Marshall 2011). As a consequence, Ca^{2+} responsiveness of the myofilaments was enhanced. However, only the HNO donor NCA was able to enhance Ca^{2+} sensitivity as well as cardiac contractility. In response to AS, only cardiac contractility was improved, whereas Ca^{2+} sensitivity was not altered. This is another example for the distinct effects of different HNO donors, which might be due to HNO release but as well due to the release and biological actions of by-products.

5.2.6 HNO and vascular function

HNO has been reported to induce vasorelaxation also during vascular diseases *in vitro* and *in vivo*. Vasorelaxation induced by HNO was demonstrated in isolated and capacity vessels isolated from dogs and rodents (Fukuto et al. 1992b;

Paolocci et al. 2003). During the first studies, Fukuto and colleagues suggested that the HNO donor AS relaxed rabbit aorta and bovine intrapulmonary artery most likely via activation of sGC (Fukuto et al. 1992a). A variety of studies using different HNO donors described vasorelaxing effects in various vascular beds, supporting independent vasorelaxing properties of HNO (Ellis et al. 2000; Wanstall et al. 2001; Irvine et al. 2003; Andrews et al. 2009, 2015; Botden et al. 2012). Interestingly and in contrast to NO, HNO treatment did not lead to vascular tolerance, suggesting that HNO might be suitable as an antihypertensive drug for a long-term treatment (Irvine et al. 2007). These protective effects under pathophysiological conditions may be due to its resistance to scavenging by superoxide (Leo et al. 2012). Therefore, HNO could be of relevance in a clinical setting as a novel therapeutic addition for the treatment of cardiovascular diseases. However, how HNO lowers blood pressure still remains elusive. Previous results in aortic and endothelium-denuded rings showed that HNO given by NCA induced a concentration-dependent relaxation (EC_{50} = 4.4 µM) (Donzelli et al. 2012). Inhibitors of sGC, CGRP and voltage-dependent K^+ channels significantly impaired the vasorelaxing response to NCA.

Previous experiments demonstrated that HNO-mediated vasorelaxation was mainly mediated by sGC. sGC is a heme-binding metalloprotein, which can be activated by HNO, as shown in *in vitro* experiments (Miller et al. 2009). It reduces Fe^{3+} to Fe^{2+} and experiments with heme-free sGC could show that the heme group was essential for the effect of HNO on enzymatic activity (Miller et al. 2009). Interestingly, HNO-induced activation of sGC was 2-3 times lower than for NO-induced activation at comparable concentrations. sGC activation in a thiol- and oxygen-free buffer was not possible (Miller et al. 2009). However, Dierks et al. attributed the vasorelaxing effect in response to HNO donors to NO release and were doubtful that HNO could activate sGC (Dierks and Burstyn 1996). In these studies, the experiments were performed in the presence of DTT, which might scavenge HNO before it could interact with sGC. Further studies supporting the idea that NO and not HNO is responsible for the vasorelaxing effect showed that sGC could not be activated by HNO in the absence of SOD, although this finding was challenged by other studies (Ellis et al. 2000; Wanstall et al. 2001; Irvine et

al. 2003; Andrews et al. 2009; Zeller et al. 2009). In addition, inhibition of sGC by 1H-[1,2,4]-oxadiazolo-[4,3-a]-quinoxalin-1-one (ODQ), a pharmacological inhibitor of sGC, did not inhibit vasorelaxation completely, suggesting that HNO might lead to vasorelaxation also by other mechanisms.

As one of those, modulation of voltage-gated potassium channels by HNO was rationalised, as 4-aminopyridine (4-AP), which blocks these channels, was able to abolish this effect in human radial or rat mesenteric arteries (Irvine et al. 2003; Favaloro and Kemp-Harper 2009; Donzelli et al. 2012). Furthermore, activation of the large conductance Ca^{2+} activated K^+ channel (BK_{Ca}) on the smooth muscle cell membrane was discussed, as iberiotoxin, its inhibitor, was able to abolish this effect (Irvine et al. 2003).

CGRP release in the context of HNO-mediated vasorelaxation was another mechanism, which was evaluated (Paolocci et al. 2001; Favaloro and Kempharper 2007; Eberhardt et al. 2014). In response to HNO donors such as AS, CGRP levels were increased in the arterial plasma of dogs. However, this finding was not consistent with observations made with other HNO donors, suggesting that this effect might be due to the donor compound itself (Paolocci et al. 2003). Furthermore, CGRP levels were also increased in the cranial dura mater or sciatic nerves in mice exposed to AS (Eberhardt et al. 2014). In addition, vasorelaxing effects in response to the HNO donor AS in coronary arteries were reduced by CGRP inhibitors, further supporting this mechanism of action (Favaloro and Kempharper 2007).

5.3 cGMP-dependent protein kinase (PKG)

The cGMP-dependent protein kinase (PKG) is a homodimeric serine/threonine kinase containing various structural elements. PKG has been classified into the AGC-branch of the kinase complement of the human genome, due to the homology of its catalytic domain and similar phosphorylation consensus sites on substrate proteins (Osborne et al. 2011; Arencibia et al. 2013). PKGI and PKGII are encoded by two different genes, namely *Prkg1* and *Prkg2,* and are distinguishable by their amino acid sequence in the N-terminus of the regulatory domain. Although PKGI and PKGII are highly homologous, they display disparate

tissue expression, localisation and have distinct substrate preferences. PKGI is especially localised in the cytosol, while PKGII is anchored to the plasma membrane by an N-terminal myristoyl residue (Francis et al. 2010). In the following, the focus has been set on PKGI isoforms, as they have been shown to be prominently involved in blood pressure homeostasis. In contrast, PKGII plays an important role in the regulation of bone remodelling (Rangaswami et al. 2009), intestinal secretion (Vaandrager et al. 1998), renin secretion (Gambaryan et al. 1998) by the kidney and aldosterone production by the adrenal gland (Gambaryan et al. 2003).

Alternative splicing of two exons of the PKGI-gene pre-mRNA yields two isoforms, PKGIα and PKGIβ, which differ in the first 90-100 amino acids of their N-terminal region (Hofmann et al. 2000). This is very important, as the respective N-terminal regions interact with isoform specific G-kinase anchoring proteins (GKAPs) that enable compartmentalised signalling events by localising the kinase into substrate vicinity (Vo et al. 1998). Furthermore, the isoform-specific differences in the N-terminal domain impact on cGMP affinity and substrate specificity (Wolfe et al. 1989; Sekhar et al. 1992; Tang et al. 1993; Ruth et al. 1997; Surks et al. 1999; Ammendola et al. 2001; Richie-Jannetta et al. 2003; Francis et al. 2010). Variations in the N-terminal region of the splice isoforms PKGIα and PKGIβ are therefore responsible for the observed functional differences. Both isoforms are commonly co-expressed, however, to a different extent in the various tissues. PKGIβ is predominantly soluble and present in high concentrations (>0.1µM) in muscle, platelets, cerebellum, hippocampus, dorsal root ganglia, neuromuscular endplate and the kidney vasculature, as well as in low concentrations in vascular endothelium, granulocytes, chondrocytes and osteoclasts (Hofmann et al. 2000; Geiselhöringer et al. 2004a). In contrast, the PKGIα isoenzyme is mainly expressed in lung, heart, platelets, cerebellum and, importantly, in smooth muscle cells of the uterus, vessels, intestine and trachea (Keilbach et al. 1992; Vo et al. 1998; Hofmann et al. 2000; Corradini et al. 2015). PKGI isoforms can change their subcellular location, mediated by the N-terminal leucine zipper (LZ) (Francis et al. 2010; Sharma et al. 2017).

Studies using PKG-targeted knock-out (KO) mice were employed to investigate

the physiological role of PKG. Conventional PKG KO mice revealed a severely reduced life span of only 6 weeks due to impaired relaxation of vascular and visceral smooth muscle cells. Furthermore, mice showed defects in axon guidance and neuronal plasticity (Pfeifer et al. 1998; Massberg et al. 1999; Hedlund et al. 2000; Schmidt et al. 2002). Due to their short life span and the necessity to investigate as well adult mice and chronic disease models, conditional PKG KO mice were generated. In these mice, tissue-specific PKG deletion was studied. Conditional PKG KO mice are fully viable and display dependent on the target tissue various phenotypes (Wegener et al. 2002; Kleppisch et al. 2003). Interestingly, mice with mutations in the LZ domain of PKGIα are basally hypertensive and display impaired cGMP-mediated vasorelaxation. Mechanistically, these mutations hinder protein dimer formation and substrate recognition and thus correct subcellular localisation, showing the functional importance of this domain. In addition, the mice also develop diastolic dysfunction and progressive left ventricular hypertrophy (Michael et al. 2008; Blanton et al. 2013). Taken together, these studies highlight that PKGI functions are crucially important for unperturbed cardiovascular function, with the functional importance of every structural element. Alteration of its structural elements results in impaired PKGI signalling and thus downstream effector signalling.

5.3.1 PKG and vasorelaxation

PKG is described as one of the major players involved in the multiple molecular signalling events leading to vasorelaxation in mammals (Geiselhöringer et al. 2004a, 2004b).

One important substrate of PKG is BK_{Ca} (**Figure 3**). Phosphorylation by PKG promotes its open-probability and leads to hyperpolarisation by increased cellular export of K^+. The hyperpolarisation facilitates closure of the voltage dependent Ca^{2+} channels and reduces thereby Ca^{2+} influx into the cells (Fukao et al. 1999; Barman et al. 2003). In addition, PKG activation results in increased PLB phosphorylation. PLB phosphorylation removes the inhibitory effect on SERCA, which imports Ca^{2+} from the cytosol into the SR. Therefore, PKG-mediated PLB phosphorylation enhances import of Ca^{2+} into the SR, consequently decreasing

cytosolic Ca^{2+} concentrations in the VSMCs and thus contributing to vasorelaxation (Lalli et al. 1999; Koller et al. 2003).

Another target of PKG is the IP_3 receptor-associated PKG-substrate (IRAG) in smooth muscle cells (Fritsch et al. 2004). Vasoconstriction is initiated by activation of the PLC-IP_3 signalling pathway (see chapter 5.1.1). However, in VSMCs, pro-contractile agonists such as noradrenaline activate PLC. As a consequence, IP_3 generation in VSMCs is increased, which results in activation of the IP_3R with subsequent Ca^{2+} release from the SR (Raeymaekers et al. 2002; Yao and Garland 2005). In order to induce vasorelaxation, PKG phosphorylates IRAG and inhibits thereby IP_3-dependent Ca^{2+} release via the IP_3R (Schlossmann et al. 2000; Fritsch et al. 2004; Geiselhöringer et al. 2004b). Additionally, PLC-dependent IP_3-production is inhibited by PKG-dependent phosphorylation of the regulator of G-protein signalling 2 (RGS2) (Obst et al. 2006; Osei-Owusu et al. 2007).

In summary, orchestrated phosphorylation of the PKG substrates BK_{Ca}, PLB, IRAG and RGS2 in VSMCs reduces intracellular Ca^{2+} levels and thereby inhibits MLCK activity (Hirano 2007). This in turn reduces phosphorylation of MLC and inhibits its ATPase activity. As a consequence, actin-myosin interaction is reduced, resulting in deceleration of cross-bridge cycling and ultimately culminating in smooth muscle cell relaxation.

Additionally, these signalling events are supported by MLCP activation, which also promotes smooth muscle relaxation. PKG phosphorylates RhoA, the activator of Rho kinase (ROCK), and prevents RhoA translocation to the membrane, an important trigger for ROCK activation. ROCK cannot be activated by RhoA and is not able to inactivate MLCP (Sauzeau et al. 2000; Sawada et al. 2001).

Furthermore, PKG activation prevents MLCP inactivation by phosphorylation of the myosin phosphatase target subunit 1 (MYPT1) of MLCP at serine (S) 695. ROCK phosphorylation of MYPT at threonine (Thr) 696 is prevented by phosphorylation of MYPT1 at Ser695 (Surks et al. 1999; Wooldridge et al. 2004; Somlyo 2007). Therefore, PKG contributes to vasorelaxation independently of intracellular Ca^{2+} fluxes.

In addition, phosphorylation of the small heat shock protein 20 (HSP20) by PKG enhances actin-binding with subsequent reduction of actin cytoskeleton reorganisation and diminished smooth muscle constriction (Beall et al. 1997, 1999).

In summary, PKG activation mediates blood vessel relaxation by decreasing intracellular Ca^{2+} concentrations, together with a reduction in myofilament Ca^{2+} sensitivity and thereby attenuation of actin-myosin interaction and cross-bridge cycling (Murphy and Walker 1998; Etter et al. 2001).

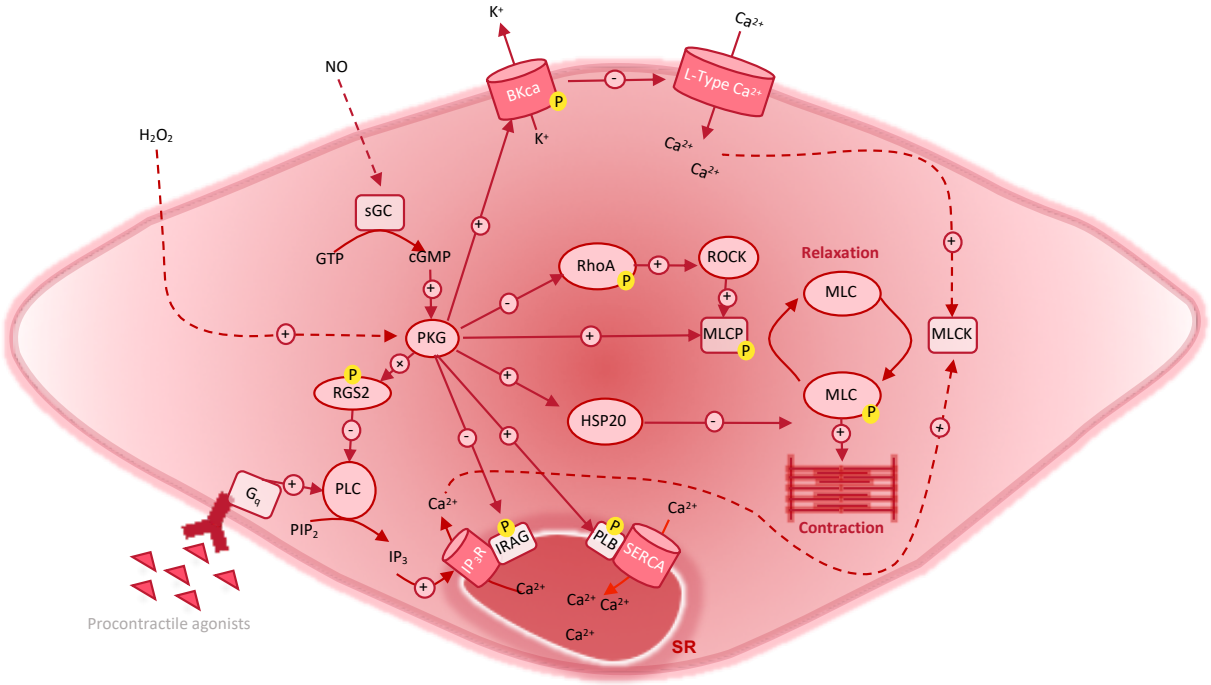

Figure 3: Targets of PKG in a VSMC that mediate vascular smooth muscle tone (adapted from Burgoyne and Eaton 2010).

5.3.2 PKG and cardiac function

NO and natriuretic peptides, such as the atrial natriuretic peptide (ANP) and the brain natriuretic peptide (BNP), are regulators of cardiac contractility and remodelling and various studies discuss the significance of PKG with regard to the NO-cGMP signalling cascade (Layland et al. 2002; Koitabashi et al. 2009; Krüger et al. 2009; Kinoshita et al. 2010). ANP and BNP are both secreted by cardiomyocytes, ANP in the atria and BNP in the ventricles, and amongst other factors in response to stretching caused by increased blood volume (Maisel et al.

2018). NO treatment of isolated adult rat ventricular myocytes (ARVMs) is associated with negative inotropic effects via PKG signalling (Layland et al. 2002). In adult mice with a conditional cardiomyocyte specific PKGI KO, cGMP analogues were not able to induce negative inotropic effects (Wegener et al. 2002). These results suggested that the reduction of myocardial contractility is mediated by activation of PKGI. With regard to isoenzyme specific effects, studies using transgenic overexpressing PKGIβ mice confirmed the anti-hypertrophic effects of NO donors (Wollert et al. 2002). Transgenic cardiomyocyte specific overexpression of PKGIα enhanced in murine ventricular myocytes in particular the NO/cGMP-induced inhibition of L-type Ca^{2+} channel activity, suggesting that this might be the underlying mechanism for NO-mediated negative inotropy (Schröder et al. 2003). Knock-in (KI) mice constitutively expressing a PKGIα mutant with replacement of C42 by a serine, displayed diastolic dysfunction and an impaired Frank-Starling mechanism (Scotcher et al. 2016). This model will be described in more detail in chapter 5.3.4. These studies showed the great importance of increasing the understanding of the molecular regulation of PKGIα by second-messenger binding and posttranslational modifications and the resulting mode of activation.

5.3.3 PKG structure

PKGIα and PKGIβ are constitutive dimeric proteins with monomers arranged in parallel (Francis et al. 2010). Each monomer consists of a regulatory and a catalytic domain. The regulatory domain can be divided into a LZ domain, a flexible linker with autoinhibitory (AI) and autophosphorylation sequences as well as two cGMP-binding sites. The catalytic domain contains the Mg^{+}/ATP-binding pockets and catalyses the transfer of one phosphate from ATP to a serine/threonine residue on target proteins (Hofmann et al. 1992, 2000; Pfeifer et al. 1999). The LZ domain promotes protein dimerization, interaction with substrate proteins and GKAPs and thereby subcellular localisation (Richie-Jannetta et al. 2003; Francis et al. 2005; Sharma et al. 2008). The AI domain functions as a pseudo-substrate and inhibits PKGI activity in the absence of cGMP by blocking the catalytic sites. Interestingly, the LZ and the AI domains

differ between PKGIα and PKGIβ and thus contribute to their substrate specificity (Surks et al. 1999; Ammendola et al. 2001; Francis et al. 2005). The LZ domain can be modified by oxidative posttranslational modifications and is essential with regard to redox-regulation and subcellular localisation of PKGIα in substrate vicinity, which will be introduced in the following chapters.

The cGMP-binding sites bind cyclic nucleotides in general. However, both cGMP-binding sites have a higher preference towards cGMP over cyclic adenosine monophosphate (cAMP). Both PKGI isoforms bind two molecules of cGMP and are very similar with regard to K_M and V_{max} and phosphorylation of synthetic peptides (Surks et al. 1999; Ammendola et al. 2001; Tang et al. 2003).

The two cGMP-binding sites, cyclic nucleotide binding site (CNB)-A and CNB-B are also defined as the high and low affinity site. Hereby, the CNB-A high affinity site displays a comparably slow dissociation of bound cGMP, whereas the CNB-B site shows a faster dissociation (Reed et al. 1996; Kim et al. 2011). Especially, the low affinity binding site is more selective for cGMP than for cAMP and appears to be responsible for cGMP selectivity in PKG (Lorenz et al. 2015). Binding of cyclic nucleotides induces a conformational change that relieves the catalytic site from autoinhibition and enables subsequent substrate phosphorylation (Wall et al. 2003; Alverdi et al. 2008).

5.3.4 Regulation of PKGIα by oxidants

Alternatively to the classical NO-cGMP pathway, PKGIα has been described to function as a redox-sensor and can be posttranslationally modified by oxidants with impact on its subcellular localisation, substrate interaction and kinase activity, independently of cGMP-binding. In response to oxidants such as H_2O_2, the kinase homodimer complex forms an interprotein disulfide via C42 in the LZ domain of PKGIα (Burgoyne et al. 2007). Structural studies confirm that C42 on each chain closely aligns to explain the susceptibility to oxidants. Due to the localisation of C42 within the LZ, it is likely that interdisulfide formation impacts on kinase localisation and translocation into substrate vicinity. Activation of PKG by cGMP increases PKG V_{max}, whereas disulfide activation increases the kinase affinity for its substrates (Burgoyne et al. 2007). The physiological importance of

this mechanism becomes evident in PKGIα-C42S KI mice, which cannot form the interprotein disulfide bond and basally display a hypertensive phenotype (Burgoyne et al. 2007). These mice were also protected from septic injury related to hypotension during sepsis, whereas wildtype (WT) mice showed increased oxidative activation of PKGIα, followed by increased blood vessel permeability, hypotension, reduced cardiac output and subsequently insufficient perfusion of end organs (Rudyk et al. 2013). Moreover, this emphasizes that oxidants might also be indispensable for the maintenance of blood pressure homeostasis as the mice are basally hypertensive and that oxidants are not only detrimental and contribute to disease, but also impact on signal transduction, summarised as redox signalling.

5.4 Redox-regulation of signalling pathways

The oxidant-dependent regulation of PKG is an example for the emerging role of reactive oxygen species (ROS) in the control of physiological and pathophysiological signalling pathways (Corcoran and Cotter 2013; Rani et al. 2014; Cuello 2017). ROS are endogenous metabolic by-products of cellular respiration and metabolic reactions, but they are also produced in a tightly controlled manner by enzymes such as nicotinamide adenine dinucleotide phosphate (NADPH) oxidases (Schröder et al. 2012; Brandes et al. 2014; Schröder 2019). Due to elevated levels of ROS in tissues during various global diseases such as cancer, inflammation and cardiovascular disorders, they were primarily associated with cell damage and aging. Based on these findings, a therapeutic strategy was to counteract ROS actions using antioxidants (Harman 1956; Gerschman et al. 2001). Whilst some preclinical studies suggested a protective effect of antioxidants, large translational trials could not confirm antioxidants in their role as a cure-all against ageing, cancer or cardiovascular diseases (Stephens et al. 1996; Chappell et al. 1999; Bjelakovic and Gluud 2007; Bjelakovic et al. 2007; Pauling et al. 2009). Especially in the field of cardiovascular diseases, studies led to the assumption that antioxidants do more harm than good (Miller et al. 2005). Together with other studies in the field of cancer research, these results paved the way for a new paradigm: ROS are to

date also regarded as physiological regulators of intracellular signalling pathways (Eaton 2006; Burgoyne et al. 2012a). Current studies suggest that oxidants play critical roles in the function of healthy tissues or adaptation to stress that limits disease progression (Cuello and Eaton 2018). In this scenario, elevated levels of oxidants may cause dysregulation by overstimulating these originally regulatory pathways and contribute in this way also causatively to the aetiology. But not just the concentration of oxidants within the cell, but also the oxidant species and the type of the oxidative posttranslational modification have an impact on protein function. Irreversible hyperoxidation may lead to protein dysfunction as described later on (Meng et al. 2002).

Oxidants can regulate signalling pathways in a tightly controlled manner by inducing a variety of protein modifications, described as posttranslational modifications. These modifications, which include for example S-glutathiolation or disulfide bond formation, can alter the structure and function of these biomolecules and thereby impact on downstream signalling events (Cuello and Eaton 2018). Within the proteins, the amino acid cysteine belongs to the most susceptible targets for posttranslational modifications and can thereby operate as a redox sensor (Couvertier et al. 2014). Evolutionally, it was shown that the cysteine content of proteins increased from 0.41% in archaea to 2.26% in mammals (Miseta and Csutora 2000). In addition, a variety of proteins contain highly conserved regions between species and organisms, in which the cysteines are embedded (Go and Jones 2013). This suggests a regulatory function beyond just structural roles, namely operating as a redox switch. The oxidation state of a cysteine thiol group is dependent on its acid dissociation constant (pK_a); a low pK_a is associated with a markedly more reactive cysteine. The pK_a of reactive cysteine thiols are mostly below the ambient pH, as in glutaredoxin with 3.5. Thereby, the thiol group is predominantly deprotonated at a cellular pH and highly reactive towards oxidation (Giles et al. 2001). In most cytoplasmic proteins, thiols have pK_a values higher than the ambient pH, concluding that they are mostly protonated and unreactive under physiological conditions (Kamynina 2017). In addition to the pK_a, the structural microenvironment, created by neighbouring amino acids, and the precise position of a cysteine residue defines its reactivity

towards redox modifications (Roos et al. 2012). Due to a great variety of different posttranslational modifications, with each potentially inducing a functional different activity or graded response, the thiol group can serve as a finely tuned redox switch. H_2O_2 for example has been observed to oxidise a variety of thiol proteins in cells and tissues, however, mostly via peroxidases (Winterbourn 2008; Cuello and Eaton 2018). Oxidised forms of cysteine thiols include sulfenic (SOH), sulfinic (SO_2H), sulfonic (SO_3H) acids, inter- and intraprotein disulfides and S-nitrosothiol (**Figure 4**) (Ullrich and Kissner 2006; Paulsen and Carroll 2013). The various modifications differ in their stability, reactivity and reversibility. Importantly, the majority of these posttranslational modifications involving cysteines are reversible. Reducing reactions and especially oxidoreductase enzymes, such as thioredoxin (Trx) or glutaredoxin, are able to reverse oxidative modifications (Berndt et al. 2007). However, sulfinic acids are mostly irreversible, when they form in proteins. This terminal reaction can impact on protein activity and may inactivate enzymes (Meng et al. 2002).

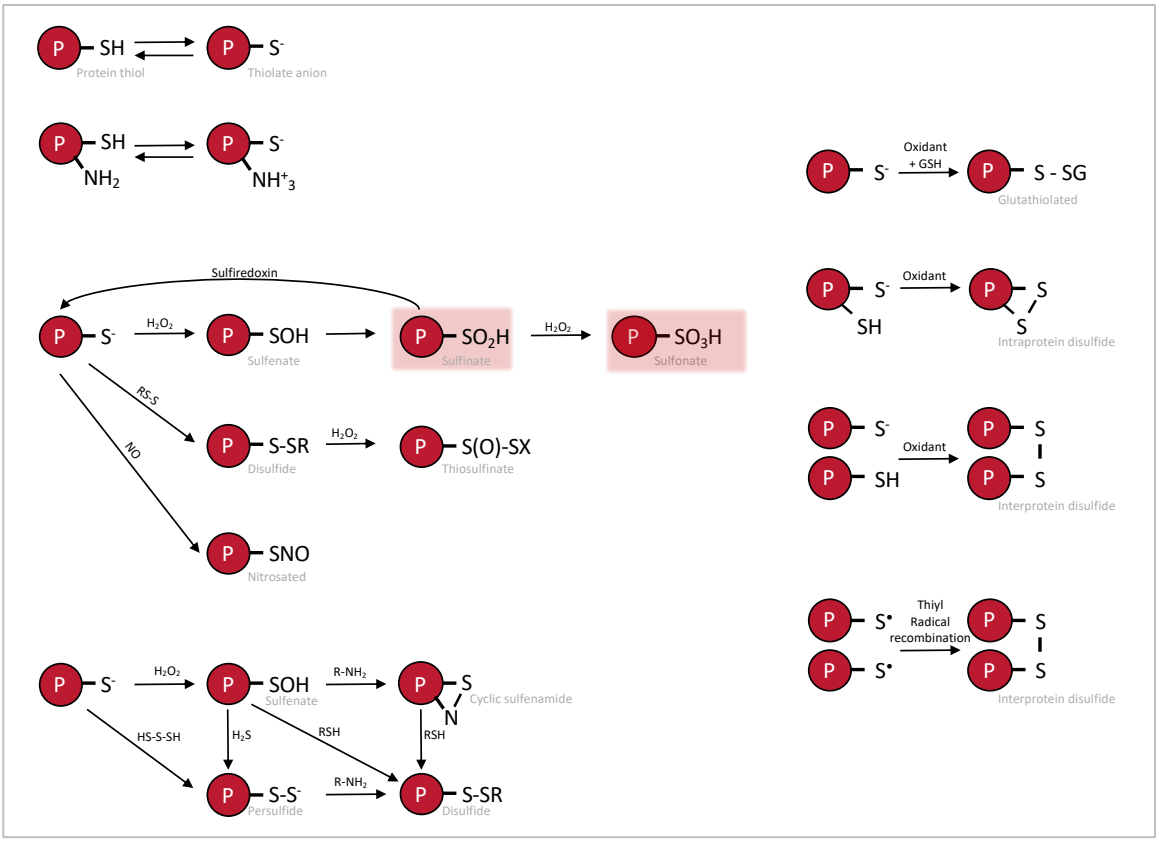

Figure 4: Posttranslational modifications in response to oxidants (adapted from Cuello and Eaton 2018).

There are proteins, which are directly regulated by the cellular redox state (Tanner et al. 2011). Posttranslational modifications of proteins at critical cysteine residues may stimulate, modulate or inhibit catalytic activity, or promote conformational changes that alter the possibility to interact with substrates, binding partners and as a consequence subcellular translocation (Kamynina 2017). Within these proteins, a catalytically important cysteine has often an enhanced reactivity towards oxidants due to a low pK_a. An oxidative modification could mediate enzyme inactivation as the essential catalytic thiol would no longer be available to perform biochemical reactions. These types of reactions occur typically in protein tyrosine phosphatases and ribonucleotide reductases (Meng et al. 2002). Moreover, oxidation of cysteines can also induce changes in protein structure, such as intra- or intermolecular disulfide bonds. PKGIα is, as described above, an example how interdisulfide bond formation in response to oxidants such as H_2O_2 alters substrate phosphorylation and physiological functions (Burgoyne et al. 2007). However, whether oxidants such as HNO might have an impact on kinase conformation, localisation and activity and thus might contribute to the HNO-mediated vasorelaxation remains incompletely understood.

5.5 Background of the study

It was shown that HNO-induced vasorelaxation was attenuated, but not completely inhibited by ODQ, a pharmacological inhibitor of sGC. Therefore, the aim of this thesis was to investigate PKGIα as potential target for HNO-mediated oxidation in the vasculature. Understanding the principles of thiol modification and subsequent disulfide formation, PKGIα might be a potential target of HNO. It has been shown that the Iα isoform of PKG is subject to oxidative modulation, besides the classical regulation by cGMP.

The combination of the unique pharmacological actions of HNO such as increased myocardial contractility and peripheral vasorelaxation opens new possibilities concerning HF therapy. Furthermore, antiaggregatory and vasorelaxing effects enable application in cardiovascular pathologies such as

angina pectoris, acute hypertensive crisis and atherosclerosis. In contrast to NO donors, which induce a tolerance phenomenon during long-term treatment, show reduced effectivity under oxidative conditions and are possibly cytotoxic under certain conditions, HNO donors do not show these adverse side effects and might be of benefit in a clinical setting as a novel therapeutic addition for the treatment of cardiovascular diseases.

5.6 Aims of this doctoral thesis

The aim of this thesis was to investigate PKGIα as a novel target of HNO-mediated oxidation. Key findings of this work have been published recently (Donzelli, Goetz et al. 2017).

6 Materials and methods

6.1 Materials

6.1.1 Chemicals

Name	Company
Acetic Acid	Merck Millipore (Billerica, USA)
Acetone	Th. Geyer (Renningen, Germany)
Acetonitrile	Th. Geyer (Renningen, Germany)
[y-^{32}P] Adenosine 5'-triphosphate (y-^{32}-ATP)	Hartmann Analytic (Braunschweig, Germany)
2-Amino-2-hydroxymethylpropane-1,3-diol (Tris)	Sigma-Aldrich (St. Louis, USA)
2-Propanol	Merck Millipore (Billerica, USA)
30% Acrylamide/ Bis Solution 37.5:1	Bio-Rad (Hercules, USA)
1,4-Dithiothreitol (DTT)	Roth (Arlesheim, Germany)
Acetic acid (glacial) 100%	Merck Millipore (Billerica, USA)
Adenosine 5'-triphosphate (ATP) 10 mmol/L	Merck Millipore (Billerica, USA)
Ammonium persulfate (APS)	BioRad (Hercules, USA)
Ampicillin trihydrate	SERVA Electrophoresis (Heidelberg, Germany)
Aqua B. Braun	B. Braun Melsungen (Melsungen, Germany)
Bacto™ Agar	BD Biosciences (San Jose, USA)
Bacto™ Tryptone	BD Biosciences (San Jose, USA)

Bacto™ Yeast Extract	BD Biosciences (San Jose, USA)
β-Escin	Sigma-Aldrich (St. Louis, USA)
β-Mercaptoethanol	Sigma-Aldrich (St. Louis, USA)
Bromophenol blue	BioRad (Hercules, USA)
Bovine Serum Albumin (BSA)	Sigma-Aldrich (St. Louis, USA)
$CaCl_2$ (20 mmol/L) 10X	New England BioLabs (Ipswich, USA)
Calcium chloride dihydrate ($CaCl_2 \cdot 2 H_2O$)	Merck (Darmstadt, Germany)
Carbon dioxide (CO_2)	SOL Deutschland (Krefeld, Germany)
cGMP	BIOLOG Life Science Institute (Bremen, Germany)
cOmplete protease inhibitor cocktail tablets	Roche (Basel, Suisse)
Coomassie Blue R250 / G250	Merck Millipore (Billerica, USA)
D(+)-Glucose	Roth (Arlesheim, Germany)
Dulbecco's Modified Eagle Medium (DMEM)	Thermo-Fisher Scientific (Waltham, USA)
Ethylene glycol bis-(β-aminoethyl ether) N,N,N′,N′-tetraacetic acid (EGTA)	Sigma-Aldrich (St. Louis, USA)
Ethylenediaminetetraacetic acid (EDTA) disodium salt dihydrate	Roth (Arlesheim, Germany)
Enhanced Chemiluminescence (ECL)	GE Healthcare (Chicago, USA)
Ethanol Absolute P. A., Reag. Ph. Eur. (Min. 99.9 %)	Th. Geyer GmbH & Co. KG (Höxter-Stahle, Germany)

Fentanyl	Janssen CILAG GmbH (Neuss, Germany)
Glycerol solution	Sigma-Aldrich (St. Louis, USA)
Guanosine 3',5'-[8-3H] cyclic monophosphate	American Radiolabeled Chemicals, Inc. (St. Louis, USA)
Glycine PUFFERAN®	Roth (Arlesheim, Germany)
HEPES PUFFERAN®	Roth (Arlesheim, Germany)
Hydrochloric acid (HCl) fuming 37%	Merck Millipore (Billerica, USA)
Lipofectamine	Thermo-Fisher Scientific (Waltham, USA)
Magnesium chloride hexahydrate ($MgCl_2 \cdot 6H_2O$)	Sigma-Aldrich (St. Louis, USA)
Magnesium sulfate heptahydrate ($MgSO_4 \cdot 7\ H_2O$)	Merck (Darmstadt, Germany)
Maleimide	Sigma-Aldrich (St. Louis, USA)
Medetomidine	Pfizer GmbH (Berlin, Germany)
Methanol	Avantor Performance Materials (Center Valley, USA)
Midazolame	Hameln Pharmaceutics GmbH (Hameln, Germany)
N,N,N',N'-Tetramethylethylendiamine (TEMED)	Bio-Rad (Hercules, USA)
Nitrogen (N_2), liquid	SOL Deutschland (Krefeld, Germany)
PD Minitrap™ G-25 column, GE28-9180-07	GE Healthcare (Chicago, USA)

Potassium chloride (KCl)	Merck (Darmstadt, Germany)
Potassium dihydrogen phosphate (KH_2PO_4)	Merck (Darmstadt, Germany)
Powdered milk	Carl Roth (Arlesheim, Germany)
ProtoGel® acrylamide solution	Thermo-Fisher Scientific (Waltham, USA)
Sodium chloride (NaCl)	Avantor Performance Materials (Center Valley, USA)
Sodium dodecyl sulfate (SDS) pellets	Carl Roth (Arlesheim, Germany)
Sodium fluoride (NaF)	Sigma-Aldrich (St. Louis, USA)
Sodium hydrogen carbonate ($NaHCO_3$)	Merck Millipore (Billerica, USA)
Sodium hydroxide (NaOH) solution 0.1 mol/L	Carl Roth (Arlesheim, Germany)
Tris(2-carboxyethyl)phosphine hydrochloride (TCEP)	Sigma-Aldrich (St. Louis, USA)
Trizma®-base	Sigma-Aldrich (St. Louis, USA)
TurboFect Transfection Reagent	Thermo-Fisher Scientific (Waltham, USA)
Tween® 20	Sigma-Aldrich (St. Louis, USA)

6.1.2 Buffers and solutions

Name	**Ingredients**	**Concentration**
Coomassie Brilliant Blue stain solution	Coomassie Blue R250 Acetic acid Methanol	0,25 % (w/v) 10% (v/v) 45% (v/v)

Denaturing alkylation buffer (DAB) buffer	Urea Tris-HCl pH 8 EDTA SDS	6 mol/L 200 mmol/L 10 mmol/L 0.5% (w/v)
Extraction buffer	Tris pH 7.4 NaCl EDTA EGTA NaF Protease inhibitor	20 mmol/L 150 mmol/L 1 mmol/L 1 mmol/L 2 mmol/L
FRET imaging buffer (FRET buffer)	NaCl KCl $MgCl_2$ Ca_2Cl HEPES pH 7.3 NaOH	140 mmol/L 5 mmol/L 1.2 mmol/L 2 mmol/L 5 mmol/L
HEK-medium	DMEM medium D(+)-glucose FCS L-glutamine Penicillin Streptomycin	 4.5 g/l 10 % 2 mmol/L 100 U/ml 100 µg/ml
HEK-Typsin/EDTA	Trypsin EDTA x 4Na in Hank's B.S.S.	0.5 g/l 0.2g/l
Intracellular-like medium (ICM)	HEPES KCl NaCl EGTA	10 mmol/L 125 mmol/L 19 mmol/L 1 mmol/L

	$CaCl_2$ pH 7.3 KOH	0.33 mmol/L
Intravital microscopy buffer	NaCl KCl $CaCl_2$ $MgSO_4$ $NaHCO_3$ KH_2PO_4 pH 7.4 by gassing with 5% CO_2 in N_2	118.4 mmol/L 3.8 mmol/L 2.5 mmol/L 1.2 mmol/L 20 mmol/L 1.2 mmol/L
In vitro kinase assay buffer	Tris pH 7.4 $MgCl_2$	30 mmol/L 15 mmol/L
Lysis buffer	Tris pH 7.4 NaCl EDTA NaF cOmplete protease inhibitor cocktail	20 mmol/L 150 mmol/L 1 mmol/L 2 mmol/L 1 tablet
Semi-dry transfer buffer	Glycine Methanol SDS Tris pH 8.3	0.29 % (w/v) 20% (v/v) 0.037 (w/v) 0.58 (w/v)
SDS-PAGE electrophoresis buffer	Glycine SDS Tris	1.44 % (w/v) 0.1 % (w/v) 0.3 % (w/v)
4 x SDS-PAGE running gel buffer	SDS Tris pH 8.7	0.4 % (w/v) 18.2 % (w/v)

4 x SDS-PAGE stacking gel buffer	SDS Tris pH 6.8	0.4 % (w/v) 6 % (w/v)
Tris pH 7.4	Tris	1 M
TTBS	Sodium chloride Tween 20 Tris pH 7.6	0,8 % (w/v) 0.1 % (v/v) 0.058 % (w/v)
TBS (x10)	TRIS base NaCl ddH2O	48.4g 160g 2000ml

6.1.3 Instruments

Name	**Company**
Accu-jet® pipette controller	BRAND (Wertheim, Germany)
AttofluorTM Cell Chamber, for microscopy	Thermo-Fisher Scientific (Waltham, USA)
Autoclave VARIOKLAV®	Sartorius (Göttingen, Germany)
Axiocam 105 digital camera	Carl Zeiss (Oberkochen, Germany)
Benchtop incubator WS 60	JULABO (Seelbach, Germany)
Bioruptor® Plus sonication device	Diagenode (Liège, Belgium)
Centrifuge 5415D	Eppendorf (Hamburg, Germany)
Centrifuge 5415R	Eppendorf (Hamburg, Germany)
CO_2 incubator HeraCell™ 240	Thermo Fisher Scientific (Waltham, USA)
DMI3000b inverted microscope with 40x objective	Leica Camera (Wetzlar, Germany)
Dry block heater Thermostat 5320	Eppendorf (Hamburg, Germany)

DV2 DualView emission splitting system	Photometrics (Tucson, USA)
Eclipse E600 optical microscope	Nikon (Minato, Japan)
ECL Semi-Dry Transfer Unit TE 77	GE Healthcare (Chicago, USA)
Electrophoresis chamber Mini-PROTEAN® 3 / Tetra Cell	Bio-Rad (Hercules, USA)
Electrophoresis chamber Sub-Cell® GT	Bio-Rad (Hercules, USA)
Eppendorf Reference® / Eppendorf Research® pipettes	Eppendorf (Hamburg, Germany)
Gel dryer Model 583	Bio-Rad (Hercules, USA)
Heat block Dri-Block® DB-1	Techne (Staffordshire, UK)
Inclined orbital shaker Polymax (2040)	Heidolph Instruments (Schwabach, Germany)
Incubator Shaker C25	Eppendorf (Hamburg, Germany)
Injection syringe 25 µL	Hamilton (Reno, USA)
Light source pE-100 (440 nm)	CoolLED (Andover, UK)
LTQ Orbitrap mass spectrometer	Thermo Fisher Scientific (Waltham, USA)
MICROMAN® pipettes	Gilson (Middleton, USA)
Mini-PROTEAN® Comb, 10- / 15-well	BioRad (Hercules, USA)
Mini Rocker Shaker MR-1	Biosan (Riga, Lativa)
Mini-Shaker Model Kühner	B. Braun Melsungen (Melsungen, Germany)

Multi-wire myograph system - 620M	Danish Myo Technology A/S (Hinnerup, Denmark)
optiMOS™ Camera	QImaging (Surrey, Canada)
Packard Tri-Carb Liquid Scintillation counter	Packard Instrument Company (Illinois, USA)
pH Meter, digital	Mettler Toledo (Columbus, USA)
PIPETMAN® pipettes	Gilson (Middleton, USA)
Pipetus®-akku	Hirschmann Laborgeräte (Eberstadt, Germany)
PowerPac Bacic Power Supply	BioRad (Hercules, USA)
Power source EC570-90	E-C Apparatus Corporation (St. Petersburg, USA)
Precision balance Pioneer®	OHAUS (Parsippany, USA)
Rotating mixer RM 5	Ingenieurbüro CAT (Ballrechten-Dottingen, Germany)
Scanner CanoScan LiDE 60	Canon (Tokyo, Japan)
Short Plate / Spacer Plate for Mini-PROTEAN®	Web Scientific (Cheshire, UK) / Bio-Rad (Hercules, USA)
Spectrophotometer NanoDrop ND-1000	Thermo Fisher Scientific (Waltham, USA)
Spectrophotometer SmartSpecTM 3000	BioRad (Hercules, USA)
Sterile working bench HeraSafe™ HS 12 class II	Thermo Fisher Scientific (Waltham, USA)

Thermomixer 5436 TissueLyser	Eppendorf (Hamburg, Germany) QIAGEN (Hilden, Germany)
TC Flask	Eppendorf (Hamburg, Germany)
Ultracentrifuge Optima L-90K with rotor SW 32 Ti	Beckman Coulter (Brea, USA)
Vacuum filtration manifold, Millipore® model 1225	Sigma-Aldrich (St. Louis, USA)
MiniVent ventilator	Harvard Apparatus (Holliston, USA)
Vortex shaker	Heidolph Instruments (Schwabach, Germany)
Water purification system Milli-Q	Merck Millipore (Billerica, USA)
Whatman® glass microfiber filters, Grade GF/C	Sigma-Aldrich (St. Louis, USA)
X-ray cassette	Wardray (Surrey, UK)
X-ray cassette 18 x 24 cm	Rego X-Ray (Augsburg, Germany)

6.1.4 Expendable materials

Name	**Company**
AccuMarQ™ Pre-stained Molecular Weight Markers	Badrilla (Leeds, UK)
Amersham™ ECL™ / ECL Select™ Western Blotting Detection Reagents	GE Healthcare (Chicago, USA)

Amersham™ Hybond™ PVDF / Amersham™ Protran™ Nitrocellulose (NC) Blotting Membranes	GE Healthcare (Chicago, USA)
Amersham™ Hyperfilm™ ECL	GE Healthcare (Chicago, USA)
Assistent® Cover glass 25 mm ø	Glaswarenfabrik Karl Hecht (Sondheim v.a. Rhön, Germany)
Assistent® Elka object slide	Glaswarenfabrik Karl Hecht (Sondheim v.a. Rhön, Germany)
Cell scraper 2-position blade	Sarstedt (Nürnbrecht, Germany)
CELLSTAR® 6 well cell culture plate Comply™ Lead Free Steam Indicator Tape	Greiner Bio-One (Frickenhausen, Germany) 3M Deutschland (Neuss, Germany)
Cuvette Disposable pipette	Sarstedt (Nürnbrecht, Germany) Sarstedt (Nümbrecht, Germany)
DMEM (high glucose)	Thermo-Fisher Scientific (Waltham, USA)
Ethanol 96%	Roth (Arlesheim, Germany)
Fuchs Rosenthal Counting Chamber	Brand (Wertheim, Germany)
Gibco® Dulbecco's phosphate-buffered saline (DPBS), no calcium, no magnesium	Thermo-Fisher Scientific (Waltham, USA)
Gibco® Fetal Bovine Serum	Thermo-Fisher Scientific (Waltham, USA)
Gibco® Medium 199 (1x), Hanks' Balanced Salts	Thermo-Fisher Scientific (Waltham, USA)

Gibco® Penicillin-Streptomycin	Thermo-Fisher Scientific (Waltham, USA)
Latex gloves powder-free	VWR International (Radnor, USA)
MICROMAN® Capillaries and Pistons	Gilson (Middleton, USA)
Nitrile Examination Gloves	Ansell (Iselin, USA)
Parafilm	Pechiney Plastic Packaging (Chicago, USA)
Pierce® Protein-Free T20 (TBS) Blocking Buffer	Thermo-Fisher Scientific (Waltham, USA)
Pipette tips 10, 200, 1000 µL	Sarstedt (Nümbrecht, Germany)
Precision Plus Protein™ All Blue / Dual Color Standards	Bio-Rad (Hercules, USA)
Rapid Fixer / Developer for medical X-ray film processing	Agfa (Mortsel, Belgium)
Reaction tubes 1.5, 2 mL	Sarstedt (Nümbrecht, Germany)
Serological pipettes 1, 2, 5, 10, 25 mL	Sarstedt (Nümbrecht, Germany)
Sterile scalpel blade	C. Bruno Bayha (Tuttlingen, Germany)
Sterile tube	Sarstedt (Nümbrecht, Germany)
Stripette® disposable serological pipette	Corning Incorporated (Corning, USA)
SYPRO™ Ruby protein gel stain	Thermo-Fisher Scientific (Waltham, USA)
Tapira® cleansing tissue	GVS-GROSSVERBRAUCHERSPEZIALISTEN (Friedewald, Germany)

Test tubes 15, 50 mL	Greiner Bio-One (Frickenhausen, Germany)
Thinwall Polyallomer Tube	Beckman Coulter Life Sciences (Brea, USA)

6.1.5 Kits

Name	Company
Cleavable iCAT Reagent – Assay Kit	SCIEX (Framingham, USA)
HiSpeed® Plasmid Maxi Kit	QIAGEN (Hilden, Germany)

6.1.6 Enzymes

Name	Origin	Company
Difco™ Trypsin 250	n/a	BD Biosciences (San Jose, USA)
PKGIα	Bovine lung	Merck Millipore (Billerica, USA)

6.1.7 Reagents for the treatment of cells and animal studies as well as *in vitro* assays

Substance	Solvent	Company
1-Nitrosocyclohexyl acetate (NCA)	DMSO	Axon Medchem (Groningen, Netherlands)
3-Isobutyl-1-methylxanthine (IBMX)	DMSO	Santa Cruz (Dallas, USA)
Angeli's salt (AS)	10 mmol/L NaOH	Cayman Chemicals (Ann Arbor, USA)
Dimethyl sulfoxide (DMSO)	-	Sigma-Aldrich (St. Louis, USA)
Forskolin (FOR)	DMSO	Sigma-Aldrich (St. Louis, USA)

Hydrogen peroxide (H_2O_2) solution 30% (w/w) in H_2O	H_2O	Sigma-Aldrich (St. Louis, USA)
1H-[1,2,4]-oxadiazolo-[4,3-a]-quinoxalin-1-one (ODQ)	DMSO	Cayman Chemicals (Ann Arbor, USA)

6.1.8 Antibodies

6.1.8.1 Primary antibodies for Western immunoblotting

Name	Company	Host	Working Dilution
Anti-PKGI, polyclonal	Enzo Life Sciences (Farmingdale, USA)	Rabbit	1:1000, in 1% milk / TBST
Anti-pVASP, polyclonal	Cell Signaling Technology (Danvers, USA)	Rabbit	1:1000, in 5% BSA/TBST

6.1.8.2 Secondary labelling antibodies and reagents for Western immunoblotting

Name	Company	Host	Working Dilution
ECL™ Anti-rabbit IgG, HRP linked whole antibody	GE Healthcare (Chicago, USA)	Sheep	1:2000, in 5% BSA/TBST or 1% milk/TBST (depending on the primary antibody dilution)

6.1.9 Cells

Name	Company
HEK293A	Thermo-Fisher Scientific (Waltham, USA)

HEK293T	Thermo-Fisher Scientific (Waltham, USA)

6.1.10 Plasmids

Name	Supplier
AKARIII	Kind gift of VO Nikolaev (University Medical Center Hamburg-Eppendorf, Germany)
pcDNA-PKGIα-WT	Kind gift of P. Eaton (King's College London, UK)
pcDNA-PKGIα-C42S	Kind gift of P. Eaton (King's College London, UK)
pcDNA-PKGIα-C117/195S	Kind gift of P. Eaton (King's College London, UK)
pcDNA-PKGIα-C42/117/195S	Kind gift of P. Eaton (King's College London, UK)

6.1.11 Bacteria

E.coli strain	Company
Subcloning Efficiency™ DH5α™	Thermo-Fisher Scientific (Waltham, USA)

6.1.12 Software

Name	Company
CanonScan Toolbox	Canon (Tokyo, Japan)
GelQuant.NET	BiochemLabSolutions.com (San Francisco, USA)

ImageJ with Fiji (version 1.5.1) and µManager (version 1.4.5)	Wayne Rasband, National Institutes of Health (Bethesda, USA)
MaxQuant	Max Planck Institute of Biochemistry (Munich, Germany)
NanoDrop® 1000 3.8.1	Thermo-Fisher Scientific (Waltham, USA)
Prism 5	GraphPad Software (La Jolla, USA)
SwissProt Database	Swiss Institute of Bioinformatics (Geneva, Switzerland)
Word, PowerPoint, Excel	Microsoft (Redmond, USA)

6.2 Methods

The experiments were performed in the working group of Prof. Dr. Friederike Cuello in the Institute of Experimental Pharmacology and Toxicology at the University Medical Center Hamburg-Eppendorf. All methods were carried out in accordance with the relevant guidelines and regulations. Experiments were approved by the relevant institutional or licensing committees as indicated in the relevant section.

6.2.1 Animal experiments

6.2.1.1 Ethical standards

Wire myography measurements were conducted in accordance with the Home Office Guidance on the Operation of the Animals (Scientific Procedures) Act 1986 in United Kingdom and approved by an institutional review committee. Intravital microscopy was performed in accordance with the German animal protection law and approved by the *Ministerium für Energiewende, Landwirtschaft, Umwelt und ländliche Räume* of Schleswig-Holstein. The isolation of primary mouse VSMCs from cGi500 transgenic mice was approved by the *Regierungspräsidium Tübingen* in compliance with the humane care and use of laboratory animals. All

animals were kept on a conventional laboratory diet and unlimited supply of municipal drinking water.

6.2.1.2 Wire myography

2nd and 3rd order mesenteric arteries were isolated from male WT C57BL/6 mice and subjected to wire myography measurements as described previously (Prysyazhna et al. 2012).

Third-order mesenteric arteries were mounted for isometric tension recordings on a wire myograph (Danish Myo Technology A/S), stretched to the optimal pre-tension conditions (using DMT Normalization Module), bathed in Krebs solution, maintained at 37°C and gassed with 95% O_2: 5% CO_2. Vasotone measurements of mesenteric arteries were assessed by determining the responses of U46619-pre-constricted vessels to the HNO donors AS (0-100 µmol/L) or NCA (0-100 µmol/L). The concentration-response curves to HNO donors were constructed in a cumulative fashion. Tension experiments were carried out using one or two vessels per animal from 4 different WT animals.

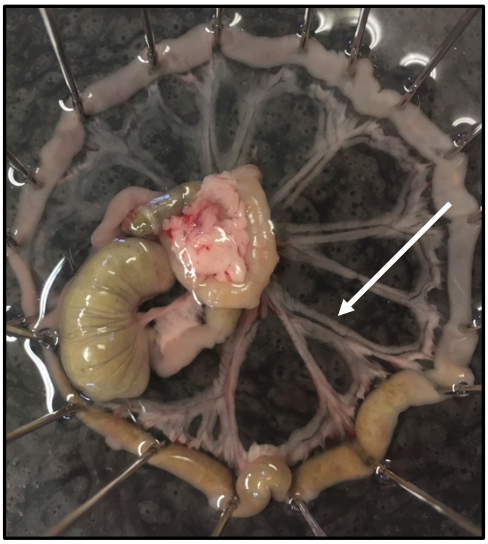

Figure 5: Preparation of the murine gastrointestinal tract. The mesenteric vessels (veins and arteries) are indicated by the white arrow.

6.2.1.3 Intravital microscopy

12-week-old male C57BL/6NCrl mice (Charles River) were used to study microvascular networks *in vivo* in the cremaster muscle using intravital microscopy as described previously (de Wit et al. 1993). Mice were anaesthetised with fentanyl (0.05 mg/kg), midazolame (5 mg/kg), and medetomidine (0.5 mg/kg) by intraperitoneal injection. After intraperitoneal injection of a first bolus of the anaesthetics, the mouse was tracheotomised to secure the respiration via a MiniVent ventilator (MiniVent, Harvard Apparatus). The animals were ventilated with a stroke volume of 0.225 mL at 160 strokes per min. In a second step, a central venous catheter was inserted into the right jugular vein for the maintenance of the anaesthesia. Next, the thin and highly vascularised cremaster muscle was prepared for intravital microscopy to study vascular responses: the right muscle was opened, detached from the testicle and spread radially as a flat sheet over a cover slip for transillumination under a compound microscope. The arteries were constantly superfused with a 35 °C prewarmed intravital microscopy buffer. In each mouse, 7 to 18 arterioles were studied using an optical microscope (Eclipse E600, Nikon) and a 20-fold objective. The microscope was equipped with a digital camera (Zeiss Axiocam 105) connected to a PC to allow image storage (Zen2 lite, Zeiss) and subsequent analysis. Arteriolar inner diameters were measured by a code written in the laboratory of Prof. de Wit using the commercially available software (LabVIEW, National Instruments). Arteriolar diameters were assessed before and during application of NCA (10 or 50 µmol/L; group 1) or AS (3 to 50 µmol/L; group 2). The respective solvent (0.1% DMSO for NCA or 0.1 mmol/L NaOH for AS) was also evaluated. To assess vascular reactivity, the effect of acetylcholine (ACh, 10 µmol/L) was also assessed. All substances were added to the superfusion solution using a roller pump and the final concentration reaching the preparation is indicated. After application of each substance, vessels were allowed to recover for 3 to 5 min, to return to their resting diameter. At the end of the experiment, mice were sacrificed by intravenous injection of pentobarbital (24 mg/kg) and both cremaster muscles of each animal were harvested for western immunoblot analysis. While the right cremaster muscle had been exposed to the HNO donors during the experiment, the left

cremaster muscle was prepared immediately after pentobarbital injection and served as the untreated control.

6.2.1.4 FRET-experiments in primary VSMCs

For Förster Resonance Energy Transfer (FRET) measurements, primary VSMCs from R26-CAG-cGi500(L1) mice were isolated (Thunemann et al. 2013b). These cells express the FRET-based biosensor cGi500 (cGMP indicator with an EC_{50} of 500 nmol/L) (Russwurm et al. 2007). VSMCs were continuously superfused with intracellular-like medium (ICM) at room temperature (RT). Cells were permeabilised by superfusion with β-Escin (100 µmol/L in ICM; 80 sec.) and subsequently exposed to ICM supplemented with increasing concentrations of cGMP (0.1, 1, 10 µmol/L; 2 min each). The individual fluorescence of cyan fluorescent protein (CFP) and yellow fluorescent protein (YFP) was recorded simultaneously using a DualView DV2 beam-splitter (Photometrics) and saved as individual TIFF images. After each cGMP application, baseline recovery of the fluorescence signals was achieved before the next drug application. After the initial series of cGMP applications, VSMCs were exposed to DMSO (0.02%; in ICM) or NCA (100 µmol/L in ICM containing 0.02% DMSO) for 30 min followed by superfusion with ICM supplemented with increasing concentrations of cGMP (0.1, 1, 10 µmol/L). Acquired images were analysed using ImageJ with Fiji and µManager and calculated using Microsoft Excel to correct for background fluorescence and the CFP/YFP ratio (R) traces, which reflect FRET changes (Dao et al. 2016). FRET responses were measured as amplitudes over baseline. The individual FRET changes (ΔR) were then normalised to the FRET change induced by the first application of cGMP (10 µmol/L; ΔR0) and are displayed as ΔR/ΔR0. Further details on measurement and evaluation of FRET signals in VSMCs are described elsewhere (Thunemann et al. 2013a, b).

6.2.2 Experiments with purified proteins

6.2.2.1 NOxICAT-Methology

Redox-modified cysteines in PKGIα in response to HNO were identified by a thiol-trapping technique using isotope-coded affinity-tag chemistry (NOxICAT) as

described previously (Lindemann and Leichert 2012). In brief, non-tagged recombinant human PKGIα, prepared as described elsewhere (Scotcher et al. 2016), was pre-treated with DTT (100 mmol/L, 30 min) in an anaerobic chamber to maintain SH-groups in a reduced state. DTT was removed by buffer exchange via passing the sample through a PD MiniTrapTM G-25 column (28-9180-07; GE Healthcare). After buffer exchange, samples were exposed to NCA (25 µmol/L, 15 min), AS (25 µmol/L, 15 min) or vehicle (DMSO) at RT. The reaction was terminated using ice-cold acetone and proteins precipitated overnight at −20 °C. On the next day, the precipitate was resuspended in a volume of 80 µL containing denaturing alkylation buffer (DAB-buffer), 20 µL acetonitrile and 1 vial ICAT reagent "light" from the cleavable ICAT methods development kit (SCIEX). Reduced cysteines were labelled under denaturing conditions at 37 °C in a thermomixer at 1300 rpm for 2 hrs. After a second acetone precipitation step, oxidised cysteines were reduced for 30 min in 80 µL DAB containing 2 mmol/L TCEP. Subsequently, one vial cleavable ICAT reagent "heavy", resuspended in 20 µL acetonitrile, was added and previously oxidised cysteines were labelled at 37 °C at 1300 rpm for 2 hrs. The reaction was stopped by acetone precipitation. The pellet was resuspended in 80 µL denaturing buffer from the cleavable ICAT reagent kit. 20 µL acetonitrile was added to the protein digest with 100 µL aqueous trypsin resuspension from the ICAT reagent kit. ICAT labelled peptides were purified by cation exchanger chromatography and affinity chromatography. Light- and heavy-ICAT-labelled peptides were analysed and quantified by reverse phase nano-liquid chromatography and detected by MS/MS with Fourier transform mass spectrometry in an LTQ Orbitrap instrument (Thermo Fisher Scientific, Waltham, USA). Peptides were identified by SwissProt database and quantified by MaxQuant.

6.2.2.2 ^{3}H-cGMP binding assays

^{3}H-cGMP binding assays were performed using recombinant PKGIα, ^{3}H-labeled cGMP, non-radioactive cGMP and assay buffer. Recombinant PKGIα (0,1 µg/µL) was diluted in assay buffer to a final concentration of 600 fmol/assay. ^{3}H-cGMP (concentration of 1 mCi/ml; specific activity of 25 Ci/mmol) solved in 50% EtOH

was diluted to a final concentration of ~5pmol/ assay in assay buffer, considering that EtOH is able to break the structure of the kinase. Non-radioactive cGMP was diluted in assay buffer with increasing final concentrations (0 nmol/L, 10 nmol/L, 30 nmol/L, 100 nmol/L, 300 nmol/L, 1 µmol/L, 3 µmol/L) to compete with ^{3}H-cGMP. To assay the ability of PKGIα-WT to bind cGMP under oxidising and reducing conditions, the kinase was either pre-treated with NCA (100 µmol/L) for 30 min on ice covered with aluminium foil to oxidise the kinase or pre-treated with DTT (100 mmol/L) for 10 min on ice to reduce the kinase. For each pre-treatment group, 24 samples were prepared in triplicates for each condition: seven different concentrations of non-radioactive cGMP and samples without PKGIα to determine cGMP-binding to the filter. Following the pre-treatment, ^{3}H-cGMP (~5 pmol/ assay) and unlabelled cGMP in the specified different concentrations were added to the assay as well as assay buffer to reach a final volume of 50 µL. Samples were incubated for 1h on ice, covered with aluminium foil and 4 ml of 4°C ice-cold $(NH_4)_2SO_4$ (3.8M) solution were added to each sample to stop the reaction. Samples were subsequently vacuum-filtered over Whatman® glass-microfiber filters previously prewetted in $(NH_4)_2SO_4$ (3.8 mol/L) using the constantly running Millipore vacuum filtration system. Due to the vacuum filtration, the filter papers dried quickly and were then incubated with 2 ml of a 2% SDS solution for 1h in the scintillation vials, dissolving the filter papers and releasing the proteins. 10 ml of Rotiszint® scintillation fluid was added to each vial, followed by intensive shaking to ascertain the formation of a homogenous suspension. The vials were finally counted for 5 min in the Packard scintillation counter using the [^{3}H]-program. With regard to data analysis, 1 µL of diluted ^{3}H-cGMP was counted in 2 ml of 2% SDS in order to allow calculation of the total specific activity of the used volume in each sample and thereby to calculate the concentration of bound ^{3}H-cGMP in each sample. The mean value of counts reached in the samples without PKGIα was subtracted from each count result as a background of cGMP-binding to the filter paper as well as counts reached in samples with cGMP (3 µmol/L) with the assumption that in these samples only unlabelled cGMP should bind to PKGIα.

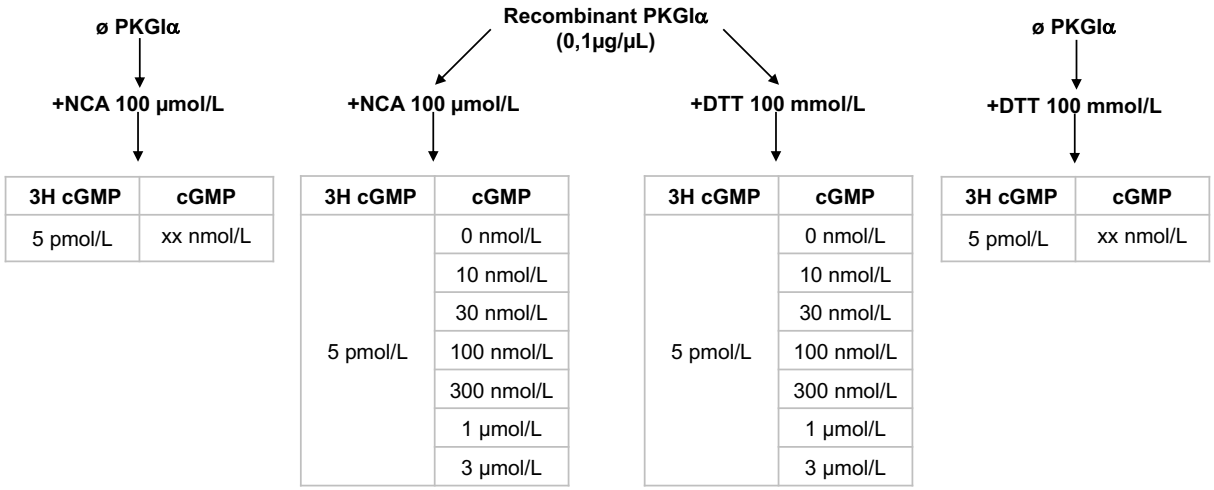

Figure 6: Experimental design of the ^{3}H-cGMP binding assays. Every condition was prepared in triplicates. Thereby, 24 samples were measured in each experiment.

6.2.3 Experiments in cells

6.2.3.1 Cell culture

All work steps were carried out under sterile cell culture conditions in a tissue culture hood. HEK293T and HEK293A cells were cultured at 37°C and 5 % CO_2 in Dulbeccos MEM (DMEM) supplemented with fetal calf serum (FCS; 10%) and penicillin/streptomycin (1%) in cell culture flasks or 6-well plates. HEK293T cells contain the SV40 Large T-antigen that promotes episomal replication and thereby amplification of transfected plasmids containing the SV40 origin of replication and are in general an ideal cell model due to their ease of growth and transfectability (Yuan et al. 2018). Cells were passaged, when they reached 70-80% confluence or when plated into culture multi-well plates. To disrupt adherent cell monolayers, the culture medium was removed, 3 ml of 37°C Trypsin/EDTA were added and cells were incubated for 2-3 min at 37°C. Subsequently, trypsin digestion was stopped by addition of 9 ml of 37°C pre-warmed DMEM, cells were carefully resuspended and transferred into 50 ml centrifuge tubes. After centrifugation for 5 min at 600 xg, the supernatant was aspirated off and the cell pellet resuspended in 10 ml or 20 ml fresh DMEM, as appropriate. Cells were counted using the hemocytometer and an appropriate volume of the cell suspension was aliquoted into freshly prepared cell culture flasks or culture multi-well plates with media.

6.2.3.2 Transformation

The pcDNA-PKGIα-WT plasmid as well as the pcDNA-PKGIα-C42S, the pcDNA-PKGIα-C117/195S and the pcDNA-PKGIα-C42/117/195S plasmid were kindly provided by the working group of Prof. Philip Eaton (King's College London, London, UK). For amplification, plasmids were transformed into competent DH5α bacteria and plasmid DNA extracted with the Plasmid Maxi Kit from QIAGEN. In brief, a bacterial colony was inoculated in 250 ml LB medium with a selective antibiotic for an overnight culture. The bacteria were harvested by centrifugation for 15 min at 6000 xg at 4°C, resuspended in buffer P1, lysed with buffer P2 and the reaction neutralised using buffer P3. The cellular debris was removed using a provided filter cartridge and a plunger and endotoxins were eliminated by adding the provided buffer ER (provided in the Plasmid Maxi Kit). The plasmid DNA was immobilised on a filter, washed with the provided buffer QC and eluted with water at RT. The DNA concentration was determined using NanoDrop®.

6.2.3.3 Transfection

For transfection of HEK293A or HEK293T cells with plasmid DNA, approximately 200 000 cells per well were plated into 6-well plates. After 24 hrs, cells were transfected with a transfection mix either consisting of Opti-MEM (400 µL), plasmid-DNA (2 µg) and TurboFect2000® (6 µL) or for FRET measurements using the A-Kinase activity reporter III (AKARIII)-sensor consisting of Opti-MEM (50 µL), plasmid-DNA (0.5 µg) and Lipofectamin® (1.15 µL) for each well under sterile conditions. When the cells were transfected with a combination of two different plasmids at the same time, the amount of plasmid-DNA was reduced to 1 µg per plasmid-type. After 20 min incubation at RT, the reaction mix was added dropwise to each well. 24 hrs after transfection, cells were used for experiments, such as FRET measurements or *in vitro* PKGIα activity assays. In cells transfected with the vasodilator-stimulated phosphoprotein (VASP)-plasmid, transfection efficiency was monitored by a microscope equipped with a red fluorescent protein (RFP)-filter due to the mCherry-sequence tag in the VASP-plasmid.

6.2.4 Assessing PKG kinase activity

6.2.4.1 VASP-phosphorylation experiments

To investigate the impact of oxidative modification of PKGIα on substrate protein phosphorylation, HEK293T cells were transfected with the mCherry-VASP-plasmid and the PKGIα-WT-plasmid or the various mutants: PKGIα-C42S, PKGIα-C117/195S. After successful transfection, cells were exposed to NCA (100 µmol/L in DMSO), 3MNCA (100 µmol/L in DMSO) or vehicle control (DMSO, 0.1%) for 30 min or exposed to AS (500 µmol/L in 10 mmol/L NaOH) or vehicle control (10 mmol/L NaOH) for 15 min or to H_2O_2 (100 µmol/L) or SperNo (100 µmol/L) for 10 min by adding the compound directly into the medium. Cells were harvested under non-reducing conditions to study oxidative modifications using Laemmli sample buffer (3x) supplemented with maleimide (100 mmol/L) or under reducing conditions to study phosphorylation using Laemmli sample buffer (3x) supplemented with 9% (v/v) β-mercaptoethanol. Prior to gel electrophoresis, non-reducing samples were homogenised, while reducing samples were heated at 95°C for 5 min.

6.2.4.2 Assessment of PKG activity by FRET

FRET measurements were performed as described elsewhere (Sprenger et al. 2012). HEK293A cells were cultured and passaged as described previously in chapter 6.2.3.1. HEK293A cells are known for their flat cell morphology and adhesive properties and were therefore suitable for these experiments (Yuan et al. 2018). For transfection of HEK293A cells with plasmid DNA, cells were plated onto round glass coverslips (ø = 24 mm), which were positioned in 6-well plates. After 24 hrs, when the cells reached 60 % confluency, the transfection mix for each well was prepared under sterile conditions as described in chapter 6.2.3.3. Cells were transfected to express PKGIα-WT or the various PKGIα-mutants, PKGIα-C42S or PKGIα-C117/195S, in combination with the AKARIII-sensor plasmid. To ensure whether the alteration of the FRET response occurs due to changes in PKGI activity and is not due to the activation of other endogenous kinases, cells were also transfected with the AKARIII-sensor alone. 24 hrs after transfection, cells were used for FRET measurements. Coverslips with HEK293A

cells were mounted in the imaging chamber. The cells were washed once with 400 µL of FRET buffer and 400 µL of fresh FRET buffer containing 3% of DMSO were added to the chamber. This step was performed to rule out vehicle effects. NCA (2 mmol/L) diluted in DMSO was stored on ice and prior to treatment diluted in FRET buffer. In the chamber, a final concentration of NCA of 30 µmol/L in 3% DMSO was achieved. FRET measurements were performed using an inverted fluorescent microscope equipped with ImageJ software. CFP, the FRET donor, was excited at 440 nm using a CoolLED single-wavelength light emitting diode. The emitted light from the sample was split into CFP and YFP signals using a dual view and detected via a CCD camera. Cells with optimal sensor expression were selected using live fluorescent light, which was switched off immediately after finding an appropriate cell to avoid photobleaching of the FRET sensor. An exposure time of 2-5 msec was commonly sufficient to yield an optimal signal-to-noise ratio and images were acquired in CFP and YFP emission channels every 5 sec. After a stable baseline of around 100 sec was reached, NCA (100 µmol/L; in FRET buffer) was added into the chamber. After approximately 500 sec, the FRET trace reached a plateau and 400 µL of FRET buffer with Forskolin (50 mmol/L) and IBMX (100 mmol/L) were added into the chamber to induce maximal activity of the sensor. FRET signals were continuously recorded, until a stable plateau was reached. FRET imaging data were analysed offline. The single CFP and YFP intensities from each cell were measured using ImageJ and copied into an Excel spreadsheet to calculate the corrected FRET ratio YFP/CFP. FRET measurements were routinely corrected for the bleed-through of the donor fluorescence (CFP) into the acceptor (YFP) channel. Cells, which showed a negative ratio were excluded.

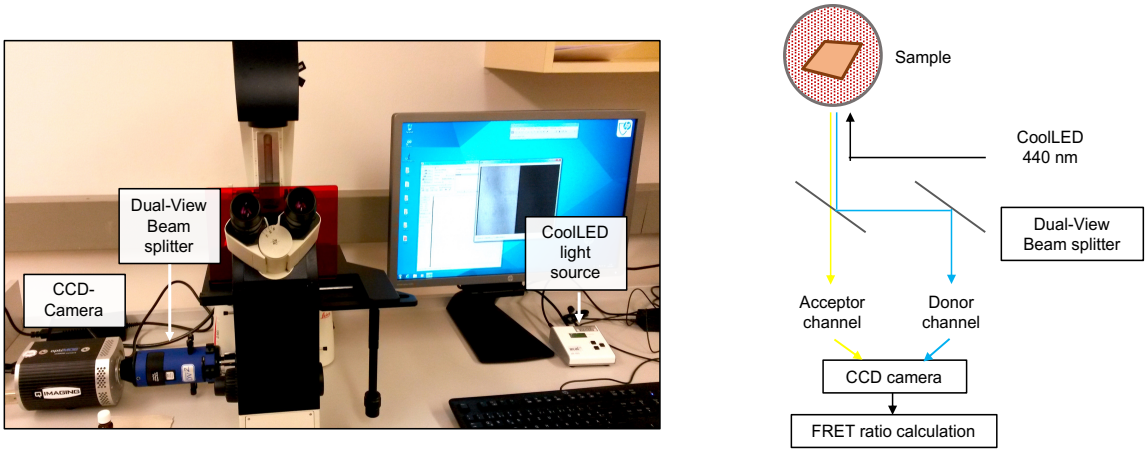

Figure 7: FRET microscope setup. The Cool LED light source is used for CFP excitation at 440 nm. The Dual View splits the emitted sample fluorescence into an acceptor channel (YFP) and a donor channel (CFP). Both signals are detected via a CCD camera and transferred to a computer that calculates the FRET ratio using ImageJ software (adapted from Sprenger et al. 2012).

6.2.4.3 *In vitro* PKGIα activity assay using a recombinant substrate

Kinase activity was investigated by assessing phosphorylation of recombinantly expressed His_6-tagged C1-M-C2 domain of cardiac myosin-binding protein C, which is an established substrate of PKG (amino acid residues 153-450) in the presence of radiolabelled γ^{32}P-ATP (GE Healthcare) (Thoonen et al. 2015; Stathopoulou et al. 2016). HEK-293T cells transfected with PKGIα-WT, PKGIα-C42S, PKGIα-C117/195S, or PKGIα-C42/117/195S were exposed to NCA (100 µmol/L, 30 min), AS (500 µmol/L, 15 min) or vehicle (NaOH for AS; DMSO for NCA) and harvested in lysis buffer. Afterwards, the samples were diluted 1:1 in *in vitro* kinase assay buffer containing ATP (100 µmol/L final concentration and spiked with γ^{32} P-ATP). The *in vitro* kinase reaction was initiated by addition of His_6-tagged C1-M-C2 (500 pmol/reaction), pre-bound to Ni-NTA agarose beads, prior equilibrated in *in vitro* kinase assay buffer. The samples were incubated for 30 min at 30 °C and 1300 rpm, followed by centrifugation for 1 min at 1000 xg. The supernatant was discarded and the agarose beads resuspended in 75 µL 3x reducing Laemmli sample buffer. Samples were heated for 5 min at 75 °C and proteins resolved by 10% SDS-PAGE. Gels were stained with Colloidal Coomassie stain to assure equal substrate content between samples, destained in 20% (v/v) methanol, incubated briefly in 20% (v/v) glycerol in water and

vacuum-dried. Experiments were analysed by autoradiography. Densitometry was subsequently performed using GelQuant NET software provided by biochemlabsolutions.com and normalised to the substrate signal obtained by Coomassie staining.

6.2.5 SDS-PAGE

Sodium dodecyl sulfate polyacrylamide gel electrophoresis (SDS-PAGE) is an analytical gelelectrophoresis method that allows the separation of proteins according to their molecular mass independently of their charge. Discontinuous gels, composed of a stacking and a running gel, were used. Electrophoresis gels with 10 or 15 wells and thickness of 1.0 mm were produced immediately before use. Running gels consisted of 7.5% acrylamide to detect PKGIα or of 10.5% acrylamide to detect VASP or C1-M-C2. Stacking gels consisted of 6% acrylamide. APS and TEMED were used to initiate polymerization of the gels. 5 µl of prestained Precision Plus Protein^{TM} Standards from BioRad Laboratories were used to estimate the molecular mass of proteins in gels. Gels were run at constant voltage of 200 V in electrophoresis chambers containing electrophoresis buffer.

Table 1: SDS-PAGE tris-glycine gel compositions.

Reagent	**Stacking gel (ml)**	**Resolving gel (ml)**	
		7.5%	**10.5%**
Stacking buffer (4x)	2.5	-	-
Resolving buffer (4x)	-	2.5	2.5
Acrylamide solution	1.16	2.5	3.5
H_2O	6.23	4.89	3.89
10% APS	0.1	0.1	0.1
TEMED	0.01	0.01	0.01
Final volume	10	10	10

6.2.5.1 Western Blotting by semi-dry transfer

Western Blotting was performed to transfer proteins, which were separated using SDS-PAGE, onto polyvinylidene fluoride (PVDF) or nitrocellulose, which was then used for immunodetection of the proteins of interest.

PVDF membranes with a size of 8.5 cm x 5.5 cm were activated in methanol for 20 sec and then incubated in transfer buffer until use. Nitrocellulose membranes were cut in a similar size and were only immersed in transfer buffer. Subsequently, a symmetric blotting sandwich was assembled containing per gel 6 buffer-soaked filter papers, a PVDF or nitrocellulose membrane and the gel. The membranes faced the anode-side of the blotting machine, since the negatively charged proteins migrate to the anode. Transfer was run for 2 hrs at constant current of 45 mA per membrane.

6.2.5.2 Immunoblotting

After protein transfer, the membranes were incubated in 10% (w/v) non-fat milk or 5% BSA in TTBS for 30 min to block unspecific binding sites. Subsequently, the membranes were incubated in primary antibodies prepared in 1% non-fat milk or 5% BSA in TTBS at 4°C overnight under rotation and afterwards washed 3 times with TTBS for 10 min to remove unbound antibodies, before incubating in the secondary antibody (goat anti-rabbit or goat anti-mouse) prepared in 1% non-fat milk or 5% BSA in TTBS solution for 1 h at RT. The secondary antibodies are conjugated to HRP and specifically interact with the respective primary antibodies.

After three additional washing steps, each membrane was incubated in 2 ml of Amersham Enhanced Chemiluminescence (ECL) reagent for 2 min.

In this step, the luminol contained in the ECL reagent becomes oxidised via catalysis by HRP and H_2O_2 under alkaline conditions, producing light as a by-product. The presence of p-iodophenol increases the HRP turnover rate and thereby enhances the light emission up to 1000-fold. The intensity of the emitted light is a result of the number of the reacting enzymes, thus proportional to the amount of bound antibody and therefore directly related to the amount of the detected protein on the blot. The emitted light is detected as a signal when

exposing the blots to autoradiography films (Amersham Hyperfilm^{TM} MP), which are then processed in developer and fixer photographic solutions. Immunoblots were analysed using the GeneTools software (Syngene, Cambridge, UK).

6.2.5.3 Coomassie Brilliant Blue staining

PVDF membranes were stained with the Coomassie Brilliant Blue stain, a triphenylmethane dye that attaches to alkaline amino acids, for 1-2 hrs and afterwards destained with Coomassie destaining solution, where appropriate, to control for equal protein loading.

6.2.6 Statistics

Differences between experimental groups during the FRET-recordings using AKARIII were analysed using Student's *t*-test, differences between more than two groups were analysed using one-way ANOVA followed by Bonferroni‟s post-hoc test as appropriate at the significance level of 0.05. Other statistical comparisons were performed by one-way ANOVA (*in vitro* kinase assays with HEK293T lysates) or two-way ANOVA *(*FRET analysis using cGi500) followed by Bonferroni's multiple comparisons test; Student's *t*-test comparing samples with the same cGMP concentration (cGMP-binding assays). Arteriolar diameter changes were normalised to the respective maximal possible response:

$$\% \text{ of maximal response} = (D_{Subst} - D_{Con})/(D_{Max} - D_{Con}) \times 100$$

where D_{Subst} is the diameter in the presence of the substance, D_{Con} the control diameter before application and D_{Max} the respective maximal diameter observed for each vessel during the experiment. Data within groups were compared using paired *t*-test and corrected according to Bonferroni for multiple comparisons. Quantitative data are given as mean ± S.E.M and a value of $P < 0.05$ was considered significant.

7 Results

7.1 HNO induces vasorelaxation in isolated murine mesenteric arteries

Mesenteric arteries are key to blood pressure regulation and contribute to a large extent to the total peripheral resistance (Christensen and Mulvany 1993). They arise from the aorta and supply the intestine with oxygen and nutrients. To confirm vasorelaxation in response to HNO donors, vasotone measurements were performed *in vitro* using isolated murine mesenteric arteries. Third-order mesenteric arteries from WT male mice on a C57BL/6 genetic background were isolated and subjected to wire myography measurements. Prior to vasotone measurements, arteries were pre-constricted with the thromboxane A2 receptor agonist U-46619 (100 nmol/L). The concentration-response curves to both HNO donors, namely the short-lasting agent AS and the longer-lasting agent NCA, were constructed in a cumulative fashion. In mesenteric arteries, AS induced concentration-dependent vasorelaxation with an EC_{50} of 0.44 µmol/L (EC_{50} 0.44 µmol/L ± 0.6 µmol/L; 1-2 vessels per mouse from 4 mice) (**Figure 8A**). Similarly, NCA was able to dilate isolated mesenteric arteries with an EC_{50} of 2.96 µmol/L (EC_{50} 2.96 ± 0.47 µmol/L; 1-2 vessels per mouse from 4 mice) (**Figure 8B**). Subsequently, western immunoblot analysis was performed in homogenates from mesenteric arteries under non-reducing conditions, using a PKGIα-antibody. The PKGIα monomer was detectable at 75 kDa, the PKGIα interdisulfide dimer at 150 kDa. Representative immunoblots revealed that both HNO donors enhanced interprotein disulfide formation in homogenates from WT mesenteric arteries (**Figure 8C**). The band corresponding to the interdisulfide dimer was absent under reducing western blotting conditions and thereby proving the oxidative character of this modification. Interestingly, the antibody detected additional bands, which migrated below the monomer in samples treated with AS and below the interdisulfide dimer band in samples treated with NCA. Due to the observation that these bands were also only detectable under non-reducing western blotting conditions, it was likely to hypothesize that they represented oxidative modifications of other cysteines in PKGIα. Interestingly, in the literature, intradisulfide formation in PKGIα had been reported previously (Landgraf et al. 1991; Eaton 2006).

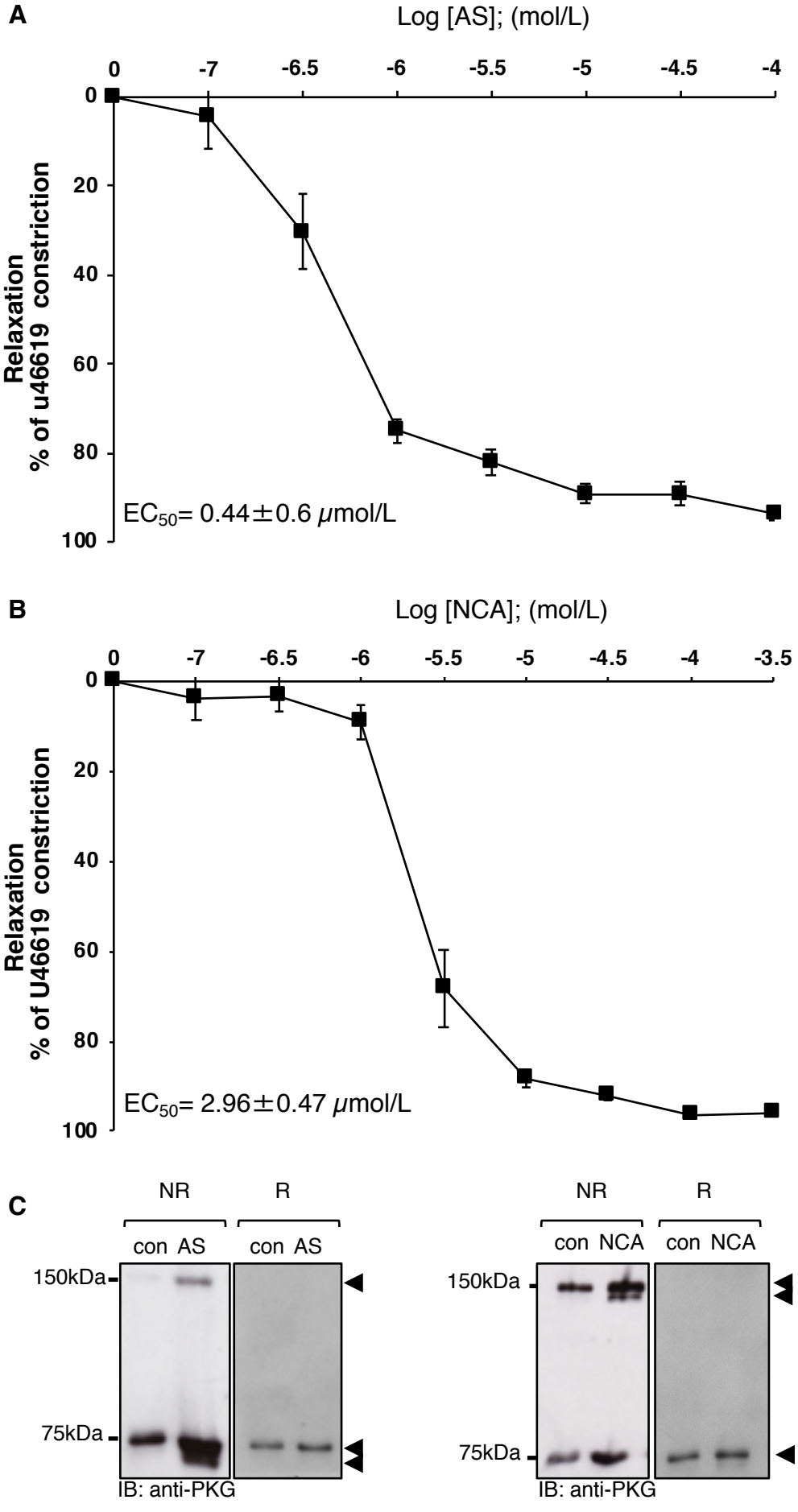
A
Log [AS]; (mol/L)
0
-7
-6.5
-6
-5.5
-5
-4.5
-4
Relaxation
% of u46619 constriction
0
20
40
60
80
100
EC50= 0.44±0.6 μmol/L
B
Log [NCA]; (mol/L)
0
-7
-6.5
-6
-5.5
-5
-4.5
-4
-3.5
Relaxation
% of U46619 constriction
0
20
40
60
80
100
EC50= 2.96±0.47 μmol/L
C
NR
R
con AS
con AS
150kDa
75kDa
IB: anti-PKG
NR
R
con NCA
con NCA
150kDa
75kDa
IB: anti-PKG

Figure 8: HNO-mediated vasorelaxation in murine mesenteric arteries *in vitro.* The effect of AS (A) or NCA (B) on vasorelaxation was assessed in isolated mesenteric arteries from WT mice. U46619 (100 nmol/L) was used to preconstrict vessels. Subsequently, increasing concentrations of NCA (0.1, 0.3, 1, 3, 10, 30, 100, 300 µmol/L) or AS (0.1, 0.3, 1, 3, 10, 30, 100 µmol/L) were administered. Experiments were performed in 1-2 vessels obtained from at least 4 animals for each HNO donor. Immunoblot analysis for PKGIα was performed under reducing (R) or non-reducing (NR) conditions to correlate kinase conformation in response to HNO donors AS and NCA in endogenous PKGIα with alterations in vascular tone. The vessels, which were used for immunoblotting were exposed to NCA (30 µmol/L for 30 min) or AS (3 µmol/L for 15 min) (adapted from Donzelli, Goetz et al. 2017).

7.2 NOxICAT analysis reveals cysteine oxidation in response to HNO donors in PKGIα

To identify redox-modified cysteines in recombinant human PKGIα, the NOxICAT methodology was combined with HNO application in collaboration with Prof. Leichert (Lindemann and Leichert 2012). These experiments were predominantly performed by Dr. Sonia Donzelli and were an essential milestone in this dissertation project. The method allowed to differentiate between reduced and HNO-oxidised cysteinyl thiol residues via selective labelling with light or heavy ICAT isotopes and subsequent analysis by mass spectrometry. Thereby, this method also allowed a quantitative as well as a qualitative analysis of cysteine oxidation.

In these experiments, pre-treatment with the reducing agent DTT was crucial, otherwise recombinant PKGIα would have been completely oxidised by air. Therefore prior to the start of the experiment, recombinant PKGIα was exposed to various DTT concentrations to ascertain that the majority of the kinase was in its reduced state, before HNO-mediated oxidation was performed in an anaerobic environment. PKGIα contains 11 cysteines. Amongst the cysteines that were found oxidised by HNO exposure, was C42 as expected (**Figure 9**). Surprisingly, C117 and C195 were also found to be modified after exposure to HNO.

Despite DTT-prereduction, C42 was already partially oxidised under basal conditions, before the treatment with the HNO donors, whilst C117 and C195 were predominantly found in their reduced state. This demonstrates that C42 is

highly susceptible to oxidative modification. In response to the HNO donor AS, C42 was completely oxidised. C117 as well as C195 were half-maximally oxidised, however, to a similar extent. In response to the HNO donor NCA, C42 as well as C117 and C195 were found to be completely oxidised. The oxidative modification of C42 in response to both HNO donors was in accordance with the previously described interdisulfide bond forming between two PKGIα monomers (Burgoyne et al. 2007). Recapitulating the similar extent of oxidation of C117 and C195, it was likely to hypothesise that these two cysteines might form an intradisulfide bond. Also, the existence of such an intradisulfide bond had been demonstrated previously by the analysis of the crystal structure (Osborne et al. 2011). As the oxidative modification particularly of C117 and C195 was more pronounced in response to NCA-treatment, further experiments focused predominantly on the experimental HNO donor NCA.

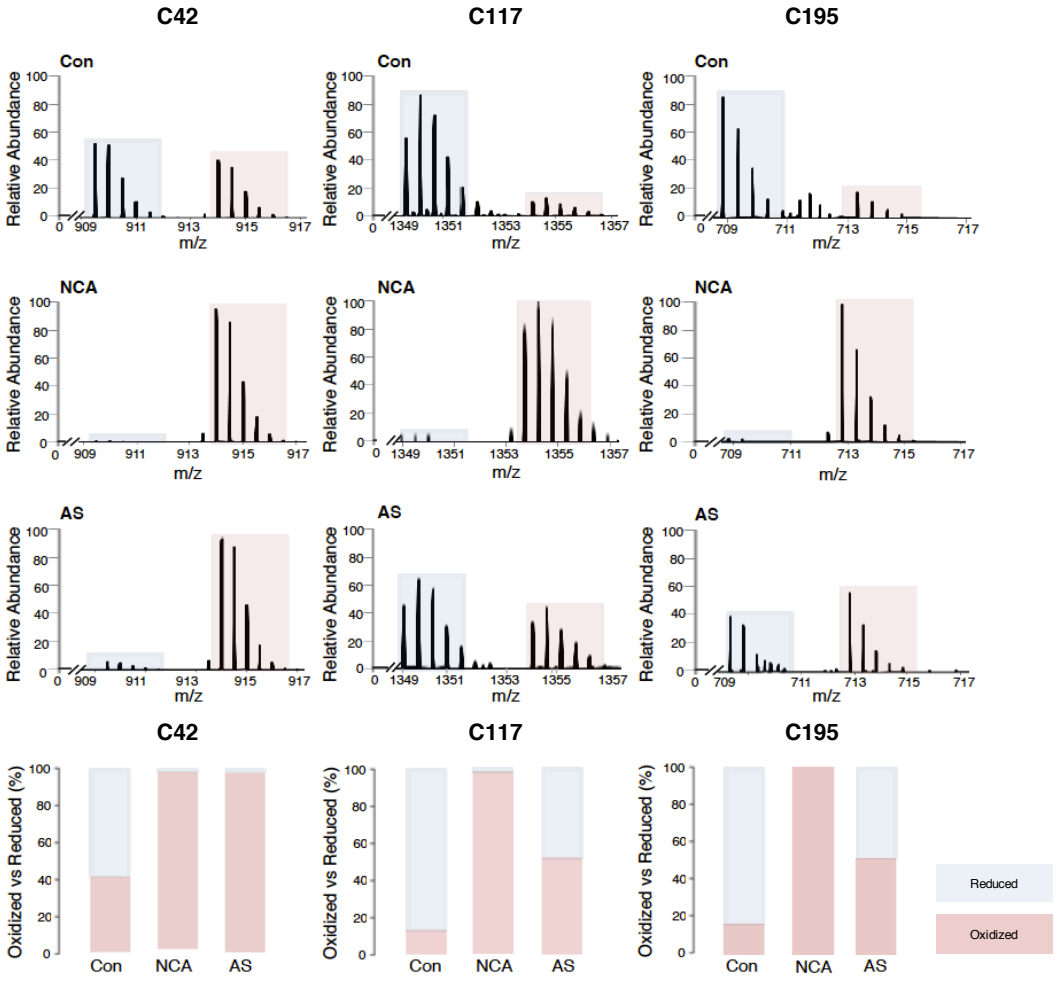

Figure 9: Identification of HNO-modified cysteines in PKGIα by NOxICAT. Exposure of recombinant human PKGIα to the HNO donors AS and NCA induced oxidation of C42, C117 and C195 in PKGIα. Fourier Transform Mass Spectrometry spectra are expressed as the relative abundance of the detected peptides in mass charge (m/z) containing C42 (left), C117 (middle) and C195 (right) in response to vehicle (top), NCA (25 mmol/L for 15 min; middle) or AS (25 µmol/L for 15 min; bottom). Quantification of the detected oxidised (pink) versus reduced (blue) peptide fraction is shown as percent of the total detected peptides (adapted from Donzelli, Goetz et al. 2017).

7.3 Assessment of PKGIα activity in cells

Interestingly, C117 and C195 are localised in the high-affinity cGMP-binding pocket of PKGIα as shown previously in the crystal structure (Osborne et al. 2011). As this is the high affinity site of second messenger binding and this might be a crucial position with regard to PKGIα activity, it could also explain effects on vasorelaxation as observed in mesenteric arteries. The vasodilator-stimulated phosphoprotein (VASP) is one of the established substrates, which is

phosphorylated by PKGIα and therefore changes in VASP phosphorylation can be directly correlated with PKGIα activity (Krause et al. 2003). To increase signal intensity and improve signal detection, the VASP signal was boosted by co-transfection of a VASP-mCherry plasmid with PKGIα-WT and the various PKGIα-mutants: the non-interdisulfide forming mutant PKGIα-C42S or the non-intradisulfide mutant PKGIα-C117/195S. Transfected and non-transfected cells were controlled using a brightlight-filter and a RFP-filter to ensure successful transfection with VASP-mCherry. Transfected cells were treated with vehicle (DMSO 0.02%, 30 min) or NCA (100 µmol/L; 30 min). Subsequently, western immunoblot analysis for phosphorylated VASP (pVASP) and PKGIα was performed under reducing (R) and under non-reducing (NR) conditions. Western immunoblot analysis for PKGIα showed under NR conditions the monomer at 75 kDa and the interprotein disulfide dimer at 150 kDa. NCA treatment increased PKGIα interprotein disulfide dimer formation (**Figure 10A**), similarly as in samples from the mesenteric arteries. The additional band below the PKGIα monomer likely corresponds to an intradisulfide that forms upon NCA exposure. The interdisulfide dimer was absent in cells transfected with the PKGIα-C42S mutant as expected, whereas the intradisulfide signal below the monomer remained. Importantly, in cells transfected with the PKGIα-C117/195S mutant, the putative intradisulfide signal was absent, strongly suggesting involvement of C117 and C195 in intradisulfide bond formation in PKGIα. The interdisulfide dimer was, as expected, detectable in cells transfected with the PKGIα-C117/195S mutant. In response to NCA, phosphorylation of VASP was enhanced in PKGIα-WT expressing cells, compared to vehicle-treated controls, suggesting an activatory effect of NCA on PKGIα-WT (**Figure 10B, 10C**). This effect was abolished in the non-interdisulfide forming PKGIα-C42S, suggesting a crucial role of this cysteine with regard to PKGIα activity, which might be due to subcellular redistribution into substrate vicinity followed by substrate phosphorylation (**Figure 10C**). In cells expressing the non-intradisulfide forming mutant, VASP phosphorylation was potentiated. However, the effect on VASP-phosphorylation

did not reach significance in cells expressing the PKGIα-mutants compared to PKGIα-WT expressing cells.

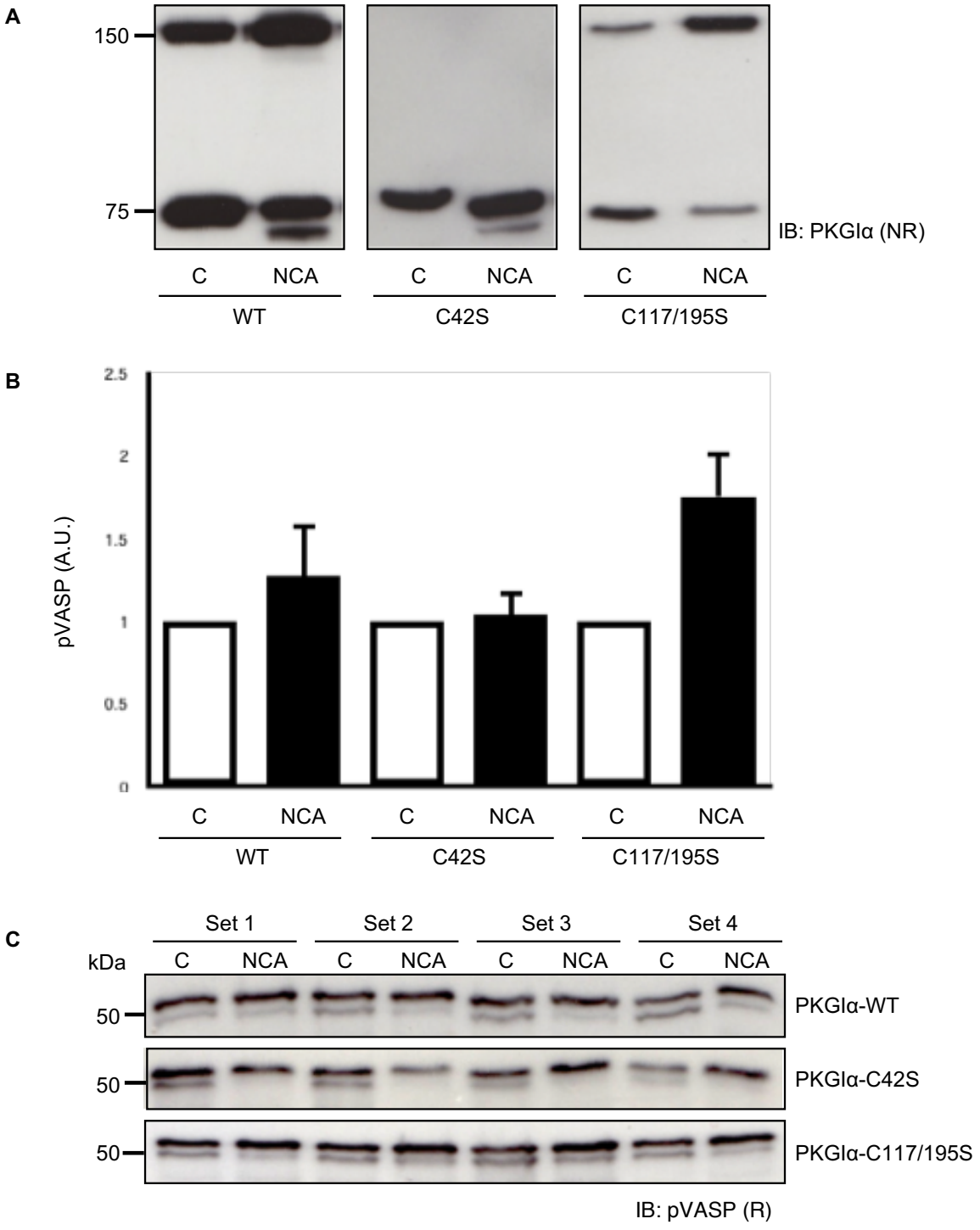

Figure 10: VASP-phosphorylation in response to the HNO donor NCA. HEK293T-cells were transfected with PKGIα-WT or PKGIα mutants PKGIα-C42S or PKGIα-C117/195S and VASP-mCherry and exposed to NCA (100 µmol/L for 30 min) or vehicle (DMSO; 0.02% for 30 min). Western-immunoblotting was performed under non-reducing (NR) conditions using a PKGIα-antibody (**A**). The

positions of monomeric (75 kDa), inter- (150 kDa) and intradisulfide (below 150 kDa) PKGIα are indicated. For detection of VASP phosphorylation (pVASP), western immunoblotting was performed under reducing conditions (R) (**C**). Densitometry was performed using ImageJ and NCA-treated samples were normalised to the respective control and shown in arbitrary units (A.U.) (**B**). Data are representative of 9 independent experiments. Data are given as mean ± SEM, using two-way ANOVA.

7.4 FRET measurements using the AKARIII-sensor

To investigate the functional consequences of the intradisulfide on PKGIα activity using an independent methodology, measurements using Förster Resonance Energy Transfer (FRET) technology were performed (Förster 1948). FRET is a well-established method, which uses a genetically encoded reporter construct expressing two fluorophores as well as a substrate- and a phosphopeptide-binding domain. Phosphorylation leads to a conformational change. Donor and acceptors are coming in close proximity, leading to an increased FRET signal (Wu and Brand 1994). As shown previously by Prof. Nikolaev and his group, the A-Kinase activity reporter III (AKARIII), generated in order to assess activity of PKA, contains a substrate domain that is also recognised by PKG and was therefore considered suitable for the present study (Allen and Zhang 2006; Gambaryan et al. 2012). The reporter was used to measure alterations in PKGIα activity in living cells. HEK293A cells were co-transfected with the AKARIII-sensor-plasmid and PKGIα-WT, PKGIα-C42S or PKGIα-C117/195S and exposed to the HNO donor NCA. NCA-exposure of cells co-transfected with PKGIα-WT enhanced the FRET signal when compared to cells transfected with AKARIII only. Thereby, it could be confirmed that the AKARIII may as well function as a suitable readout for the assessment of PKGIα kinase activity. In cells expressing the PKGIα-C42S mutant, the AKARIII FRET-response was significantly reduced compared to cells expressing PKGIα-WT (**Figure 11**). In cells expressing the non-intradisulfide forming mutant PKGIα-C117/195S, the FRET signal was slightly reduced compared to PKGIα-WT-expressing cells, however, remained statistically non-significant. Regarding the values of single measurements, particularly the cells transfected with PKGIα-WT displayed a broader scatter when compared to the PKGIα-C42S mutant transfected cells

(**Figure 11, right panel**). The FRET measurements suggested that PKGIα-activity in response to NCA was dependent on C42 oxidation and less affected by intradisulfide formation between C117/195, as the FRET ratio was diminished to a lesser extent when these cysteines were mutated.

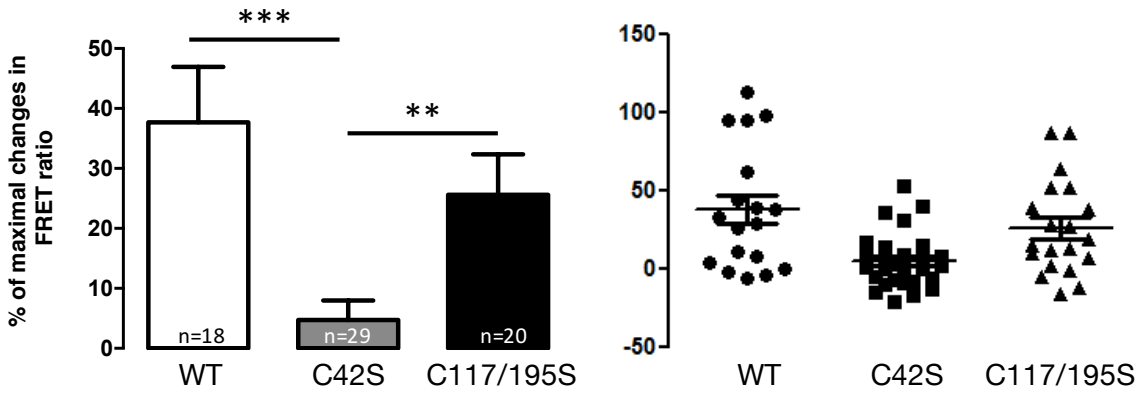

Figure 11: Assessment of PKGIα activity using AKARIII FRET-measurements. HEK293A cells were plated onto cover slips and co-transfected with PKGIα-WT or PKGIα mutants PKGIα-C42S or PKGIα-C117/195S and the AKARIII sensor. After 48 hrs, the cells were transferred to the FRET setup and controlled for cell viability. Cells with optimal sensor expression were selected for subsequent experiments. After 3 min and at a stable baseline, NCA (100 µmol/L) was added to the chamber. When a plateau of the response was reached, Forskolin (50 mmol/L) and IBMX (100 mmol/L) were added to induce a maximal FRET response. FRET results in response to NCA are shown in relation to the maximal response induced by Forskolin/IBMX. Bar charts summarise the data obtained from 18-29 cells. Data are given as mean ± SEM. ** indicates $P<0.006$ for Brown-Forsythe-test, *** indicates $P<0.008$ for ordinary one-way Anova.

7.5 Assessment of PKGIα activity *in vitro*

In order to establish a further readout for PKGIα activity, HEK293T-cells were transfected with PKGIα-WT, PKGIα-C42S, PKGIα-C117/195S or PKGIα-C42/117/195S. Non-transfected cells served as a control. Transfected and non-transfected cells were exposed to AS (500 µmol/L for 15 min) or NCA (100 µmol/L for 30 min). Kinase activity was analysed by assessing substrate phosphorylation in the presence of radiolabelled γ^{32}P-ATP and autoradiography. PKGIα-WT activity was significantly increased in response to the HNO donor NCA as reflected by enhanced phosphorylation of the recombinantly expressed C1-M-C2 domain of cardiac myosin-binding protein C, an established substrate of PKGIα (**Figure 12A**) (Thoonen et al. 2015). Replacement of C42 or C117/195 by an

oxidation-resistant serine significantly reduced substrate phosphorylation in response to NCA and AS, which was completely abolished in the triple mutant PKGIα-C42/117/195S (**Figure 12A, 12B**). These results suggest that NCA and AS activate PKGIα as reflected by increased substrate phosphorylation in PKGIα-WT and that activity is dependent on the oxidative modification of C42, C117 and C195. Interestingly, NCA and AS showed a distinct behaviour with regard to their impact on substrate phosphorylation: whilst NCA-induced substrate phosphorylation was significantly reduced after replacement of C117/195 (**Figure 12A)**, AS induced substrate phosphorylation was more dependent on the presence of C42 (**Figure 12B**).

Western immunoblotting under non-reducing conditions using a PKGIα-antibody was used to correlate the PKGIα oxidation status with PKGIα substrate phosphorylation in response to NCA and AS (**Figure 12C**). Western immunoblotting revealed monomeric PKGIα migrating at 75 kDa and the PKGIα interprotein disulfide dimer at 150 kDa in cells transfected with PKGIα-WT in response to NCA or AS. Interestingly, an additional band below the dimer was again detectable, potentially representative of the intradisulfide in PKGIα. This was particularly evident in samples treated with NCA, but also in PKGIα-WT samples treated with AS. Under both experimental conditions, the intradisulfide was detectable below the dimer. The intradisulfide was absent in samples treated with decomposed NCA (100µmol/L; 30 min) or DMSO as the corresponding solvent for NCA (0.02%; 30 min) (**Figure 12C; upper panel**). Furthermore, in samples treated with NaOH as a solvent control of AS, nitrite (NO_2^-), a by-product released during decomposition of AS, or decomposed AS (500 µmol/L for 15 min), there was no intradisulfide detectable (**Figure 12C; lower panel**), providing evidence that the release of HNO rather than a by-product was responsible for the oxidative modification in PKGIα. In cells expressing PKGIα-C42S, as expected, no interdisulfide formation was detectable, with only the monomer and the intradisulfide band below the monomer apparent in response to NCA treatment. Importantly, replacement of either C117 or C195 was sufficient to abolish the appearance of the lower band, again consistent with the hypothesis that formation of an intradisulfide between C117 and C195 is responsible for the

appearance of the additional band. In the triple mutant, only monomeric PKGIα was detectable after HNO treatment. Importantly, treatment with 2-mercaptoethanol reduced the interdisulfide-linked dimer and also the faster migrating bands, an observation consistent with an oxidative nature of the modification in PKGIα. Taken altogether, these findings further supported the formation of an intradisulfide in PKGIα.

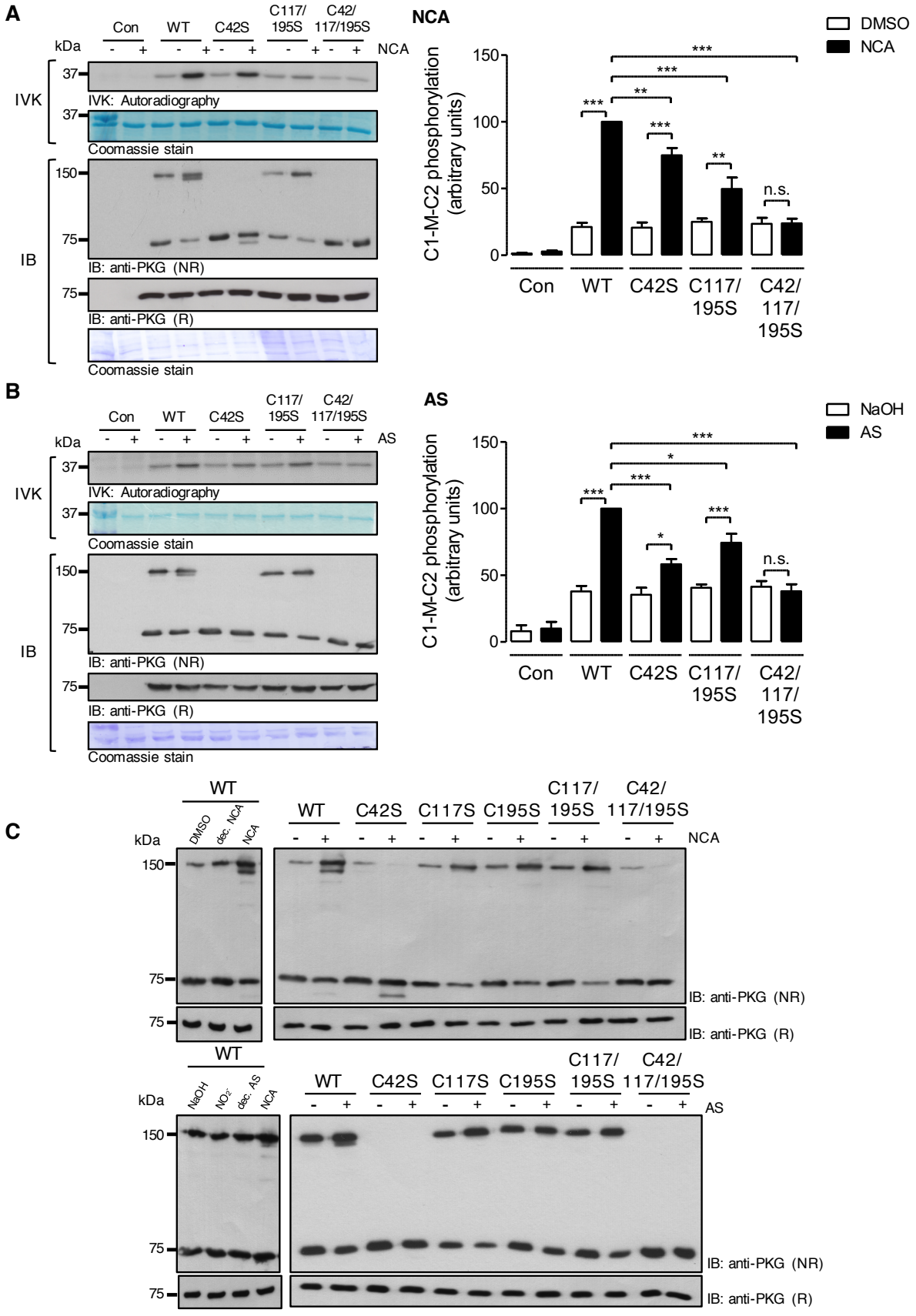
A
Con
WT
C42S
C117/ 195S
C42/ 117/195S
kDa
NCA
IVK
37
IVK: Autoradiography
Coomassie stain
IB
150
75
IB: anti-PKG (NR)
IB: anti-PKG (R)
NCA
DMSO
C1-M-C2 phosphorylation (arbitrary units)
n.s.
B
AS
NaOH
C
DMSO
dec. NCA
C117S
C195S
NO2-
dec. AS

Figure 12: Effect of HNO-mediated PKGIα oxidation on kinase activity. HEK293T cells were transfected to express PKGIα-WT or various mutants PKGIα-C42S, PKGIα-C117/195S, PKGIα-C42/117/195S and exposed to (**A**) NCA (100 µmol/L for 30 min), (**B**) AS (500 µmol/L for 15 min). *In vitro* kinase (IVK) assays were performed in cell lysates by addition of recombinant His_6-tagged C1-M-C2 domain of cardiac myosin-binding protein C as a substrate in the presence of γ^{32}P-ATP. Substrate phosphorylation was detected by autoradiography. Bar charts represent the results of 5 independent experiments. Data are expressed as $^{*}P < 0.05$, $^{**}P < 0.01$, $^{***}P < 0.001$ by comparison against each respective unstimulated control or WT after HNO-exposure. Immunoblotting for PKGIα under non-reducing (NR) or reducing (R) conditions was performed in the same samples (**C**). In addition, HEK293T cells were transfected to express PKGIα-WT and exposed to NCA (100 µmol/L for 30 min) or the respective controls, namely DMSO or decomposed NCA donor compound; AS (500 µmol/L for 15 min) or the respective controls NaOH, nitrite ($NO2^{-}$) or decomposed AS. Representative immunoblots show PKGIα migrating at 75 kDa (monomer) and 150 kDa (dimer). n.s.: non-significant; dec: decomposed (adapted from Donzelli, Goetz et al. 2017).

7.6 FRET measurements in murine VSMCs using cGi500

Intradisulfide formation may modulate kinase activity by affecting cGMP-binding to the kinase. This hypothesis was addressed in permeabilised mouse VSMCs isolated from transgenic mice, stably expressing the FRET-based cGMP-biosensor cGi500 comprising the cGMP-binding domains of PKGIα including C117 and C195. The FRET-sensor binds cGMP with an EC_{50} of 500 nmol/L and relates conformational changes upon cGMP-binding into changes in the FRET ratio. To exclude the possibility of endogenous cGMP formation by sGC in response to HNO donor-treatment, cells were permeabilised with β-Escin to maintain intracellular cGMP concentrations low. Furthermore, experiments with ODQ, a pharmacological inhibitor of sGC were performed to further exclude FRET-alterations that are mediated by cGMP-production by sGC and to be able to correlate changes in the FRET ratio exclusively to superfused cGMP (data not shown).

Isolated VSMCs of transgenic mice expressing the FRET-based cGMP-biosensor cGi500 were subjected to increasing cGMP concentrations before and after exposure to NCA and simultaneously FRET signals were recorded (**Figure 13A**). Hereby, an increased FRET ratio reflects cGMP-binding to the sensor. As shown by the representative FRET trace, cGMP addition leads to enhanced

FRET signals in a concentration-dependent manner, as expected. DMSO had no effect on the FRET-ratio. Exposure to NCA alone induced an increased FRET signal in the absence of cGMP (**Figure 13B**). This result suggests that NCA-induced oxidation of the sensor - and thereby intradisulfide formation - induces a conformational change that may mimic cGMP-binding. Moreover, subsequent exposure to increasing cGMP concentrations resulted in significantly smaller FRET-changes than the same cGMP-concentration prior to NCA treatment, suggesting a competition of intradisulfide formation and cGMP-binding. Based on this observation, it is possible that oxidation of endogenous PKGIα during conditions of enhanced generation and release of ROS may impact on cGMP-binding to the kinase.

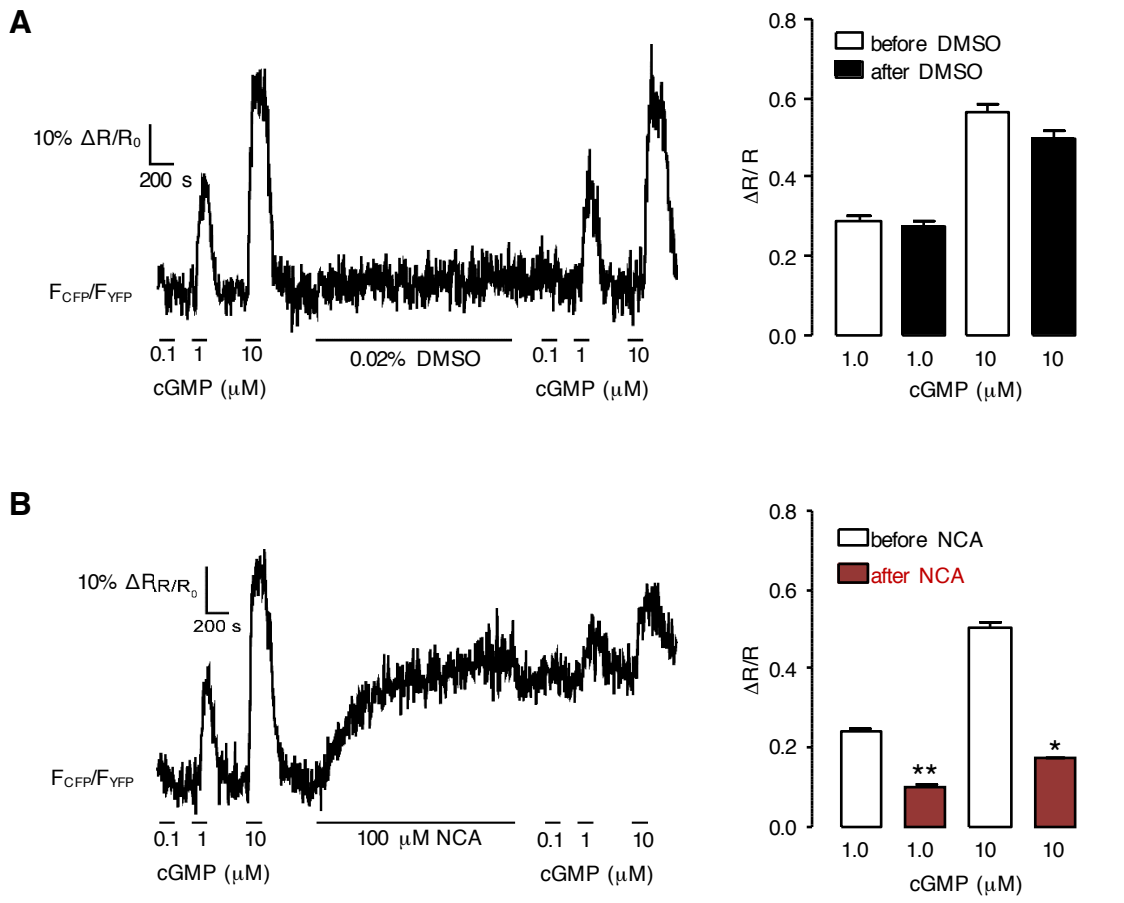

Figure 13: Assessment of intradisulfide-induced changes in the cGMP-binding domain of PKGIα. β-Escin-permeabilised primary mouse VSMCs stably expressing the FRET sensor cGi500 were superfused with intracellular-like medium (ICM) containing increasing concentrations of cGMP (0.1, 1, 10 µmol/L).

This was followed by incubation with DMSO (0.02%, **A**) or NCA (100 µmol/L, **B**) and by another incubation with ICM supplemented with increasing concentrations of cGMP (0.1, 1, 10 µmol/L). Changes of the FRET signals were recorded by FRET-microscopy. Representative FRET traces are shown on the left. The bar charts on the right summarise the FRET results from 10 cells per group as the ΔR/ΔR0 (amplitude relative to the signal induced by the first application of 10 µmol/L cGMP) induced by cGMP incubation before (white bars) or after exposure to DMSO (black; **A**) or NCA (red; **B**). $*P < 0.01$, $**P < 0.01$, $***P < 0.001$, comparing cGMP-induced changes in FRET ratio before and after DMSO or NCA by two-way ANOVA (adapted from Donzelli, Goetz et al. 2017).

7.7 cGMP-binding assays using ^{3}H-cGMP

As suggested by previous results, the intradisulfide forms in the high affinity binding domain in response to NCA and might alter cGMP-binding to the kinase. Therefore, cGMP-binding assays were performed. Recombinant human PKGIα was reduced by exposure to DTT (100 mmol/L) or oxidised by exposure to the HNO donor NCA (100 µmol/L) in order to induce inter- and intradisulfide bond formation.

Recombinant reduced or oxidised PKGIα was incubated with increasing concentrations of unlabelled cGMP that was spiked with ^{3}H-cGMP. ^{3}H-cGMP binding to the kinase was analysed using scintillation counting and the bound fraction of cGMP was calculated (**Figure 14**). cGMP-binding to the NCA-oxidised kinase was significantly reduced compared to the DTT-reduced kinase, corroborating previous results that the intradisulfide might counteract cGMP-binding to PKGIα.

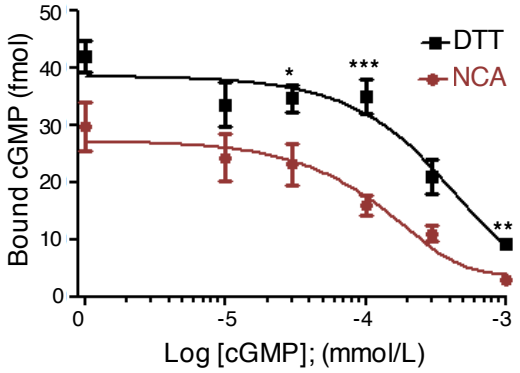

Figure 14: *In vitro* cGMP-binding to PKGIα after exposure to DTT (100 mmol/L for 10 min; black squares) or NCA (100 µmol/L for 30 min; red dots) was

investigated by measuring binding of ^{3}H-cGMP in the presence of increasing concentrations of unlabelled cGMP (0, 10, 30, 100, 300, 1000 nmol/L). The data are representative of 5 independent experiments. *$P < 0.05$, **$P < 0.01$, ***$P < 0.001$, comparing exposure to DTT or NCA at the same cGMP concentrations by *t*-test (adapted from Donzelli, Goetz et al. 2017).

7.8 NCA by-products in combination with oxidants induce intraprotein disulfide bond formation

To test whether other oxidant stimuli are able to induce intradisulfide formation, HEK293T cells were transfected to express the PKGIα-C42S mutant and were subsequently exposed to various oxidative stimuli. By using the PKGIα-C42S mutant, the aim was to exclude interdisulfide formation and focus solely on the intradisulfide. However, only after exposure to NCA, the intradisulfide was detectable, but not after exposure to other oxidants (**Figure 15A**).

The scaffold compound of NCA, 3MNCA, which does not release HNO in a significant manner, was demonstrated in previous studies to induce the formation of GSSG from GSH (Shoman et al. 2011). Regarding our observation that NCA induced the formation of an intrasulfide on PKGIα and treatment with other HNO donors resulted in less pronounced intradisulfide formation, it was hypothesised that the scaffold might be of structural importance for intradisulfide formation. To evaluate the role of the scaffold, HEK239T cells were transfected with the PKGIα-C42S mutant and were treated with a combination of various oxidative stimuli and the scaffold compound 3MNCA (**Figure 15B**). Combined treatment with oxidants and the scaffold compound 3MNCA resulted in intradisulfide formation in PKGIα. To determine, whether 3MNCA alone is sufficient to induce intradisulfide formation, the extent of intradisulfide formation was compared and quantified in cells transfected with PKGIα-WT, which were exposed to NCA or 3MNCA (**Figure 15C**). 3MNCA was able to slightly induce intradisulfide formation, however, this effect was significantly increased after exposure to NCA.

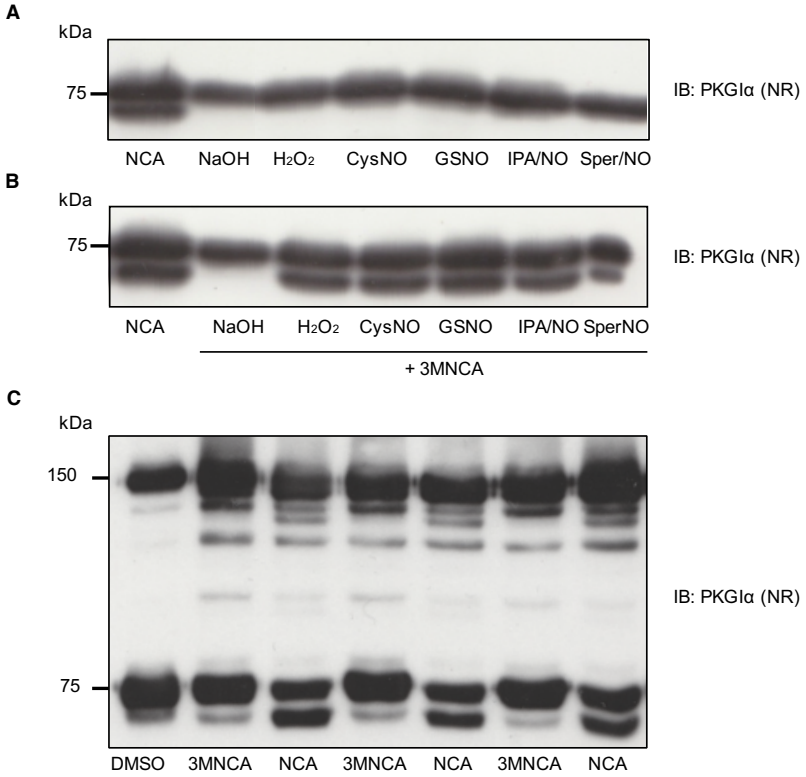

Figure 15: Combined treatment of 3MNCA and oxidants induce intraprotein disulfide bond formation in PKGIα. HEK239T cells were transfected with PKGIα-C42S (**A,B**) or PKGIα-WT (**C**). Cells were exposed to NCA (100 µmol/L for 30 min), NaOH (10 µmol/L for 15 min), H_2O_2 (100 µmol/L for 10 min), CysNO (100 µmol/L for 10 min), GSNO (100 µmol/L for 10 min), IpaNO (100 µmol/L for 10 min) and SperNO (100 µmol/L for 10 min). Cells were additionally treated with 3MNCA (100 µmol/L for 30 min) (**B, C**). Cells were harvested under non-reducing conditions and probed using a PKGIα-antibody. Intradisulfide bond formation was detectable in cells treated with NCA as well as in cells, which were treated with a combination of 3MNCA and other oxidants. 3MNCA was sufficient to induce formation of the intradisulfide bond albeit with a low stoichiometry (**C**).

7.9 Regulation of cremaster arteriolar dilation by HNO donor compounds

After molecular characterisation of the intradisulfide *in vitro,* the next aim was to correlate HNO application *in vivo* with intradisulfide formation in endogenous PKGIα. In collaboration with Prof. C. de Wit and Dr. K. Schmidt, well-established intravital imaging of the cremaster muscle microcirculation was performed. In anesthetised and ventilated mice, the thin, highly vascularised cremaster muscle was prepared for intravital microscopy to study microvascular networks including arterioles (NCA; n = 68 arterioles in 6 mice; AS; n = 73 arterioles in 6 mice) (Wölfle and Wit 2005). Vascular responses were recorded during the experiment and

quantified afterwards. Prior to the experiments, the diameter of the arterioles was assessed (maximal diameters between 13 and 49 µm) and the average diameter was comparable between the intervention groups (NCA: 27.6 ± 0.8 µm; AS 29.2 ± 0.9) (**Figure 16A, B**). The arterioles showed spontaneous tone (depicted as the quotient of the resting and maximal diameter) with a mean of 40 ± 1% (ranging from 10 to 85%). The spontaneous tone exhibited by the arterioles was similar in both groups (NCA: 41 ± 2%, AS: 40 ± 2% of maximal diameter; p = 0.63). Every artery was used as its own control and predilated with the endothelium-dependent vasodilator ACH (10 µmol/ L) to ensure vascular responsiveness in each experiment. After washout, DMSO was applied as a vehicle for NCA and washed out again. Addition of NCA (50 µmol/L) nearly doubled arteriolar diameter. A summary of independent experiments revealed that ACH as a positive control was able to induce approximately 80% of the maximum response in both intervention groups showing intact endothelial function and dilator capacity (NCA: 82 ± 3%; AS 91 ± 2% of the maximum response). DMSO did not induce vasorelaxation, but on the contrary, a small constriction (from 11.6 ± 0.8 to 19 ± 0.8; p <0.05). However, NCA (10 µmol/L) induced vasorelaxation was comparable to the response evoked by ACH (dilation from 11.0 ± 0.9 to 24.6 ± 0.8 µm). At a higher concentration, NCA (50 µmol/L) induced an even more pronounced vasorelaxation (26.3 ± 0.8 µm; p <0.05 vs. 10 µmol/L NCA). Similarly, application of 3 µmol/L AS induced a significant vasorelaxation in arterioles (from 11.6 ± 0.8 µm to 19.0 ± 0.8 µm) and a higher concentration of AS (50 µmol/L) dilated the arterioles even more (to 23.8 ± 0.8 µm). By western immunoblotting, kinase oxidation state was correlated under NR conditions and showed predominantly intradisulfide formation in response to NCA. These results are in line with the vasotone measurements in mesenteric arteries.

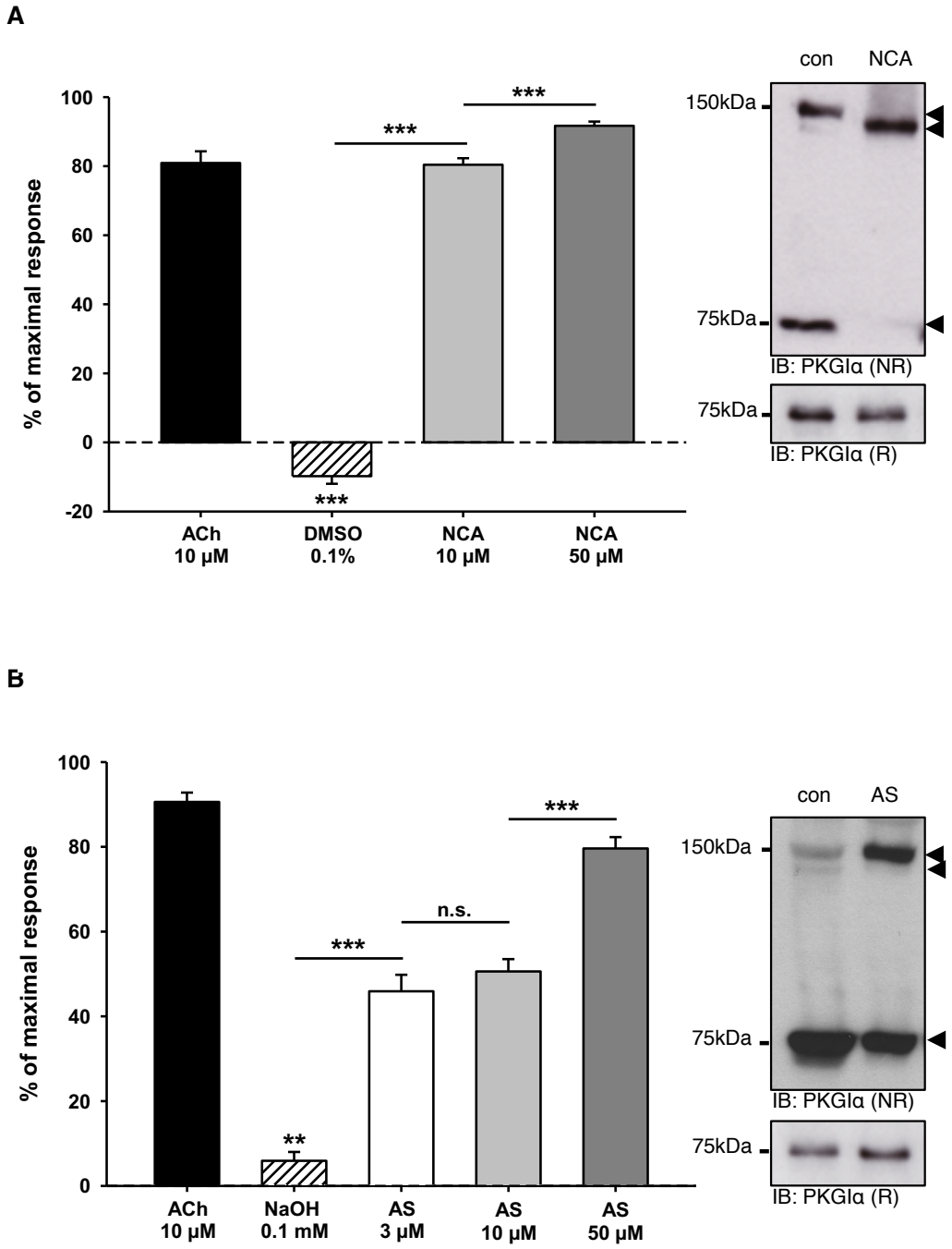

Figure 16: Correlation of intradisulfide formation in endogenous PKGIα with HNO-mediated vasorelaxation *in vivo*. Both HNO donors induced concentration-dependent vasorelaxation in arterioles *in vivo*. The effect of NCA was studied in 68 vessels from 6 mice. The effect of AS was studied in 73 vessels from 6 mice. Data are given as mean ± SEM. *** indicates $P < 0.001$ for paired comparisons (*t*-test). Western immunoblot analysis for PKGIα was performed under reducing (R) and non-reducing (NR) conditions in isolated cremaster muscles exposed to NCA (50 µmol/L) or AS (50 µmol/L). Black arrows indicate

the positions of monomeric (75 kDa), inter- (150 kDa) and intradisulfide (below 150 kDa) PKGIα (adapted from Donzelli, Goetz et al. 2017).

8 Discussion

Studies support the contemporary view that oxidants have cellular signalling properties and are crucial for the maintenance of organ and tissue homeostasis (Cuello and Eaton 2018). Thereby, the opinion that oxidative posttranslational modifications in target proteins are responsible for transducing an oxidant signal into a biological response has only started to emerge. The present study contributes a puzzle piece to the broader understanding on how oxidants regulate vasotone and thus might be therapeutically exploited. It demonstrates and characterises thoroughly intradisulfide bond formation in PKGIα, precisely in the high affinity cGMP-binding pocket (Donzelli, Goetz et al. 2017). This is not entirely new, in fact, Hofmann and colleagues were the first to describe the presence of an intradisulfide bond in PKGIα that formed in response to metal-ion induced oxidative stress *in vitro* (Landgraf et al. 1991). Later-on, it was also observed in the crystal structure of the regulatory domain of PKGIα, suggesting a constitutive rather than an inducible character of this modification (Osborne et al. 2011). The initial observation in the present study that HNO donors induced oxidative modification of C117 and C195 that are forming the intradisulfide was a chance finding and thus unexpected. Central focus of this thesis project was to rationally elucidate whether this intradisulfide might impact on the function of PKGIα.

8.1 HNO induces vasorelaxation in isolated murine mesenteric arteries

The vasorelaxing effect of HNO donors such as NCA was described previously. This was confirmed experimentally in the present thesis. It was shown that HNO-mediated vasorelaxation was partially dependent on the modulation of voltage-dependent K^+-channels and CGRP receptors (Donzelli et al. 2012), with sGC activation contributing as the main effector. Consequently, in sGC KO mice studied by Zhu et al., vasorelaxation in response to the HNO donor CXL-1020 was abolished, whilst the positive inotropic effect was maintained (Zhu et al. 2014). However, these mice might have potential adaptational issues due to the genetic deletion of sGC. Other groups demonstrated that HNO-induced vasorelaxation was attenuated, but not completely abolished by pretreatment with the sGC inhibitor ODQ, suggesting additional targets of HNO in the

vasculature that contribute to HNO-mediated vasorelaxation. A candidate was initially postulated to be interdisulfide formation via C42 in PKGIα. This was logical to assume, as NCA shares the oxidant properties of H_2O_2. Dimer formation of PKGIα induced by H_2O_2 was described to activate the kinase independently of sGC by altering its subcellular localisation (Burgoyne et al. 2007). This is a topic of intense discussion in the current literature as the leucine zipper is structurally distant from the catalytic site of the kinase and thus the impact of interdisulfide formation on the activity status of PKG is difficult to reconcile (Moon et al. 2018; Sheehe et al. 2018).

To evaluate qualitative and quantitative HNO-mediated modifications of PKGIα, a differential isotope-based thiol-trapping mass spectrometry-based approach was used, namely NOxICat methodology. PKGIα contains a total of 11 cysteines (Takio et al. 1984), some of which have been described and characterised previously as redox sensors (Landgraf et al. 1991; Burgoyne et al. 2007). Using NOxICAT, oxidative modification of C42, C117 and C195 in PKGIα upon exposure to HNO could be demonstrated. These data showed that C42 was susceptible to oxidation also under basal conditions, whilst C117 and C195 were only oxidised in response to HNO donors. Equal levels of oxidation of C117 and C195 caused by NCA or AS treatment were indicative of a modification involving both cysteines such as an intradisulfide bond formation. Whilst interprotein disulfide formation via C42 has been extensively investigated and characterised, information regarding the putative impact of C117 and C195 oxidation on PKGIα functions is scarce (Burgoyne et al. 2007; Prysyazhna et al. 2012; Burgoyne et al. 2012b; Kalyanaraman et al. 2017).

This intradisulfide, which forms in the high affinity cGMP-binding site and can be considered to be in a more rational position for regulating kinase activity than C42 in the leucine zipper domain.

The intradisulfide between C117 and C195 was observed in the crystal structure comprising the regulatory domain of PKGIα (Osborne et al. 2011). This observation would be consistent with a constitutive disulfide. Indeed, in these studies from the Dostmann laboratory, it was suggested that this intradisulfide most likely mediated the oxidative activation of the kinase. However, it is clear

from the observations reported here that cellular PKGIα, and especially C117 and C195, are predominantly found in their reduced state under basal conditions, with cysteine modifications including disulfide bond formation only accumulating when oxidant levels are elevated. In the crystallography experiments, the kinase was crystallised at ambient molecular oxygen and in buffer conditions that are free from thiol-reducing agents such as TCEP, thioredoxin or glutathione, which could help to capture solvent accessible cysteinyl thiols in their reduced state. This might explain the presence of the intradisulfide in the crystal structure. Interprotein disulfides in PKGIα or protein kinase A RI (PKARI) have been originally described as constitutive structural bonds (Monken and Gill 1980; Sarma et al. 2010), but were found later to be basally absent without pro-oxidant interventions (Brennan et al. 2006; Burgoyne et al. 2007). Recently, S-guanylation of C195 by nitro-cGMP was reported as a novel modification of PKGIα, leading to persistent kinase activity (Akashi et al. 2016). As S-guanylation occurs at reduced thiols, this provides independent corroboration of the observations made here that the intradisulfide is largely not present in the absence of pro-oxidant conditions.

Taken together, the results showing cysteine oxidation in PKGIα would be consistent with structural studies showing that PKGIα forms an intradisulfide at this location. However, NOxICAT analysis cannot give a definitive proof of this modification.

8.2 VASP Phosphorylation

Changes in VASP phosphorylation can be linked to changes in cellular PKGIα activity also with regard to its various and partially kinase-specific phosphorylation sites, namely S157 and S239, with the latter being primarily a target of PKG phosphorylation. Nevertheless, also other phosphorylation sites might be targeted by PKGIα. Therefore, in our studies we used a pVASP-antibody, specifically detecting phosphorylation at S239. Assaying changes in VASP-phosphorylation showed an activatory effect of the HNO donor NCA on PKGIα-WT-activity, suggesting that indeed part of the vasorelaxation induced by HNO donors may be mediated by PKG activation. The reduction of VASP-

phosphorylation observed in the PKGIα-C42 mutant confirms a link between deficiency in interdisulfide formation and impaired kinase activity. Phosphorylation of VASP in cells transfected with the PKGIα-C117/195S mutant remained unchanged compared to PKGIα-WT expressing cells. In the present experiments, VASP phosphorylation by the phosphospecific antibody revealed a double band. Here, the upper band migrating at approximately 50 kDa of the signal was used as a readout of VASP-phosphorylation. The double band can be rationalised by the fact that phosphorylation might induce a molecular weight shift from 46 kDa to 50 kDa in this case (Holt et al. 2016). One could consider the whole signal as well as a readout of VASP phosphorylation, which was calculated as well but revealed no difference. Moreover, results were calculated from the absolute values and controlled for equal loading using coomassie staining. An alternative would be to calculate the ratio of pVASP and total VASP amount (tVASP), which was in our hands indifferent, but might be more precise. Taken together, the results showed a substantial variance between the different experiments. As an alternative, we also looked therefore for VASP phosphorylation in serum starved cells, to exclude effects of the serum or growth factors included in the serum on signalling pathways. Unfortunately, overnight cell-starvation did not improve signal quality and did not reduce the variance (results not shown).

Even though this experiment showed a trend, it did not allow to make a definitive conclusion on whether PKG activity was altered in response to HNO due to the variance between experiments. Moreover, this could be interpreted that VASP was maybe not a favoured target of HNO-modulated PKGIα. Congruent with this, Eaton et al. showed that new antihypertensive compounds, which increase interprotein disulfide in PKGIα bond formation leading to vasorelaxation, did not increase VASP phosphorylation at S239, whereas exposure to 8-br-cGMP had the ability to do so (Burgoyne et al. 2017). Moreover, further studies could show that phosphorylation of PKGIα targets in cardiomyocytes can behave differently after oxidant- or cGMP- induced activation, which might explain the findings in these studies (Scotcher et al. 2016). Due to its proximity to the leucin zipper domain, the interdisulfide involving C42 might be in a more rationale position for

regulation kinase localisation and thereby induce target phosphorylation and confer downstream signalling.

Taken together, these studies could mainly confirm activation of PKG by NCA and increased VASP phosphorylation in PKGIα-WT-transfected cells, but the experimental setup was found not suitable to evaluate the role of the intradisulfide.

8.3 FRET measurements using the AKARIII-sensor

FRET measurements were performed in HEK293A cells co-transfected with the AKARIII-sensor as well as the various PKGIα constructs. Only the more adherent HEK293A-subtype was found suitable to perform FRET-experiments in living cells, whereas HEK293T cells detached during the experiments and thus disrupted the FRET measurements. Prior to the experiments, the HNO donor NCA was tested in a cell-free chamber to exclude autofluorescence of the compound itself contributing to the measurement. HEK293A-cells were used as the cell-line of choice as they are easy to transfect and do not express large quantities of the relevant components of the here studied PKGIα signalling cascade (Thomas and Smart 2005). In HEK293A-cells transfected solely with the AKARIII-sensor, it was evaluated whether NCA might target or activate the sensor directly, which was not the case. Moreover, 3MNCA, the scaffold of NCA, which does not release HNO was tested in cells transfected with AKARIII and PKGIα-WT, to ensure that observed effects on the fluorescence ratio are due to HNO release by NCA and not due to an effect of a by-product. Also, DMSO was tested in the applied concentration (0.01%) to exclude any vehicle effects. After ~25 frames of (= 125 secs.) baseline measurement NCA was applied to the cells followed by forskolin (Brophy et al. 2002). The majority of WT-transfected cells showed an increase in the FRET signal, suggesting PKGIα activation in response to NCA. This was significantly reduced as expected in cells transfected with the PKGIα-C42S mutant and supported previous findings regarding PKGIα activity in response to oxidants (Burgoyne et al. 2007). In the double mutant, alterations in the FRET-signal were very similar to PKGIα-WT-expressing cells, suggesting that formation of an intradisulfide would have no effect on PKGIα activity.

However, it is important to keep in mind that in these experiments the AKARIII sensor was employed that has been developed to assay PKA activity (Gambaryan et al. 2012; Zhu et al. 2016). To date there is no G-Kinase FRET sensor available, but with regard to the shared consensus domain of the AGC-kinase family, usage of the AKARIII could be considered suitable, when employing appropriate controls (Arencibia et al. 2013). Nevertheless, the A-kinase sensor might display a differential sensitivity with regard to measuring G-Kinase activity and therefore, these results represent more a trial rather than a proof of concept. During the experiments, a number of cells, which responded with a decline below basal fluorescence were observed. This might indicate that through a conformational change, the fluorophores move further apart, leading to a reduction in basal sensor fluorescence. However, due to the defined exclusion/inclusion criteria prior to the onset of the study that enrolled all cells that responded to forskolin, these cells were included in the present study.

Another variable was the time-course of the experiment: whilst the incubation time for NCA was set to 30 min in HEK293T-cell studies, the FRET-signal after NCA reached a plateau already after 100 frames (~8 min). Longer incubation times would probably have led to other results. Also, the cells were exposed to light and ambient temperature when measured under the microscope, which would have impaired the results during longer measuring times as well. Taken together, the FRET experiments performed in HEK293A cells represented an experimental setup, which made it difficult to control for temperature during the measurement.

8.4 PKGIα-dependent substrate phosphorylation *in vitro* in response to the HNO donor NCA

Due to experimental flaws experienced with the FRET experiments that were performed in transfected HEK293T cells, a more robust assay system was tested. Therefore *in vitro* kinase assays were performed to evaluate potential functional effects of the nascent intradisulfide on PKGIα activity. HEK293T cells were transfected with PKGIα-WT, the non-interdisulfide forming mutant PKGIα-C42S or the non-intradisulfide forming mutant PKGIα-C117/195S as well as a triple

mutant and kinase activity was analysed using autoradiography. As a substrate the recombinant C1-M-C2 domain of cardiac myosin-binding protein C was used, which was described in the literature as an established substrate of PKGIα (Thoonen et al. 2015). As already observed in previous experiments, phosphorylation and consequently PKGIα-activity was significantly increased in cells transfected with PKGIα-WT in response to the HNO donors. As seen with other experimental setups, PKGIα-activity was found to be reduced in cells transfected with PKGIα-C42S. Here, surprisingly, also cells expressing the PKGIα-C117/195S mutant that cannot form the intradisulfide, showed significantly reduced substrate phosphorylation in response to HNO donors compared to PKGIα-WT expressing cells. Substrate phosphorylation was completely abolished in cells expressing the PKGIα-C42/117/195S mutant. From these results we concluded that not just the formation of the interprotein disulfide, but also the formation of the intraprotein disulfide via C117 and C195 apparently increased kinase activity. Thus, interdisulfide formation via C42 as well as intradisulfide formation via C117 and C195 appeared to be crucial for PKG activity in response to HNO donors. However, the nature of the oxidative modification depended on the HNO donor. Whilst the C42 mutation induced a significant reduction in PKGIα activity in cells treated with AS, replacement of C117 and C195 led to a greater reduction in cells treated with NCA. Also, when western immunoblot analysis was performed under non-reducing conditions, the band migrating below the interdisulfide dimer that most likely represented the combinatory inter/intradisulfide in PKGIα, was reproducibly detectable in cells treated with NCA, but to a lesser extent in response to AS. This confirmed again the consent in the literature regarding the distinct chemical properties of the HNO donor compounds. These findings are also in accordance with the NOxICAT results showing that NCA and AS modified the same spectrum of cysteines in PKGIα, albeit to a different extent. Both donors oxidised the highly susceptible C42, however, NCA was superior to AS with regard to oxidation of C117 and C195. However, as both donors induced the same post-translational modification in PKGIα and induced a similar biological action, namely the activation of a signal

transduction pathway, it is logical to conclude that this was likely due to HNO release, especially as this is the only common nominator of these compounds. Another potential contributing factor for the apparent differences in HNO donors to modulate proteins by oxidising cysteines may be also the different half-lives of their HNO release: whilst AS has a half-life of 2 min (Hughes and Cammack 1999), NCA has a half-life of 2 hrs (Shoman et al. 2011). Releasing initially large amounts of HNO by AS may facilitate self-consumption, potentially by reducing the amount of HNO available for target oxidation. Moreover, these two HNO donors differ as well in the release of by-products as well as in their structure. When AS decomposes into HNO, an equivalent of biologically active nitrite and a small amount of NO is also generated (Dutton et al. 2004). NCA in comparison releases HNO and a thiol-reactive scaffold moiety (Sha et al. 2006). These respective by-products themselves exert biological effects that have to be taken into account (Lundberg et al. 2008). Distinct behaviour with regard to target oxidation and functional effects induced by different HNO donors has in fact been extensively described (Shoman et al. 2011). NCA belongs to the acyloxy nitroso compounds, which have been reported to induce also in other proteins interprotein disulfides (Mitroka et al. 2013). The scaffold by-product of NCA may by itself facilitate the formation of a disulfide of vicinal thiol residues.

A potential explanation for the discrepancy between the different kinase activity experiments performed in the present thesis might be as well that the analysis of VASP phosphorylation and PKG-activity measured by FRET analysis were performed in whole cells. Compartmentalisation within cells should therefore be taken into account (Sugiura et al. 2008; Kato et al. 2015; Cuello and Nikolaev 2020).

Another important finding when evaluating the western immunoblots are the previously described distinct migration patterns that allowed visual distinction between the posttranslational modifications: inter- or intradisulfides can be assessed using non-reducing western immunoblotting, as the oxidations induce higher or lower molecular weight shifts of proteins in gels that can be reversed by addition of a reducing agent such as DTT (Eaton 2006; Rudyk and Eaton 2014). Indeed, non-reducing western immunoblot analysis of cell homogenates mirror

exactly the NOxICAT data, with a basal level of C42 interdisulfide detectable under control conditions, whereas the intradisulfide only formed upon oxidant-exposure. The HNO donor intervention concomitantly elevated cGMP, which has been shown here to compete with the formation of the intradisulfide. This might explain that the intradisulfide induced by HNO had an apparent low stoichiometry. It is evident that the interplay of mechanisms that control PKGIα activity is complex, especially as cGMP-binding negatively influenced oxidation of C42 (Burgoyne et al. 2012b, 2012a; Müller et al. 2012; Prysyazhna et al. 2016). A significant finding of this study was that the interdisulfide that formed in position C42 attenuated the formation of the intradisulfide, as PKGIα-C42S showed markedly potentiated intradisulfide formation in response to HNO. This complex array of interrelated, interacting and modulating mechanisms may serve as a feedback that delimits over-activation or over-recruitment of the kinase to regulatory stimuli.

The overall important conclusion to reiterate here once more is the primary novel finding of this work, namely that PKGIα formed an intradisulfide and this activated the kinase. This conclusion is rationally based on the structure and is consistent with S-guanylation also activating the kinase at the same position (Osborne et al. 2011; Akashi et al. 2016). Perhaps either of these oxidative activation mechanisms that target C195 disrupts the interaction of the autoinhibitory domain with the catalytic domain gaining catalytic competence. This is in essence similar to what cGMP achieves, when it binds to its high affinity-binding site in the kinase that also contains this redox active cysteine (Chu et al. 1997).

8.5 FRET measurements using cGi500

With regard to the complex interplay between oxidative modification and cGMP-binding, FRET experiments were performed in VSMCs isolated from transgenic mice constitutively expressing a FRET-biosensor comprising the cGMP-binding sites of PKGIα. This approach has several advantages. Firstly, measurements are performed in a relevant cell type, namely in VSMCs that regulate vasotone. Secondly, these experiments do not require transfection and long-term culturing of the cells, which might be prone to artefacts. In summary, these experiments

allowed to evaluate the impact of HNO-induced intradisulfide formation in the FRET sensor on cGMP-binding in a relevant cellular context. Indeed, exposure to HNO increased the FRET response in the absence of cGMP, reflecting kinase activation. This FRET-response was comparable to that achieved by cGMP-dependent stimulation and demonstrates once more that the kinase was activated by intradisulfide formation and would be consistent with a modification relieving the autoinhibition of the catalytic domain. Importantly, these experiments were repeated in the presence of the sGC inhibitor ODQ and revealed a similar response thus excluding the potential influence of HNO donors on sGC activation in this scenario. Increasing cGMP concentrations did not further enhance the FRET signal primarily induced by the HNO donor NCA, consistent with the intradisulfide limiting second messenger binding. Future experiments involving recombinant mutant PKGIα or VSMCs isolated from KI animals expressing mutant kinase would be valuable in establishing whether the difference in cGMP-binding to PKGIα is definitely mediated by oxidant-induced intradisulfide formation.

In this experiment, an established well characterised FRET sensor construct was applied, which had been specifically designed to detect spatiotemporal changes in cGMP signalling by cGMP-binding (Thunemann et al. 2013a, 2013b). Here, we repurposed this sensor for our needs, to study the effects of HNO-induced intradisulfide formation in the presence or absence of controlled cGMP addition. Given the design of the sensor, which contains a cGMP-binding domain sandwiched between two fluorescent proteins with FRET-changes occurring upon conformational changes normally caused by the binding of cGMP, this represented almost native conditions (Russwurm et al. 2007). Both cysteines of our interest, C117 and C195, but not the LZ-localised C42 are present in this cGMP-binding domain. A possible explanation for such a cGMP-alike effect is most likely an intradisulfide bond formation in this cGMP-sensor, which can be studied in the absence of effects on C42.

8.6 cGMP-binding assays using ^{3}H-cGMP

These experiments were substantiated by ^{3}H-cGMP binding experiments, which showed that oxidative modification of the recombinantly expressed and purified PKG protein using HNO donors delimited cGMP-binding to the kinase, possibly by inducing a conformational change in the cGMP-binding pocket. Future experiments using the mutant-recombinant PKGIα with replacement of the critical cysteines C42, C117, C195 would help to further substantiate this statement.
Taken together, these experiments emphasize the finding of the present study, namely that the HNO-induced intradisulfide might mimic cGMP-binding, thereby activating the kinase but at the same time competing with cGMP-binding to the kinase.

8.7 Cremaster muscle microcirculation in response to the HNO donor NCA

Recapitulating the previous findings, the HNO-mediated intradisulfide formation in PKGIα most likely contributes mechanistically to the previously described impact of HNO on blood pressure reduction. This is supported by the fact that HNO induced significant amounts of intradisulfide in endogenous PKGIα, as shown in the cremaster muscle vasculature. This activated the kinase, and so provided a rational link between vasorelaxation and oxidation of endogenous PKGIα observed in two different vascular beds, namely mesenteric arteries as well as cremaster muscle vasculature *in vivo*.

However, it remained unclear, which mechanisms were involved and to which extent and whether sGC might contribute to the observed HNO donor mediated vasorelaxation. Studies using enzyme-specific KO, global, tissue specific or conditional animal models could be useful in evaluating this question *in vivo* in future studies. In fact, it would be especially interesting to investigate, to what extent HNO is released from each donor *in vivo* and to which extent its by-products might be involved in exerting functional biological responses.
Moreover, future studies are required to pinpoint whether a pharmacological compound could target specifically the functionally important cysteines. Other

groups have already demonstrated that it might be possible to employ a pro-oxidant therapy to induce interprotein disulfide bond formation via C42 and lower blood pressure and this might only be the starting point in the development of drugs, which modulate disease-specific posttranslational modifications without global inhibition of a protein or a signal transduction pathway (Burgoyne et al. 2017). A crucial question, which needs to be answered as well is which of the cysteines, C117 or C195, might be the one representing the switch to induce a conformational change, leading to kinase activation and concomitant vasorelaxation (Akashi et al. 2016). Moreover, a number of studies suggested that targets of PKGIα might be different in response to oxidant-induced activation or classical activation by cGMP and whether this might be occurring endogenously with a biological rationale.

To date, the present study demonstrated that HNO donors such as AS and NCA exerted direct effects on PKGIα activity and functions by promoting disulfide bond formation between critical cysteine residues, by mediating interprotein disulfide bond formation including C42 and additionally and novel, an intraprotein disulfide bond between C117 and C195 in the high affinity cGMP-binding domain. Mechanistically, the intraprotein disulfide mimics cGMP-binding, thereby activating the kinase and contributing to HNO-induced vasorelaxation.

9 Abstract

In cardiovascular pathology, nitric oxide (NO)-releasing drugs are clinically used to induce coronary vasorelaxation, improve oxygenation and thereby relieve pain. Unfortunately, they possess a major setback, namely the well-recognised “tolerance” phenomenon. In recent years, nitroxyl (HNO), the one-electron reduced sibling of NO, has emerged as a novel regulator of cardiovascular function with cardio- and vasoprotective properties. Importantly, HNO maintains its vasorelaxing effects without resulting in vascular tolerance. Therefore, HNO could be of relevance in a clinical setting as a novel therapeutic addition for the treatment of cardiovascular diseases. But to date, the underlying molecular mechanisms of HNO induced vasorelaxation are not fully understood. In mesenteric arteries isolated from WT-mice, two HNO donors with different kinetic properties of HNO release induced concentration-dependent vasorelaxation. We hypothesised that HNO-mediated oxidative posttranslational modification of cGMP-dependent protein kinase Iα (PKGIα) might impact on protein kinase activity and thus could represent a further molecular mechanism of HNO-mediated vasorelaxation. The data of this dissertation demonstrate that HNO induces interprotein disulfide formation between two cysteine 42 (C42) residues on adjacent chains of the PKGIα homodimer. This has been described previously to activate the kinase independently of the classical NO-cGMP-signalling pathway. Additionally, the formation of a previously unknown intradisulfide between C117 and C195 within the high-affinity cGMP-binding region was identified. To estimate the impact on second messenger signalling, cGMP-binding assays with recombinant PKGIα were performed and revealed reduced cGMP-binding affinity after HNO exposure of PKGIα. To determine whether HNO-induced intradisulfide formation is activatory or inhibitory, fluorescence energy transfer experiments (FRET) using a kinase activity reporter containing an AGC kinase phosphorylation consensus sequence were employed. HEK293Tcells were co-transfected with the FRET reporter as well as PKGIα wild-type (WT) or various oxidation-deficient PKGIα mutants. In WT transfected cells, HNO significantly increased the FRET signal compared to cells transfected with the FRET reporter only. Interestingly, the enhanced FRET response was

attenuated in cells transfected with the PKGIα-C42S mutant. PKGIα-C117/195S expressing cells were comparable to WT transfected cells. Furthermore, the phosphorylation status of the established PKGIα substrate VASP at serine 239 was assessed as a readout of protein kinase activity. Western immunoblot analysis of WT expressing cells exposed to HNO displayed higher VASP phosphorylation compared to vehicle-treated control cells. VASP phosphorylation was reduced in cells expressing the PKGIα-C42S mutant. In cells expressing the PKGIα-C117/195S mutant, VASP phosphorylation was again comparable to WT expressing cells. *In vitro* kinase activity was monitored using the phosphorylation of a recombinantly expressed substrate protein of PKGIα in the presence of ^{32}P-ATP. This revealed HNO enhanced WT kinase activity, an effect significantly attenuated in inter- or intradisulfide-deficient PKGIα. PKGIα-C42/117/195S, which is not susceptible to oxidation, was completely resistant to HNO-induced activation. Consistent with our previous observations, HNO induced concentration-dependent vasorelaxation *in vivo* as shown in cremaster arterioles by intravital microscopy. Vasorelaxation *in vivo* was correlated with enhanced inter- and intradisulfide formation in PKGIα. The results of this dissertation allow the conclusion that HNO exposure induces disulfide formation in PKGIα with impact on kinase activity and subsequent vasorelaxation.

9.1 Zusammenfassung

Im Rahmen kardiovaskulärer Erkrankungen werden oftmals Stickstoffmonoxid (NO) basierte Medikamente verabreicht, um durch eine Relaxation der Koronargefäße die Sauerstoffversorgung der Herzmuskelzellen zu verbessern. So können pektanginöse Beschwerden der Patienten gelindert werden. Gleichzeitig führt allerdings die andauernde Verwendung dieser NO basierten Medikamente zur Toleranz und die Wirkung wird dadurch vermindert. Die Säure des reduzierten Stickstoffmonoxids, die als Nitroxyl (HNO) bezeichnet wird, weist ebenfalls vasorelaxierende sowie positiv inotrope Effekte auf, ohne dabei eine Toleranz zu induzieren. Gegenwärtig werden diese Effekte in klinischen Studien überprüft. Ungeklärt bleibt nach wie vor, wie die pro-oxidativ wirkenden HNO Donatoren ihren vorbeschriebenen vasorelaxierenden Effekt ausüben.

Im Rahmen dieser Studie führten zwei HNO Donatoren mit unterschiedlichen kinetischen Eigenschaften in murinen Wildtyp (WT) Mesenterialarterien zu einer konzentrationsabhängigen Vasorelaxation. Die zugrunde liegende Hypothese dieser Arbeit hinterfragt, ob eine HNO-vermittelte oxidative posttranslationale Modifikation der cGMP-abhängigen Proteinkinase Iα (PKGIα) die Aktivität dieser Kinase beeinflusst und somit als molekulare Grundlage der HNO vermittelten Vasorelaxation interpretiert werden kann.

In vorangehenden Studien wurde bereits eine Interdisulfidbrücke zwischen dem jeweiligen Cystein 42 (C42) der benachbarten Aminosäureketten des PKGIα Homodimers beschrieben. Es konnte gezeigt werden, dass diese Interdisulfidbrücke zu einer cGMP-unabhängigen Aktivierung der Kinase und dadurch zur Vasorelaxation führt. Diese zeigte sich nun auch nach einer Behandlung der Zellen mit HNO Donatoren. Gleichzeitig stellte sich infolge der HNO Donatoren eine Intradisulfidbrücke zwischen C117 und C195 innerhalb der hochaffinen cGMP-Domäne dar. Zur weiteren Charakterisierung der Auswirkungen dieser neuartigen Intradisulfidbrücke wurden die Bindungseigenschaften von cGMP an rekombinanter PKGIα untersucht. HNO Donatoren reduzierten die cGMP Affinität zur Kinase. Unter Verwendung eines spezifischen Fluoreszenz Energie Transfer (FRET) Sensors mit einer übereinstimmenden Phosphorylierungsdomäne für AGC-Kinasen sollte nun die

Auswirkung auf die Kinaseaktivität experimentell untersucht werden. HEK293T Zellen wurden mit dem FRET Sensor und WT-PKGIα oder oxidationsdefizienten PKGIα Mutanten transfiziert. In Zellen mit PKGIα-WT Expression resultierte die Applikation von HNO Donatoren in einer gesteigerten FRET-Aktivität gegenüber Zellen, die nur mit dem FRET Sensor transfiziert worden waren. Gleichzeitig zeigte sich in Zellen mit PKGIα-C42S eine verminderte FRET Aktivität gegenüber den PKGIα-WT Zellen. Die Zellen mit PKGIα-C117/195S zeigten eine vergleichbare FRET-Aktivität. Als weiterer Surrogatparameter zur Einschätzung der PKGIα-Aktivität in Abhängigkeit von HNO Donatoren wurden Zellen mit dem bereits etablierten Phosphorylierungssubstrat VASP (Phosphorylierungsstelle Serin 239) transfiziert. Auch hier zeigte die Analyse der Western-Immunoblots eine gesteigerte VASP-Phosphorylierung im PKGIα-WT Modell infolge der HNO Donatoren, im Vergleich zu Zellen, die nur mit einer Kontrolllösung behandelt worden waren. Gleichzeitig war die VASP-Phosphorylierung in Zellen mit der PKGIα-C42S Mutante vermindert. Eine mit dem WT vergleichbare VASP-Phosphorylierung wurde in Zellen mit der PKGIα-C117/195S Mutante gesehen. Anschließend wurde die Kinaseaktivtät zuletzt auch in *in vitro* Kinase Analysen unter Verwendung eines etablierten, rekombinant exprimierten Substratproteins von PKGIα und ^{32}P-ATP bestimmt. Erneut konnte infolge der Behandlung mit HNO Donatoren eine gesteigerte Aktivität der PKGIα-WT Kinase beschrieben werden. Dieser Effekt war signifikant reduziert in Zellen mit den Intra- bzw. Interdisulfidbrücken Mutanten PKGIα-C42S und PKGIα-C117/195S. Die oxidationsdefiziente PKGIα-C42/117/195S Mutante zeigte keinerlei Kinaseaktivität infolge der HNO Donatoren. Abschließend konnte im *in vivo* Modell mittels intravitaler Mikroskopie von murinen Musculus cremaster Arteriolen die vasorelaxierende Wirkung der HNO Donatoren bestätigt werden. Es zeigte sich eine Korrelation der Vasorelaxation *in vivo* mit der Formierung der Inter- sowie Intradisulfidbrücken. Die Ergebnisse dieser Doktorarbeit liefern eine umfassende Charakterisierung der HNO vermittelten Disulfidbrückenbildung in PKGIα und deren Auswirkung auf die Aktivität der Kinase und der daraus resultierenden Vasorelaxation.

10 Literature

Agvald P, Adding LC, Artlich A, Persson MG, Gustafsson LE. Mechanisms of nitric oxide generation from nitroglycerin and endogenous sources during hypoxia in vivo. Brit J Pharmacol. 2002;135(2):373–82.

Akashi S, Ahmed KA, Sawa T, Ono K, Tsutsuki H, Burgoyne JR, Ida T, Horio E, Prysyazhna O, Oike Y, Rahaman M, Eaton P, Fujii S, Akaike T. Persistent activation of cGMP-dependent protein kinase by a nitrated cyclic nucleotide via site specific protein S-guanylation. Biochemistry-us. 2016;55(5):751–61.

Allen MD, Zhang J. Subcellular dynamics of protein kinase A activity visualized by FRET-based reporters. Biochem Bioph Res Co. 2006;348(2):716–21.

Alpha-Tocopherol, Beta Carotene Cancer Prevention Study Group. The effect of vitamin E and beta carotene on the incidence of lung cancer and other cancers in male smokers. New Engl J Med. 1994;330(15):1029–35.

Alverdi V, Mazon H, Versluis C, Hemrika W, Esposito G, van den Heuvel R, Scholten A, Heck A. cGMP-binding prepares PKG for substrate binding by disclosing the C-terminal domain. J Mol Biol. 2008;375(5):1380–93.

Ammendola A, Geiselhöringer A, Hofmann F, Schlossmann J. Molecular determinants of the interaction between the inositol 1,4,5-trisphosphate receptor-associated cGMP kinase substrate (IRAG) and cGMP kinase Ibeta. J Biological Chem. 2001;276(26):24153–9.

Andrews KL, Irvine JC, Tare M, Apostolopoulos J, Favaloro JL, Triggle CR, Kemp-Harper B. A role for nitroxyl (HNO) as an endothelium-derived relaxing and hyperpolarizing factor in resistance arteries. Brit J Pharmacol. 2009;157(4):540–50.

Andrews KL, Lumsden NG, Farry J, Jefferis AM, Kemp-Harper BK, Chin-Dusting JPF. Nitroxyl: a vasodilator of human vessels that is not susceptible to tolerance. Clin Sci. 2015;129(2):179–87.

Arencibia JM, Pastor-Flores D, Bauer AF, Schulze JO, Biondi RM. AGC protein kinases: From structural mechanism of regulation to allosteric drug development for the treatment of human diseases. Biochimica Et Biophysica Acta Bba - Proteins Proteom. 2013;1834(7):1302–21.

Barman SA, Zhu S, Han G, White RE. cAMP activates BKCa channels in pulmonary arterial smooth muscle via cGMP-dependent protein kinase. Am J Physiology Lung Cell Mol Physiology. 2003;284(6):L1004-11.

Bartberger MD, Fukuto JM, Houk KN. On the acidity and reactivity of HNO in aqueous solution and biological systems. Proc National Acad Sci. 2001;98(5):2194–8.

Beall A, Bagwell D, Woodrum D, Stoming TA, Kato K, Suzuki A, Rasmussen H, Brophy C. The small heat shock-related protein, HSP20, is phosphorylated on serine 16 during cyclic nucleotide-dependent relaxation. J Biol Chem. 1999;274(16):11344–51.

Beall AC, Kato K, Goldenring JR, Rasmussen H, Brophy CM. Cyclic nucleotide-dependent vasorelaxation is associated with the phosphorylation of a small heat shock-related protein. J Biol Chem. 1997;272(17):11283–7.

Berndt C, Lillig CH, Holmgren A. Thiol-based mechanisms of the thioredoxin and glutaredoxin systems: implications for diseases in the cardiovascular system. Am J Physiol-heart C. 2007;292(3):H1227–36.

Bevegård S, Orö L. Effect of prostaglandin E1 on forearm blood flow. Scand J Clin Laboratory Investigation. 1969;23(4):347–53.

Bjelakovic G, Gluud C. Surviving antioxidant supplements. Jnci J National Cancer Inst. 2007;99(10):742–3.

Bjelakovic G, Nikolova D, Gluud LL, Simonetti RG, Gluud C. Mortality in randomized trials of antioxidant supplements for primary and secondary prevention: systematic review and meta-analysis. Jama. 2007;297(8):842.

Blanton RM, Takimoto E, Aronovitz M, Thoonen R, Kass DA, Karas RH, Mendelsohn M. Mutation of the protein kinase I alpha leucine zipper domain produces hypertension and progressive left ventricular hypertrophy: a novel mouse model of age-dependent hypertensive heart disease. Journals Gerontology Ser Biological Sci Medical Sci. 2013;68(11):1351–5.

Botden IPG, Batenburg WW, Vries R de, Langendonk JG, Sijbrands EJG, Danser AHJ. Nitrite- and nitroxyl-induced relaxation in porcine coronary (micro-) arteries: underlying mechanisms and role as endothelium-derived hyperpolarizing factor(s). Pharmacol Res. 2012;66(5):409–18.

Brandes RP, Weissmann N, Schröder K. Redox-mediated signal transduction by cardiovascular Nox NADPH oxidases. J Mol Cell Cardiol. 2014;73:70–9.

Brennan JP, Bardswell SC, Burgoyne JR, Fuller W, Schröder E, Kentish JC, ., Eaton P. Direct activation of type I PKA by oxidants independently of cAMP is mediated by RI subunit interprotein disulphide bond formation. J Mol Cell Cardiol. 2006;40(6):928–9.

Brophy CM, Woodrum DA, Pollock J, Dickinson M, Komalavilas P, Cornwell TL, Lincoln T. cGMP-dependent protein kinase expression restores contractile function in cultured vascular smooth muscle cells. J Vasc Res. 2002;39(2):95–103.

Burgoyne JR, Eaton P. Oxidant sensing by protein kinases a and g enables integration of cell redox state with phosphoregulation. Sensors Basel Switz. 2010;10(4):2731–51.

Burgoyne JR, Madhani M, Cuello F, Charles RL, Brennan JP, Schroder E, Browning D, Eaton P. Cysteine redox sensor in PKGIa enables oxidant-induced activation. Science. 2007;317(5843):1393–7.

Burgoyne JR, Mongue-Din H, Eaton P, Shah AM. Redox signaling in cardiac physiology and pathology. Circ Res. 2012a;111(8):1091–106.

Burgoyne JR, Prysyazhna O, Richards DA, Eaton P. Proof of principle for a novel class of antihypertensives that target the oxidative activation of PKG Iα (Protein Kinase G Iα). Hypertension. 2017;70(3):577–86.

Burgoyne JR, Prysyazhna O, Rudyk O, Eaton P. cGMP-dependent activation of protein kinase G precludes disulfide activation. Hypertension. 2012b;60(5):1301–8.

Chappell LC, Seed PT, Briley AL, Kelly FJ, Lee R, Hunt BJ, Parmar K., Bewley S, Shennan A, Steer P, Poston L. Effect of antioxidants on the occurrence of pre-eclampsia in women at increased risk: a randomised trial. Lancet. 1999;354(9181):810–6.

Chen G, Suzuki H, Weston AH. Acetylcholine releases endothelium-derived hyperpolarizing factor and EDRF from rat blood vessels. Brit J Pharmacol. 1988;95(4):1165–74.

Chobanian AV, Bakris GL, Black HR, Cushman WC, Green LA, Izzo JL, Jones D, Materson B, Oparil S, Wright J, Roccella E, Institute J, Committee N. Seventh report of the joint national committee on prevention, detection, evaluation, and treatment of high blood pressure. Hypertension. 2003;42(6):1206–52.

Christensen KL, Mulvany MJ. Mesenteric arcade arteries contribute substantially to vascular resistance in conscious rats. J Vasc Res. 1993;30(2):73–9.

Chu D-M, Corbin JD, Grimes KA, Francis SH. Activation by cyclic GMP binding causes an apparent conformational change in cGMP-dependent protein kinase. J Biol Chem. 1997;272(50):31922–8.

Clague MJ, Wishnok JS, Marletta MA. Formation of N δ -cyanoornithine from N G-Hydroxy-l-arginine and hydrogen peroxide by neuronal nitric oxide synthase: implications for mechanism †. Biochemistry-us. 1997;36(47):14465–73.

Colica C, Renzo LD, Trombetta D, Smeriglio A, Bernardini S, Cioccoloni G, Miranda R, Gualtieri P, Salimei P, Lorenzo A. Antioxidant effects of a hydroxytyrosol-based pharmaceutical formulation on body composition, metabolic state, and gene expression: a randomized double-blinded, placebo-controlled crossover trial. Oxid Med Cell Longev. 2017;2017:1–14.

Conti CR. Re-thinking angina. Clin Cardiol. 2007;30(S1):I1–3.

Corcoran A, Cotter TG. Redox regulation of protein kinases. Febs J. 2013;280(9):1944–65.

Corradini E, Burgers PP, Plank M, Heck AJR, Scholten A. Huntingtin-associated protein 1 (HAP1) is a cGMP-dependent kinase anchoring protein (GKAP) specific for the cGMP-dependent protein kinase Iβ isoform. J Biological Chem. 2015;290(12):7887–96.

Cortese-Krott MM, Kuhnle GGC, Dyson A, Fernandez BO, Grman M, DuMond JF, Barrow M, McLeod G, Nakagawa H, Ondrias K, Nagy P, King S, Saavedra J, Keefer L, Singer M, Kelm M, Butler A, Feelisch M. Key bioactive reaction products of the NO/H2S interaction are S/N-hybrid species, polysulfides, and nitroxyl. P Natl Acad Sci Usa. 2015;112(34):E4651-60.

Couvertier SM, Zhou Y, Weerapana E. Chemical-proteomic strategies to investigate cysteine posttranslational modifications. Biochimica Et Biophysica Acta Bba - Proteins Proteom. 2014;1844(12):2315–30.

Cowart D, Venuti RP, Lynch K, Guptill JT, Noveck RJ, Foo SY. A phase 1 randomized study of single intravenous infusions of the novel nitroxyl donor BMS-986231 in Healthy Volunteers. J Clin Pharmacol. 2019;59(5):717–30.

Cuello F. Redox regulation of kinases in the heart. Free Radical Bio Med. 2017;112:2.

Cuello F, Eaton P. Cysteine-based redox sensing and its role in signaling by cyclic nucleotide-dependent kinases in the cardiovascular system. Annu Rev Physiol. 2018;81(1):63–87.

Cuello F, Nikolaev VO. Cardiac cGMP signaling in health and disease: location, location, location. J Cardiovasc Pharm. 2020;75(5):399–409.

Dai T, Tian Y, Tocchetti CG, Katori T, Murphy AM, Kass DA, Paolocci N, Gao W. Nitroxyl increases force development in rat cardiac muscle: Nitroxyl and myofilament sensitization to Ca 2+. J Physiology. 2007;580(3):951–60.

Dao D, Fraser AN, Hung J, Ljosa V, Singh S, Carpenter AE. CellProfiler Analyst: interactive data exploration, analysis and classification of large biological image sets. Bioinformatics. 2016;32(20):3210–2.

DeMaster EG, Redfern B, Nagasawa HT. Mechanisms of inhibition of aldehyde dehydrogenase by Nitroxyl, the active metabolite of the alcohol deterrent agent cyanamide. Biochem Pharmacol. 1998;55(12):2007–15.

Dharmashankar K, Widlansky ME. Vascular endothelial function and hypertension: insights and directions. Curr Hypertens Rep. 2010;12(6):448–55.

Dierks EA, Burstyn JN. Nitric oxide (NO•), the only nitrogen monoxide redox form capable of activating soluble guanylyl cyclase. Biochem Pharmacol. 1996;51(12):1593–600.

Doctorovich F, Bikiel DE, Pellegrino J, Suárez SA, Martí MA. Reactions of HNO with metal porphyrins: underscoring the biological relevance of HNO. Accounts Chem Res. 2014;47(10):2907–16.

Donzelli S, Espey MG, Flores-Santana W, Switzer CH, Yeh GC, Huang J, Stuehr D, King S, Miranda K, Wink D. Generation of nitroxyl by heme protein-mediated peroxidation of hydroxylamine but not N-hydroxy-L-arginine. Free Radic Biology Medicine. 2008;45(5):578–84.

Donzelli S, Espey MG, Thomas DD, Mancardi D, Tocchetti CG, Ridnour LA, Paolocci N, King S, Miranda K, Lazzarino G, Fukuto J, Wink D. Discriminating formation of HNO from other reactive nitrogen oxide species. Free Radical Bio Med. 2006;40(6):1056–66.

Donzelli S, Fischer G, King BS, Niemann C, DuMond JF, Heeren J, Wieboldt H, Baldus S, Gerloff C, Eschenhagen T, Carrier L, Böger R, Espey M. Pharmacological characterization of 1-nitrosocyclohexyl acetate, a long-acting nitroxyl donor that shows vasorelaxant and antiaggregatory effects. J Pharmacol Exp Ther. 2012;344(2):339–47.

Donzelli S, Goetz M, Schmidt K, Wolters M, Stathopoulou K, Diering S, Prysyazhna O, Polat V, Scotcher J, Dees C, Subramanian H, Butt E, Kamynina A, Schobesberger S, King S, Nikolaev V, de Wit C, Leichert L, Feil R, Eaton P, Cuello F. (2017). Oxidant sensor in the cGMP-binding pocket of PKGIα regulates nitroxyl-mediated kinase activity Scientific Reports 7(1), 9938.

Doyle MP, Mahapatro SN, Broene RD, Guy JK. Oxidation and reduction of hemoproteins by trioxodinitrate(II). The role of nitrosyl hydride and nitrite. J Am Chem Soc. 1988;110(2):593–9.

Dudzinski DM, Igarashi J, Greif D, Michel T. The regulation and pharmacology of endothelial nitric oxide synthase. Annu Rev Pharmacol. 2006;46(1):235–76.

DuMond JF, King SB. The chemistry of nitroxyl-releasing compounds. Antioxid Redox Sign. 2011;14(9):1637–48.

Dutton AS, Fukuto JM, Houk KN. Mechanisms of HNO and NO production from Angeli's salt: density functional and CBS-QB3 theory predictions. J Am Chem Soc. 2004;126(12):3795–800.

Eaton P. Protein thiol oxidation in health and disease: Techniques for measuring disulfides and related modifications in complex protein mixtures. Free Radical Bio Med. 2006;40(11):1889–99.

Eberhardt M, Dux M, Namer B, Miljkovic J, Cordasic N, Will C, Kichko T, Roche J, Fischer M, Suárez S, Bikiel D, Dorsch K, Leffler A, Babes A, Lampert A, Lennerz J, Jacobi J, Martí M, Doctorovich F, Högestätt E, Zygmunt P, Ivanovic-Burmazovic I, Messlinger K, Reeh P, Filipovic M. H2S and NO cooperatively regulate vascular tone by activating a neuroendocrine HNO-TRPA1-CGRP signalling pathway. Nat Commun. 2014;5(1):4381.

El-Armouche A, Wahab A, Wittköpper K, Schulze T, Böttcher F, Pohlmann L, King S, DuMond J, Gerloff C, Böger R, Eschenhagen T, Carrier L, Donzelli S. The new HNO donor, 1-nitrosocyclohexyl acetate, increases contractile force in normal and β-adrenergically desensitized ventricular myocytes. Biochem Bioph Res Co. 2010;402(2):340–4.

Ellis A, Li CG, Rand MJ. Differential actions of L-cysteine on responses to nitric oxide, nitroxyl anions and EDRF in the rat aorta. Brit J Pharmacol. 2000;129(2):315–22.

Etter EF, Eto M, Wardle RL, Brautigan DL, Murphy RA. Activation of myosin light chain phosphatase in intact arterial smooth muscle during nitric oxide-induced relaxation. J Biol Chem. 2001;276(37):34681–5.

Favaloro J, Kempharper B. The nitroxyl anion (HNO) is a potent dilator of rat coronary vasculature. Cardiovasc Res. 2007;73(3):587–96.

Favaloro JL, Kemp-Harper BK. Redox variants of NO (NO• and HNO) elicit vasorelaxation of resistance arteries via distinct mechanisms. Am J Physiology Hear Circulatory Physiology. 2009;296(5):H1274-80.

Felker GM, Borentain M, Cleland JG, DeSouza MM, Kessler PD, O'Connor CM, Seiffert D, Teerlink J, Voors A, McMurray J. Rationale and design for the development of a novel nitroxyl donor in patients with acute heart failure. Eur J Heart Fail. 2019;21(8):1022–31.

Filipovic MR, Eberhardt M, Prokopovic V, Mijuskovic A, Orescanin-Dusic Z, Reeh P, Ivanovic-Burmazovic I. Beyond H2S and NO interplay: hydrogen sulfide and nitroprusside react directly to give nitroxyl (HNO). A new pharmacological source of HNO. J Med Chem. 2013;56(4):1499–508.

Förster T. Zwischenmolekulare Energiewanderung und Fluoreszenz. Ann Phys-berlin. 1948;437(1–2):55–75.

Förstermann U, Sessa WC. Nitric oxide synthases: regulation and function. Eur Heart J. 2011;33(7):829–37, 837a–837d.

Francis SH, Blount MA, Zoraghi R, Corbin JD. Molecular properties of mammalian proteins that interact with cGMP: protein kinases, cation channels, phosphodiesterases, and multi-drug anion transporters. Front Biosci. 2005;10(1–3):2097.

Francis SH, Busch JL, Corbin JD, Sibley D. cGMP-dependent protein kinases and cGMP phosphodiesterases in nitric oxide and cGMP action. Pharmacol Rev. 2010;62(3):525–63.

Fritsch RM, Saur D, Kurjak M, Oesterle D, Schlossmann J, Geiselhöringer A, Hofmann F, Allescher H. InsP 3 R-associated cGMP Kinase Substrate (IRAG) Is essential for nitric oxide-induced Inhibition of calcium signaling in human colonic smooth muscle. J Biol Chem. 2004;279(13):12551–9.

Froehlich JP, Mahaney JE, Keceli G, Pavlos CM, Goldstein R, Redwood AJ, Sumbilla C, Lee D, Tocchetti C, Kass D, Paolocci N, Toscano J. Phospholamban thiols play a central role in activation of the cardiac muscle sarcoplasmic reticulum calcium pump by nitroxyl. Biochemistry-us. 2008;47(50):13150–2.

Fukao M, Mason HS, Britton FC, Kenyon JL, Horowitz B, Keef KD. Cyclic GMP-dependent protein kinase activates cloned BK Ca channels expressed in mammalian cells by direct phosphorylation at serine 1072. J Biol Chem. 1999;274(16):10927–35.

Fukuto JM, Bartberger MD, Dutton AS, Paolocci N, Wink DA, Houk KN. The physiological chemistry and biological activity of Nitroxyl (HNO): The neglected, misunderstood, and enigmatic nitrogen oxide. Chem Res Toxicol. 2005a;18(5):790–801.

Fukuto JM, Carrington SJ. HNO signaling mechanisms. Antioxid Redox Sign. 2011;14(9):1649–57.

Fukuto JM, Chiang K, Hszieh R, Wong P, Chaudhuri G. The pharmacological activity of nitroxyl: a potent vasodilator with activity similar to nitric oxide and/or endothelium-derived relaxing factor. J Pharmacol Exp Ther. 1992a;263(2):546–51.

Fukuto JM, Hszieh R, Gulati P, Chiang KT, Nagasawa HT. N,O-Diacylated-N-hydroxyarylsulfonamides: Nitroxyl precursors with potent smooth muscle relaxant properties. Biochem Bioph Res Co. 1992b;187(3):1367–73.

Fukuto JM, Switzer CH, Miranda KM, Wink DA. Nitroxyl (HNO): chemistry, biochemistry, and pharmacology. Annu Rev Pharmacol. 2005b;45(1):335–55.

Furchgott RF, Cherry PD, Zawadzki JV, Jothianandan D. Endothelial cells as mediators of vasodilation of arteries. J Cardiovasc Pharm. 1984;6(NA;):S336–43.

Gambaryan S, Butt E, Kobsar A, Geiger J, Rukoyatkina N, Parnova R, Nikolaev V, Walter U. The oligopeptide DT-2 is a specific PKG I inhibitor only in vitro, not in living cells. Brit J Pharmacol. 2012;167(4):826–38.

Gambaryan S, Butt E, Marcus K, Glazova M, Palmetshofer A, Guillon G, Smolenski A. cGMP-dependent protein kinase type II regulates basal level of aldosterone production by zona glomerulosa cells without increasing expression of the steroidogenic acute regulatory protein gene. J Biol Chem. 2003;278(32):29640–8.

Gambaryan S, Wagner C, Smolenski A, Walter U, Poller W, Haase W, Kurtz A, Lohmann S. Endogenous or overexpressed cGMP-dependent protein kinases inhibit cAMP-dependent renin release from rat isolated perfused kidney, microdissected glomeruli, and isolated juxtaglomerular cells. Proc National Acad Sci. 1998;95(15):9003–8.

Gao Y, Marshall P. An experimental and computational study of the reaction of ground-state sulfur atoms with carbon disulfide. J Chem Phys. 2011;135(14):144306.

Gao WD, Murray CI, Tian Y, Zhong X, DuMond JF, Shen X, Stanley BA, Foster DB, Wink DA, King SB, Van Eyk JE, Paolocci N (2012) Nitroxyl-mediated disulfide bond formation between cardiac myofilament cysteines enhances contractile function. Circ Res. 111:1002–1011

Geiselhöringer A, Gaisa M, Hofmann F, Schlossmann J. Distribution of IRAG and cGKI-isoforms in murine tissues. Febs Lett. 2004a;575(1–3):19–22.

Geiselhöringer A, Werner M, Sigl K, Smital P, Wörner R, Acheo L, Stieber J, Weinmeister P, Feil R, Feil S, Wegener J, Hofmann F, Schlossmann J. IRAG is essential for relaxation of receptor-triggered smooth muscle contraction by cGMP kinase. Embo J. 2004b;23(21):4222–31.

Gerschman R, Gilbert D, Nye SW, Dwyer P, Fenn WO. Oxygen poisoning and X-irradiation: a mechanism in common. 1954. Nutrition Burbank Los Angeles Cty Calif. 2001;17(2):162.

Giles GI, Tasker KM, Jacob C. Hypothesis: the role of reactive sulfur species in oxidative stress. Free Radical Bio Med. 2001;31(10):1279–83.

Go Y-M, Jones DP. Thiol/disulfide redox states in signaling and sensing. Crit Rev Biochem Mol. 2013;48(2):173–81.

Hamer M, Suarez SA, Neuman NI, Alvarez L, Muñoz M, Marti MA, Doctorovich F. Discussing endogenous NO• /HNO interconversion aided by phenolic drugs and vitamins. Inorg Chem. 2015;54(19):9342–50.

Harman D. Aging: A theory based on free radical and radiation chemistry. J Gerontology. 1956;11(3):298–300.

Hartman JC, Rio CL del, Reardon JE, Zhang K, Sabbah HN. Intravenous infusion of the novel HNO donor BMS-986231 is associated with beneficial inotropic, lusitropic, and vasodilatory properties in 2 canine models of heart failure. Jacc Basic Transl Sci. 2018;3(5):625–38.

Hedlund P, Aszodi A, Pfeifer A, Alm P, Hofmann F, Ahmad M, Fassler R, Andersson K. Erectile dysfunction in cyclic GMP-dependent kinase I-deficient mice. Proc National Acad Sci. 2000;97(5):2349–54.

Hirano K. Current topics in the regulatory mechanism underlying the Ca2+ sensitization of the contractile apparatus in vascular smooth muscle. J Pharmacol Sci. 2007;104(2):109–15.

Hofmann F, Ammendola A, Schlossmann J. Rising behind NO: cGMP-dependent protein kinases. J Cell Sci. 2000;113 (Pt 10):1671–6.

Hofmann F, Dostmann W, Keilbach A, Landgraf W, Ruth P. Structure and physiological role of cGMP-dependent protein kinase. Biochimica Et Biophysica Acta Bba - Mol Cell Res. 1992;1135(1):51–60.

Hogg N, Singh RJ, Kalyanaraman B. The role of glutathione in the transport and catabolism of nitric oxide. Febs Lett. 1996;382(3):223–8.

Hollander W. Role of hypertension in atherosclerosis and cardiovascular disease. Am J Cardiol. 1976;38(6):786–800.

Holt AW, Martin DN, Shaver PR, Adderley SP, Stone JD, Joshi CN, Francisco J, Lust R, Weidner D, Shewchuk B, Tulis D. Soluble guanylyl cyclase-activated cyclic GMP-dependent protein kinase inhibits arterial smooth muscle cell migration independent of VASP-serine 239 phosphorylation. Cell Signal. 2016;28(9):1364–79.

Huges MN, Wimbledon PE. The chemisry of trioxodinitrates. Part I. Decompostion of sodium trioxodinitrate (Angeli's salt) in aqueous solution. J Chem Soc Dalton Transactions. 1976;0(8):703.

Hughes MN, Cammack R. Methods in enzymology. Methods Enzymol. 1999;301:279–87.

Ignarro LJ. Endothelium-derived nitric oxide: actions and properties. Faseb J. 1989;3(1):31–6.

Ignarro LJ, Buga GM, Wood KS, Byrns RE, Chaudhuri G. Endothelium-derived relaxing factor produced and released from artery and vein is nitric oxide. Proc National Acad Sci. 1987;84(24):9265–9.

Irigoyen M-C, Angelis KD, Santos F dos, Dartora DR, Rodrigues B, Consolim-Colombo FM. Hypertension, blood pressure variability, and target organ lesion. Curr Hypertens Rep. 2016;18(4):31.

Irvine JC, Favaloro JL, Kemp-Harper BK. NO − activates soluble guanylate cyclase and Kv channels to vasodilate resistance arteries. Hypertension. 2003;41(6):1301–7.

Irvine JC, Favaloro JL, Widdop RE, Kemp-Harper BK. Nitroxyl anion donor, angeli's salt, does not develop tolerance in rat isolated aortae. Hypertension. 2007;49(4):885–92.

Irvine JC, Ritchie RH, Favaloro JL, Andrews KL, Widdop RE, Kemp-Harper BK. Nitroxyl (HNO): the cinderella of the nitric oxide story. Trends Pharmacol Sci. 2008;29(12):601–8.

Kalyanaraman H, Zhuang S, Pilz RB, Casteel DE. The activity of cGMP-dependent protein kinase Iα is not directly regulated by oxidation-induced disulfide formation at cysteine 43. J Biol Chem. 2017;292(20):8262–8.

Kamato D, Thach L, Bernard R, Chan V, Zheng W, Kaur H, Brimble M, Osman N, Little P. Structure, function, pharmacology, and therapeutic potential of the G Protein, Gα/q,11. Frontiers Cardiovasc Medicine. 2015;2:14.

Kamynina A. Furthering the understanding of the redox control of soluble Epoxide Hydrolase and Protein Kinase G in the cardiovascular system. Doctoral dissertation. King's College London. 2017.

Kaplan RC, Psaty BM, Heckbert SR, Smith NL, Lemaitre RN. Blood pressure level and incidence of myocardial infarction among patients treated for hypertension. Am J Public Health. 1999;89(9):1414–7.

Kato S, Chen J, Cornog KH, Zhang H, Roberts JD. The Golgi apparatus regulates cGMP-dependent protein kinase I compartmentation and proteolysis. Am J Physiology Cell Physiology. 2015;308(11):C944-58.

Keilbach A, Ruth P, Hofmann F. Detection of cGMP dependent protein kinase isozymes by specific antibodies. Eur J Biochem. 1992;208(2):467–73.

Kemp-Harper BK. Nitroxyl (HNO): A novel redox signaling molecule. Antioxid Redox Sign. 2011;14(9):1609–13.

Kim JJ, Casteel DE, Huang G, Kwon TH, Ren RK, Zwart P, Headd J, Brown N, Chow D, Palzkill T, Kim C. Co-crystal structures of PKG Iβ (92-227) with cGMP and cAMP reveal the molecular details of cyclic-nucleotide binding. Plos One. 2011;6(4):e18413.

Kinoshita H, Kuwahara K, Nishida M, Jian Z, Rong X, Kiyonaka S, Kuwabara Y, Kurose H, Inoue R, Mori Y, Li Y, Nakagawa Y, Usami S, Fujiwara M, Yamada Y, Minami T, Ueshima K, Nakao K. Inhibition of TRPC6 channel activity contributes to the antihypertrophic effects of natriuretic peptides-guanylyl cyclase-A signaling in the heart. Circ Res. 2010;106(12):1849–60.

Kleppisch T, Wolfsgruber W, Feil S, Allmann R, Wotjak CT, Goebbels S, Nave K, Hofmann F, Feil R. Hippocampal cGMP-dependent protein kinase I supports an age- and protein synthesis-dependent component of long-term potentiation but is not essential for spatial reference and contextual memory. J Neurosci. 2003;23(14):6005–12.

Klinke R, Pape HC, Kurtz A, Silbernagl S. Physiologie: Lehrbuch. Vol. 9. 2009.

Kohr MJ, Kaludercic N, Tocchetti CG, Gao WD, Kass DA, Janssen PML, Paolocci N, Ziolo M. Nitroxyl enhances myocyte Ca2+ transients by exclusively targeting SR Ca2+ -cycling. Front Biosci. 2010;E2(2):614–26.

Koitabashi N, Aiba T, Hesketh GG, Rowell J, Zhang M, Takimoto E, Tomaselli G, Kass D. Cyclic GMP/PKG-dependent inhibition of TRPC6 channel activity and expression negatively regulates cardiomyocyte NFAT activation novel mechanism of cardiac stress modulation by PDE5 inhibition. J Mol Cell Cardiol. 2009;48(4):713–24.

Koller A, Schlossmann J, Ashman K, Uttenweiler-Joseph S, Ruth P, Hofmann F. Association of phospholamban with a cGMP kinase signaling complex. Biochem Bioph Res Co. 2003;300(1):155–60.

Krause M, Dent EW, Bear JE, Loureiro JJ, Gertler FB. Ena/VASP Proteins: regulators of the actin cytoskeleton and cell migration. Annu Rev Cell Dev Bi. 2003;19(1):541–64.

Krüger M, Kötter S, Grützner A, Lang P, Andresen C, Redfield MM, Butt E, Remedios C, Linke W. Protein kinase G modulates human myocardial passive stiffness by phosphorylation of the titin springs. Circ Res. 2009;104(1):87–94.

Lalli MJ, Shimizu S, Sutliff RL, Kranias EG, Paul RJ. [Ca 2+] i homeostasis and cyclic nucleotide relaxation in aorta of phospholamban-deficient mice. Am J Physiol-heart C. 1999;277(3):H963–70.

Lancel S, Zhang J, Evangelista A, Trucillo MP, Tong X, Siwik DA, Cohen R, Colucci W. Nitroxyl activates SERCA in cardiac myocytes via glutathiolation of cysteine 674. Circ Res. 2009;104(6):720–3.

Landgraf W, Regulla S, Meyer HE, Hofmann F. Oxidation of cysteines activates cGMP-dependent protein kinase. J Biological Chem. 1991;266(25):16305–11.

Layland J, Li J-M, Shah AM. Role of cyclic GMP-dependent protein kinase in the contractile response to exogenous nitric oxide in rat cardiac myocytes. J Physiology. 2002;540(2):457–67.

Leo CH, Joshi A, Hart JL, Woodman OL. Endothelium-dependent nitroxyl-mediated relaxation is resistant to superoxide anion scavenging and preserved in diabetic rat aorta. Pharmacol Res. 2012;66(5):383–91.

Lindemann C, Leichert LI. Methods in molecular biology. Methods Mol Biology Clifton N J. 2012;893:387–403.

Little PJ, Neylon CB, Tkachuk VA, Bobik A. Endothelin-1 and endothelin-3 stimulate calcium mobilization by different mechanisms in vascular smooth muscle. Biochem Bioph Res Co. 1992;183(2):694–700.

Lorenz R, Bertinetti D, Herberg FW. Handbook of experimental pharmacology. Handb Exp Pharmacol. 2015;105–22.

Lundberg JO, Weitzberg E, Gladwin MT. The nitrate-nitrite-nitric oxide pathway in physiology and therapeutics. Nat Rev Drug Discov. 2008;7(2):156–67.

Lymar SV, Shafirovich V, Poskrebyshev GA. One-electron reduction of aqueous Nitric Oxide: a mechanistic revision. Inorg Chem. 2005;44(15):5212–21.

Maisel AS, Duran JM, Wettersten N. Natriuretic peptides in heart failure. Heart Fail Clin. 2018;14(1):13–25.

Massberg S, Sausbier M, Klatt P, Bauer M, Pfeifer A, Siess W, Fässler R, Ruth P, Krombach F, Hofmann F. Increased adhesion and aggregation of platelets lacking cyclic guanosine 3′,5′-monophosphate kinase I. J Exp Med. 1999;189(8):1255–64.

McGregor M. Pathogenesis of angina pectoris and role of nitrates in relief of myocardial ischemia. Am J Medicine. 1983;74(6):21–7.

Members Task Force, Montalescot G, Sechtem U, Achenbach S, Andreotti F, Arden C, Budaj A, Bugiardini R, Crea F, Cuisset T, Mario C, Ferreira J, Gersh B, Gitt A, Hulot J, Marx N, Opie L, Pfisterer M, Prescott E, Ruschitzka F, Sabaté M, Senior R, Taggart D, Wall E, Vrints C, Zamorano J, Achenbach S, Baumgartner H, Bax J, Bueno H, Dean V, Deaton C, Erol C, Fagard R,

Ferrari R, Hasdai D, Hoes A, Kirchhof P, Knuuti J, Kolh P, Lancellotti P, Linhart A, Nihoyannopoulos P, Piepoli M, Ponikowski P, Sirnes P, Tamargo J, Tendera M, Torbicki A, Wijns W, Windecker S, Knuuti J, Valgimigli M, Bueno H, Claeys M, Donner-Banzhoff N, Erol C, Frank H, Funck-Brentano C, Gaemperli O, Gonzalez-Juanatey J, Hamilos M, Hasdai D, Husted S, James S, Kervinen K, Kolh P, Kristensen S, Lancellotti P, Maggioni A, Piepoli M, Pries A, Romeo F, Rydén L, Simoons M, Sirnes P, Steg P, Timmis A, Wijns W, Windecker S, Yildirir A, Zamorano J. 2013 ESC guidelines on the management of stable coronary artery disease: the task force on the management of stable coronary artery disease of the european society of cardiology. Eur Heart J. 2013;34(38):2949–3003.

Meng T-C, Fukada T, Tonks NK. Reversible oxidation and inactivation of protein tyrosine phosphatases In Vivo. Mol Cell. 2002;9(2):387–99.

Michael SK, Surks HK, Wang Y, Zhu Y, Blanton R, Jamnongjit M, Aronovitz M, Baur W, Ohtani K, Wilkerson M, Bonev A, Nelson M, Karas R, Mendelsohn M. High blood pressure arising from a defect in vascular function. P Natl Acad Sci Usa. 2008;105(18):6702–7.

Miller ER, Pastor-Barriuso R, Dalal D, Riemersma RA, Appel LJ, Guallar E. Meta-analysis: high-dosage vitamin E supplementation may increase all-cause mortality. Ann Intern Med. 2005;142(1):37.

Miller TW, Cherney MM, Lee AJ, Francoleon NE, Farmer PJ, King SB, Hobbs A, Miranda K, Burstyn J, Fukuto J. The effects of nitroxyl (HNO) on soluble guanylate cyclase activity: interactions at ferrous heme and cysteine thiols. J Biological Chem. 2009;284(33):21788–96.

Miranda KM, Dutton AS, Ridnour LA, Foreman CA, Ford E, Paolocci N, Katori T, Tocchetti C, Mancardi D, Thomas D, Espey M, Houk K, Fukuto J, Wink D. Mechanism of Aerobic Decomposition of Angeli's Salt (Sodium Trioxodinitrate) at physiological pH. J Am Chem Soc. 2005;127(2):722–31.

Miranda KM, Nims RW, Thomas DD, Espey MG, Citrin D, Bartberger MD, Paolocci N, Fukuto J, Feelisch M, Wink D. Comparison of the reactivity of nitric oxide and nitroxyl with heme proteins. J Inorg Biochem. 2003a;93(1–2):52–60.

Miranda KM, Paolocci N, Katori T, Thomas DD, Ford E, Bartberger MD, Espey M, Kass D, Feelisch M, Fukuto J, Wink D. A biochemical rationale for the discrete behavior of nitroxyl and nitric oxide in the cardiovascular system. Proc National Acad Sci. 2003b;100(16):9196–201.

Miseta A, Csutora P. Relationship Between the Occurrence of Cysteine in Proteins and the Complexity of Organisms. Mol Biol Evol. 2000;17(8):1232–9.

Mitroka S, Shoman ME, DuMond JF, Bellavia L, Aly OM, Abdel-Aziz M, Kim-Shapiro D, King S. Direct and nitroxyl (HNO)-mediated reactions of acyloxy nitroso compounds with the thiol-containing proteins glyceraldehyde 3-phosphate dehydrogenase and alkyl hydroperoxide reductase subunit C. J Med Chem. 2013;56(17):6583–92.

Mohamed AA. Advances in the coordination chemistry of nitrogen ligand complexes of coinage metals. Coordin Chem Rev. 2010;254(17–18):1918–47.

Mondoro TH, Ryan BB, Hrinczenko BW, Schechter AN, Vostal JG, Alayash AI. Biological action of nitric oxide donor compounds on platelets from patients with sickle cell disease. Brit J Haematol. 2001;112(4):1048–54.

Monken CE, Gill GN. Structural analysis of cGMP-dependent protein kinase using limited proteolysis. J Biological Chem. 1980;255(15):7067–70.

Moon TM, Sheehe JL, Nukareddy P, Nausch LW, Wohlfahrt J, Matthews DE, Blumenthal D, Dostmann W. An N-terminally truncated form of cyclic GMP-dependent protein kinase Iα (PKG Iα) is monomeric, autoinhibited, and provides a model for activation. J Biological Chem. 2018;293(21):7916–29.

Müller PM, Gnügge R, Dhayade S, Thunemann M, Krippeit-Drews P, Drews G, Feil R. H_2O_2 lowers the cytosolic Ca^{2+} concentration via activation of cGMP-dependent protein kinase Iα. Free Radic Biology Medicine. 2012;53(8):1574–83.

Münzel T, Daiber A, Mülsch A. Explaining the phenomenon of nitrate tolerance. Circ Res. 2005;97(7):618–28.

Murphy RA, Walker JS. Inhibitory mechanisms for cross-bridge cycling: the nitric oxide-cGMP signal transduction pathway in smooth muscle relaxation. Acta Physiol Scand. 1998;164(4):373–80.

Nagao T, Vanhoutte PM. Characterization of endothelium-dependent relaxations resistant to nitro-l-arginine in the porcine coronary artery. Brit J Pharmacol. 1992;107(4):1102–7.

Neuhauser H, Kuhnert R, Born S. 12-Monats-Prävalenz von Bluthochdruck in Deutschland. Journal of Health Monitoring. n.d.;

Niketić V, Stojanović S, Nikolić A, Spasić M, Michelson AM. Exposure of Mn and FeSODs, but not Cu/ZnSOD, to NO leads to nitrosonium and nitroxyl ions generation which cause enzyme modification and inactivation: an in vitro study. Free Radical Bio Med. 1999;27(9–10):992–6.

Obst M, Tank J, Plehm R, Blumer KJ, Diedrich A, Jordan J, Luft F, Gross V. NO-dependent blood pressure regulation in RGS2-deficient mice. Am J Physiology-regulatory Integr Comp Physiology. 2006;290(4):R1012–9.

Oparil S, Acelajado MC, Bakris GL, Berlowitz DR, Cífková R, Dominiczak AF Grassi G, Jordan J, Poulter N, Rodgers A, Whelton P. Hypertension. Nat Rev Dis Primers. 2018;4(1):18014.

Osborne BW, Wu J, McFarland CJ, Nickl CK, Sankaran B, Casteel DE, Woods V, Kornev A, Taylor S, Dostmann W. Crystal structure of cGMP-dependent protein kinase reveals novel site of interchain communication. Struct Lond Engl 1993. 2011;19(9):1317–27.

Osei-Owusu P, Sun X, Drenan RM, Steinberg TH, Blumer KJ. Regulation of RGS2 and second messenger signaling in vascular smooth muscle cells by cGMP-dependent protein kinase. J Biol Chem. 2007;282(43):31656–65.

Palmer RMJ, Ferrige AG, Moncada S. Nitric oxide release accounts for the biological activity of endothelium-derived relaxing factor. Nature. 1987;327(6122):524–6.

Paolocci N, Jackson MI, Lopez BE, Miranda K, Tocchetti CG, Wink DA, Hobbs A, Fukuto J. The pharmacology of nitroxyl (HNO) and its therapeutic potential: Not just the janus face of NO. Pharmacol Therapeut. 2007;113(2):442–58.

Paolocci N, Katori T, Champion HC, John MES, Miranda KM, Fukuto JM, Wink D, Kass D. Positive inotropic and lusitropic effects of HNO/NO- in failing hearts: Independence from adrenergic signaling. Proc National Acad Sci. 2003;100(9):5537–42.

Paolocci N, Saavedra WF, Miranda KM, Martignani C, Isoda T, Hare JM, Espey M, Fukuto J, Feelisch M, Wink D, Kass D. Nitroxyl anion exerts redox-sensitive positive cardiac inotropy in vivo by calcitonin gene-related peptide signaling. Proc National Acad Sci. 2001;98(18):10463–8.

Pauling L, Pauling L, Moertel C. A Proposition: Megadoses of vitamin C are valuable in the treatment of cancer. Nutr Rev. 2009;44(1):28–9.

Paulsen CE, Carroll KS. Cysteine-mediated redox signalling: chemistry, biology, and tools for discovery. Chem Rev. 2013;113(7):4633–79.

Pfeifer A, Klatt P, Massberg S, Ny L, Sausbier M, Hirneiß C, Wang G, Korth M, Aszódi A, Andersson K, Krombach F, Mayerhofer A, Ruth P, Fässler R, Hofmann F. Defective smooth muscle regulation in cGMP kinase I-deficient mice. Embo J. 1998;17(11):3045–51.

Pfeifer A, Ruth P, Dostmann W, Sausbier M, Klatt P, Hofmann F. Reviews of physiology, biochemistry and pharmacology. Rev Physiol Bioch P. 1999;135:105–49.

Prysyazhna O, Burgoyne JR, Scotcher J, Grover S, Kass D, Eaton P. Phosphodiesterase 5 inhibition limits doxorubicin-induced heart failure by attenuating protein kinase G Iα oxidation. J Biological Chem. 2016;291(33):17427–36.

Prysyazhna O, Rudyk O, Eaton P. Single atom substitution in mouse protein kinase G eliminates oxidant sensing to cause hypertension. Nat Med. 2012;18(2):286–90.

Pucci G, Ranalli MG, Battista F, Schillaci G. Effects of β-Blockers with and without vasodilating properties on central blood pressure: systematic review and meta-analysis of randomized trials in hypertension. Hypertens Dallas Tex 1979. 2015;67(2):316–24.

Pufahl RA, Wishnok JS, Marletta MA. Hydrogen peroxide-supported oxidation of NG-Hydroxy-L-Arginine by nitric oxide synthase. Biochemistry-us. 1995;34(6):1930–41.

Raeymaekers L, Nilius B, Voets T, Missiaen L, Baelen KV, Vanoevelen J, Wuytack F. Novartis foundation symposia. 2002;71–80.

Rangaswami H, Marathe N, Zhuang S, Chen Y, Yeh J-C, Frangos JA, Boss G, Pilz R. Type II cGMP-dependent protein kinase mediates osteoblast mechanotransduction. J Biological Chem. 2009;284(22):14796–808.

Rani V, Mishra S, Yadav T, Yadav UCS, Kohli S. Free radicals in human health and disease. 2014;105–16.

Reed RB, Sandberg M, Jahnsen T, Lohmann SM, Francis SH, Corbin JD. Fast and slow cyclic nucleotide-dissociation sites in cAMP-dependent protein kinase are transposed in type Ibeta cGMP-dependent protein kinase. J Biological Chem. 1996;271(29):17570–5.

Richie-Jannetta R, Francis SH, Corbin JD. Dimerization of cGMP-dependent protein kinase Iβ is mediated by an extensive amino-terminal leucine zipper motif, and dimerization modulates enzyme function. J Biol Chem. 2003;278(50):50070–9.

Roos G, Foloppe N, Messens J. Understanding the pK(a) of redox cysteines: the key role of hydrogen bonding. Antioxid Redox Sign. 2012;18(1):94–127.

Rudyk O, Eaton P. Biochemical methods for monitoring protein thiol redox states in biological systems. Redox Biol. 2014;2:803–13.

Rudyk O, Phinikaridou A, Prysyazhna O, Burgoyne JR, Botnar RM, Eaton P. Protein kinase G oxidation is a major cause of injury during sepsis. P Natl Acad Sci Usa. 2013;110(24):9909–13.

Russwurm M, Mullershausen F, Friebe A, Jäger R, Russwurm C, Koesling D. Design of fluorescence resonance energy transfer (FRET)-based cGMP indicators: a systematic approach. Biochem J. 2007;407(1):69–77.

Ruth P, Pfeifer A, Kamm S, Klatt P, Dostmann WR, Hofmann F. Identification of the amino acid sequences responsible for high affinity activation of cGMP kinase Ialpha. J Biological Chem. 1997;272(16):10522–8.

Sabbah HN, Tocchetti CG, Wang M, Daya S, Gupta RC, Tunin RS, Mazhari R, Takimoto E, Paolocci N, Cowart D, Colucci W, Kass D. Nitroxyl (HNO): A novel approach for the acute treatment of heart failure. Circulation Hear Fail. 2013;6(6):1250–8.

Saleem M, Ohshima H. Xanthine oxidase converts nitric oxide to nitroxyl that inactivates the enzyme. Biochem Bioph Res Co. 2004;315(2):455–62.

Sarma GN, Kinderman FS, Kim C, Daake S von, Chen L, Wang B-C, Taylor S. Structure of D-AKAP2:PKA RI complex: insights into AKAP specificity and selectivity. Struct Lond Engl 1993. 2010;18(2):155–66.

Sauzeau V, Jeune HL, Cario-Toumaniantz C, Smolenski A, Lohmann SM, Bertoglio J, Chardin P, Pacaud P, Loirand G. Cyclic GMP-dependent protein kinase signaling pathway inhibits RhoA-induced Ca2+ sensitization of contraction in vascular smooth muscle. J Biol Chem. 2000;275(28):21722–9.

Sawada N, Itoh H, Yamashita J, Doi K, Inoue M, Masatsugu K, Fukunaga Y, Sakaguchi S, Sone M, Yamahara K, Yurugi T, Nakao K. cGMP-dependent protein kinase phosphorylates and inactivates RhoA. Biochem Bioph Res Co. 2001;280(3):798–805.

Schlossmann J, Ammendola A, Ashman K, Zong X, Huber A, Neubauer G Wang G, Allescher H, Korth M, Wilm M, Hofmann F, Ruth P. Regulation of intracellular calcium by a signalling complex of IRAG, IP3 receptor and cGMP kinase Iβ. Nature. 2000;404(6774):197–201.

Schmidt H, Werner M, Heppenstall PA, Henning M, Moré MI, Kühbandner S, Lewin G, Hofmann F, Feil R, Rathjen F. cGMP-mediated signaling via cGKIalpha is required for the guidance and connectivity of sensory axons. J Cell Biology. 2002;159(3):489–98.

Schröder F, Klein G, Fiedler B, Bastein M, Schnasse N, Hillmer A, Ames S, Gambaryan S, Drexler H, Walter U, Lohmann S, Wollert K. Single L-type Ca(2+) channel regulation by cGMP-dependent protein kinase type I in adult

cardiomyocytes from PKG I transgenic mice. Cardiovasc Res. 2003;60(2):268–77.

Schröder K. NADPH oxidase-derived reactive oxygen species: Dosis facit venenum. Exp Physiol. 2019;104(4):447–52.

Schröder K, Zhang M, Benkhoff S, Mieth A, Pliquett R, Kosowski J, Kruse C, Luedike P, Michaelis U, Weissmann N, Dimmeler S, Shah A, Brandes R. Nox4 is a protective reactive oxygen species generating vascular NADPH oxidase. Circ Res. 2012;110(9):1217–25.

Schulz E, Gori T, Münzel T. Oxidative stress and endothelial dysfunction in hypertension. Hypertens Res Official J Jpn Soc Hypertens. 2011;34(6):665–73.

Scotcher J, Prysyazhna O, Boguslavskyi A, Kistamas K, Hadgraft N, Martin ED, Worthington J, Rudyk O, Cutillas P, Cuello F, Shattock M, Marber M, Conte M, Greenstein A, Greensmith D, Venetucci L, Timms J, Eaton P. Disulfide-activated protein kinase G Iα regulates cardiac diastolic relaxation and fine-tunes the Frank-Starling response. Nat Commun. 2016;7(1):13187.

Sekhar KR, Hatchett RJ, Shabb JB, Wolfe L, Francis SH, Wells JN, Jastorff B, Butt E, Chakinala M, Corbin J. Relaxation of pig coronary arteries by new and potent cGMP analogs that selectively activate type I alpha, compared with type I beta, cGMP-dependent protein kinase. Mol Pharmacol. 1992;42(1):103–8.

Sha X, Isbell TS, Patel RP, Day CS, King SB. Hydrolysis of Acyloxy Nitroso Compounds Yields Nitroxyl (HNO). J Am Chem Soc. 2006;128(30):9687–92.

Shafirovich V, Lymar SV. Nitroxyl and its anion in aqueous solutions: Spin states, protic equilibria, and reactivities toward oxygen and nitric oxide. Proc National Acad Sci. 2002;99(11):7340–5.

Sharma AK, Birrane G, Anklin C, Rigby AC, Alper SL. NMR insight into myosin-binding subunit coiled-coil structure reveals binding interface with protein kinase G-Iα leucine zipper in vascular function. J Biological Chem. 2017;292(17):7052–65.

Sharma AK, Zhou G-P, Kupferman J, Surks HK, Christensen EN, Chou JJ, Mendelsohn M, Rigby A. Probing the interaction between the coiled coil leucine zipper of cGMP-dependent protein kinase Ialpha and the C terminus of the myosin binding subunit of the myosin light chain phosphatase. J Biological Chem. 2008;283(47):32860–9.

Sheehe JL, Bonev AD, Schmoker AM, Ballif BA, Nelson MT, Moon TM, Dostmann W. Oxidation of cysteine 117 stimulates constitutive activation of

the type Iα cGMP-dependent protein kinase. J Biol Chem. 2018;293(43):16791–802.

Shoman ME, DuMond JF, Isbell TS, Crawford JH, Brandon A, Honovar J, Vitturi D, White C, Patel R, King S. Acyloxy nitroso compounds as nitroxyl (HNO) donors: kinetics, reactions with thiols, and vasodilation properties. J Med Chem. 2011;54(4):1059–70.

Sivakumaran V, Stanley BA, Tocchetti CG, Ballin JD, Caceres V, Zhou L, Keceli G, Rainer P, Lee D, Huke S, Ziolo M, Kranias E, Toscano J, Wilson G, O'Rourke B, Kass D, Mahaney J, Paolocci N. HNO enhances SERCA2a activity and cardiomyocyte function by promoting redox-dependent phospholamban oligomerization. Antioxid Redox Sign. 2013;19(11):1185–97.

Somlyo AP, Somlyo AV. Signal transduction and regulation in smooth muscle. Nature. 1994;372(6503):231–6.

Somlyo AV. Cyclic GMP regulation of myosin phosphatase: a new piece for the puzzle? Circ Res. 2007;101(7):645–7.

Sprenger JU, Perera RK, Götz KR, Nikolaev VO. FRET microscopy for real-time monitoring of signaling events in live cells using unimolecular biosensors. J Vis Exp Jove. 2012;(66):e4081.

Stathopoulou K, Wittig I, Heidler J, Piasecki A, Richter F, Diering S, Velden J, Buck F, Donzelli S, Schröder E, Wijnker P, Voigt N, Dobrev D, Sadayappan S, Eschenhagen T, Carrier L, Eaton P, Cuello F. S-glutathiolation impairs phosphoregulation and function of cardiac myosin-binding protein C in human heart failure. Faseb J Official Publ Fed Am Soc Exp Biology. 2016;30(5):1849–64.

Stephens NG, Parsons A, Brown MJ, Schofield PM, Kelly F, Cheeseman K, Mitchinson M. Randomised controlled trial of vitamin E in patients with coronary disease: Cambridge Heart Antioxidant Study (CHAOS). Lancet. 1996;347(9004):781–6.

Suarez SA, Neuman NI, Muñoz M, Álvarez L, Bikiel DE, Brondino CD, Ivanović-Burmazović I, Miljkovic J, Filipovic M, Martí M, Doctorovich F. Nitric oxide is reduced to HNO by proton-coupled nucleophilic attack by ascorbate, tyrosine, and other alcohols. A new route to HNO in biological media? J Am Chem Soc. 2015;137(14):4720–7.

Sugiura T, Nakanishi H, Roberts JD. Proteolytic processing of cGMP-dependent protein kinase I mediates nuclear cGMP signaling in vascular smooth muscle cells. Circ Res. 2008;103(1):53–60.

Surks HK, Mochizuki N, Kasai Y, Georgescu SP, Tang KM, Ito M, Lincoln T, Mendelsohn M. Regulation of myosin phosphatase by a specific interaction

with cGMP- dependent protein kinase Ialpha. Sci New York N Y. 1999;286(5444):1583–7.

Switzer CH, Flores-Santana W, Mancardi D, Donzelli S, Basudhar D, Ridnour LA, Miranda K, Fukuto J, Paolocci N, Wink D. The emergence of nitroxyl (HNO) as a pharmacological agent. Biochim Biophys Acta. 2009;1787(7):835–40.

Takio K, Wade RD, Smith SB, Krebs EG, Walsh KA, Titani K. Guanosine cyclic 3',5'-phosphate dependent protein kinase, a chimeric protein homologous with two separate protein families. Biochemistry-us. 1984;23(18):4207–18.

Tang C, Hsu HK, Chen XY, Liu MS. Externalization and internalization of (Na+ + K+)-ATPase in rat heart during different phases of sepsis. Circ Shock. 1993;41(1):19–25.

Tang KM, Wang G, Lu P, Karas RH, Aronovitz M, Heximer SP, Kaltenbronn K, Blumer K, Siderovski D, Zhu Y, Mendelsohn M, Tang M, Wang G. Regulator of G-protein signaling-2 mediates vascular smooth muscle relaxation and blood pressure. Nat Med. 2003;9(12):1506–12.

Tanner JJ, Parsons ZD, Cummings AH, Zhou H, Gates KS. Redox regulation of protein tyrosine phosphatases: structural and chemical aspects. Antioxid Redox Sign. 2011;15(1):77–97.

Thomas P, Smart TG. HEK293 cell line: A vehicle for the expression of recombinant proteins. J Pharmacol Toxicol. 2005;51(3):187–200.

Thoonen R, Giovanni S, Govindan S, Lee DI, Wang G-R, Calamaras TD, Takimoto E, Kass D, Sadayappan S, Blanton R. Molecular screen identifies cardiac myosin-binding protein-C as a protein kinase G-Iα substrate. Circulation Hear Fail. 2015;8(6):1115–22.

Thunemann M, Fomin N, Krawutschke C, Russwurm M, Feil R. Visualization of cGMP with cGi biosensors. Methods Mol Biology Clifton N J. 2013a;1020:89–120.

Thunemann M, Wen L, Hillenbrand M, Vachaviolos A, Feil S, Ott T, Han X, Fukumura D, Jain R, Russwurm M, Wit C, Feil R. Transgenic mice for cGMP imaging. Circ Res. 2013b;113(4):365–71.

Tita C, Gilbert EM, Bakel ABV, Grzybowski J, Haas GJ, Jarrah M, Dunlap S, Gottlieb S, Klapholz M, Patel P, Pfister R, Seidler T, Shah K, Zieliński T, Venuti R, Cowart D, Foo S, Vishnevsky A, Mitrovic V. A Phase 2a dose-escalation study of the safety, tolerability, pharmacokinetics and haemodynamic effects of BMS-986231 in hospitalized patients with heart failure with reduced ejection fraction. Eur J Heart Fail. 2017;19(10):1321–32.

Tocchetti CG, Stanley BA, Murray CI, Sivakumaran V, Donzelli S, Mancardi D, Pagliaro P, Gao W, Eyk J, Kass D, Wink D, Paolocci N. Playing with cardiac “redox switches”: the “HNO way” to modulate cardiac function. Antioxid Redox Sign. 2011;14(9):1687–98.

Tocchetti CG, Wang W, Froehlich JP, Huke S, Aon MA, Wilson GM, Benedetto G, O’Rourke B, Gao W, Wink D, Toscano J, Zaccolo M, Bers D, Valdivia H, Cheng H, Kass D, Paolocci N. Nitroxyl Improves Cellular Heart Function by Directly Enhancing Cardiac Sarcoplasmic Reticulum Ca 2+ Cycling. Circ Res. 2007;100(1):96–104.

Ullrich V, Kissner R. Redox signaling: Bioinorganic chemistry at its best. J Inorg Biochem. 2006;100(12):2079–86.

Vaandrager AB, Smolenski A, Tilly BC, Houtsmuller AB, Ehlert EME, Bot AGM, Edixhoven M, Boomaars W, Lohmann S, Jonge H. Membrane targeting of cGMP-dependent protein kinase is required for cystic fibrosis transmembrane conductance regulator Cl- channel activation. Proc National Acad Sci. 1998;95(4):1466–71.

Vo NK, Gettemy JM, Coghlan VM. Identification of cGMP-dependent protein kinase anchoring proteins (GKAPs). Biochem Bioph Res Co. 1998;246(3):831–5.

Wall ME, Francis SH, Corbin JD, Grimes K, Richie-Jannetta R, Kotera J, Macdonald B, Gibson R, Trewhella J. Mechanisms associated with cGMP binding and activation of cGMP-dependent protein kinase. Proc National Acad Sci. 2003;100(5):2380–5.

Wanstall JC, Jeffery TK, Gambino A, Lovren F, Triggle CR. Vascular smooth muscle relaxation mediated by nitric oxide donors: a comparison with acetylcholine, nitric oxide andnitroxyl ion. Brit J Pharmacol. 2001;134(3):463–72.

Wegener JW, Nawrath H, Wolfsgruber W, Kühbandner S, Werner C, Hofmann F, Feil R. cGMP-dependent protein kinase I mediates the negative inotropic effect of cGMP in the murine myocardium. Circ Res. 2002;90(1):18–20.

Williams B, Mancia G, Spiering W, Rosei EA, Azizi M, Burnier M, Clement D, Coca A, Simone G, Dominiczak A, Kahan T, Mahfoud F, Redon J, Ruilope L, Zanchetti A, Kerins M, Kjeldsen S, Kreutz R, Laurent S, Lip G, McManus R, Narkiewicz K, Ruschitzka F, Schmieder R, Shlyakhto E, Tsioufis C, Aboyans V, Desormais I, Group E, Backer G, Heagerty A, Agewall S, Bochud M, Borghi C, Boutouyrie P, Brguljan J, Bueno H, Caiani E, Carlberg B, Chapman N, Cífková R, Cleland J, Collet J, Coman I, Leeuw P, Delgado V, Dendale P, Diener H, Dorobantu M, Fagard R, Farsang C, Ferrini M, Graham I, Grassi G, Haller H, Hobbs F, Jelakovic B, Jennings C, Katus H, Kroon A, Leclercq C, Lovic D, Lurbe E, Manolis A, McDonagh T, Messerli F, Muiesan

M, Nixdorff U, Olsen M, Parati G, Perk J, Piepoli M, Polonia J, Ponikowski P, Richter D, Rimoldi S, Roffi M, Sattar N, Seferovic P, Simpson I, Sousa-Uva M, Stanton A, Borne P, Vardas P, Volpe M, Wassmann S, Windecker S, Zamorano J, Barbato E, Dean V, Fitzsimons D, Gaemperli O, Hindricks G, Iung B, Jüni P, Knuuti J, Lancellotti P, Januszewics A, Manolis A, Benkhedda S, Zelveian P, Siostrzonek P, Najafov R, Pavlova O, Pauw M, Dizdarevic-Hudic L, Raev D, Karpettas N, Linhart A, Shaker A, Viigimaa M, Metsärinne K, Vavlukis M, Halimi J, Pagava Z, Schunkert H, Thomopoulos C, Páll D, Andersen K, Shechter M, Mercuro G, Bajraktari G, Romanova T, Trušinskis K, Saade G, Sakalyte G, Noppe S, DeMarco D, Caraus A, Wittekoek J, Aksnes T, Jankowski P, Vinereanu D, Baranova E, Foscoli M, Dikic A, Filipova S, Fras Z, Bertomeu-Martínez V, Burkard T, Sdiri W, Aydogdu S, Sirenko Y, Brady A, Weber T, Lazareva I, Backer T, Sokolovic S, Widimsky J, Pörsti I, Denolle T, Krämer B, Stergiou G, Miglinas M, Gerdts E, Tykarski A, Rodrigues M, Chazova I, Segura J, Gottsäter A, Pechère-Bertschi A, Erdine S. 2018 ESC/ESH Guidelines for the management of arterial hypertension. Eur Heart J. 2018;39(33):3021–104.

Winterbourn CC. Reconciling the chemistry and biology of reactive oxygen species. Nat Chem Biol. 2008;4(5):278–86.

Wit C de, Bismarck P von, Pohl U. Mediator role of prostaglandins in acetylcholine-induced vasodilation and control of resting vascular diameter in the hamster cremaster microcirculation in vivo. J Vasc Res. 1993;30(5):272–8.

Wolfe L, Francis SH, Corbin JD. Properties of a cGMP-dependent monomeric protein kinase from bovine aorta. J Biological Chem. 1989;264(7):4157–62.

Wölfle SE, Wit C de. Intact endothelium-dependent dilation and conducted responses in resistance vessels of hypercholesterolemic mice in vivo. J Vasc Res. 2005;42(6):475–82.

Wollert KC, Fiedler B, Gambaryan S, Smolenski A, Heineke J, Butt E, Trautwein C, Lohmann S, Drexler H. Gene Transfer of cGMP-dependent protein kinase I enhances the antihypertrophic effects of nitric oxide in cardiomyocytes. Hypertension. 2002;39(1):87–92.

Wong PS-Y, Hyun J, Fukuto JM, Shirota FN, DeMaster EG, Shoeman DW, Nagasawa H. Reaction between S-Nitrosothiols and thiols: generation of nitroxyl (HNO) and subsequent chemistry. Biochemistry-us. 1998;37(16):5362–71.

Wooldridge AA, MacDonald JA, Erdodi F, Ma C, Borman MA, Hartshorne DJ, Haystead T. Smooth muscle phosphatase is regulated in vivo by exclusion of phosphorylation of threonine 696 of MYPT1 by phosphorylation of serine 695 in response to cyclic nucleotides. J Biol Chem. 2004;279(33):34496–504.

Wu PG, Brand L. Resonance energy transfer: methods and applications. Anal Biochem. 1994;218(1):1–13.

Yao X, Garland CJ. Recent developments in vascular endothelial cell transient receptor potential channels. Circ Res. 2005;97(9):853–63.

Yong Q-C, Hu L-F, Wang S, Huang D, Bian J-S. Hydrogen sulfide interacts with nitric oxide in the heart: possible involvement of nitroxyl. Cardiovasc Res. 2010;88(3):482–91.

Yuan J, Xu WW, Jiang S, Yu H, Poon HF. The scattered twelve tribes of HEK293. Biomed Pharmacol J. 2018;11(2):621–3.

Yuill KH, Yarova P, Kemp-Harper BK, Garland CJ, Dora KA. A novel role for HNO in local and spreading vasodilatation in rat mesenteric resistance arteries. Antioxid Redox Sign. 2010;14(9):1625–35.

Zeller A, Wenzl MV, Beretta M, Stessel H, Russwurm M, Koesling D, Schmidt K, Mayer B. Mechanisms underlying activation of soluble guanylate cyclase by the nitroxyl donor Angeli's salt. Mol Pharmacol. 2009;76(5):1115–22.

Zhu G, Groneberg D, Sikka G, Hori D, Ranek MJ, Nakamura T, Takimoto E, Paolocci N, Berkowitz D, Friebe A, Kass D. Soluble guanylate cyclase is required for systemic vasodilation but not positive inotropy induced by nitroxyl in the mouse. Hypertens Dallas Tex 1979. 2014;65(2):385–92.

Zhu X, Xiong M, Liu H, Mao G, Zhou L, Zhang J, Hu X, Zhang X, Tan W. A FRET-based ratiometric two-photon fluorescent probe for dual-channel imaging of nitroxyl in living cells and tissues. Chem Commun Camb Engl. 2016;52(4):733–6.

11 Acknowledgement

I would like to express my gratitude to everyone who contributed to this project and granted me the opportunity to do research under their supervision.

First, I would like to thank Prof. Dr. Friederike Cuello, who was and still is an exceptional supervisor and mentor for the entire duration of our project and my studies. She motivated me from the very first day and still motivates me by her incomparable enthusiasm and passion for science. She introduced me into the field of cardiovascular research and gave me the possibility to present our results at various meetings so I could see the beautiful world of science with all its aspects. She always showed great commitment when preparing presentations and posters. Working with her on these projects was always a lot of fun and always very honest. Her ability of always being part of the project and being at the bench whenever needed contributed to this project and created a lot of unforgettable memories. Friederike will always be an inspiring role model – as a scientist but also on a personal level.
Thank you for your continuing support.

I would also like to thank Sonia Donzelli. She taught me many methods I applied in this thesis. She also performed the NOxICAT analysis shown in this thesis. Sonia supported me and my studies right from the beginning and helped me out, whenever needed. Sonia is a very passionate scientist and I am grateful for her motivation and drive she offered me during this project.

I am very thankful for Angelika Piasecki, as she keeps the lab and even the whole institute together. She taught me how to do the cell culturing techniques, she shared her incredible cake recipes, the joy of cooking (as this is comparable to lab work and needs the same attention for details) and I owe her wonderful christmas party memories (such as the launch of our Christmas band). Angelika creates a family-like feeling and always has an open ear for problems and worries. I thank her for taking care of my experiments whenever I had a seminar at the university, as I could trust her unconditionally.

In addition, I would like to thank Konstantina Stathopoulou, who is always incredibly helpful but also a great sparring partner for troubleshooting. Ntina makes evenings in the lab enjoyable and offers always great guidance when performing experiments. From our very first day in the lab Simon Diering was a great colleague. I particularly remember the lab visit in Goettingen and I am especially thankful for the time we worked together on the project evolving around the cAMP-dependent protein kinase and protein phosphatase 2A. Also, Steven Schulz was a great lab colleague. I admire his ability to reflect on experiments and improve his methods continuously. Sophie Schobesberger considerably contributed to the analysis of the FRET measurements. I would like to thank Josef Schnittger who introduced me to the lab and shared the insights of a medical student doing an experimental thesis with me. Josef made the beginning in the lab and in the group very easy and enjoyable. Overall, the years in the working group *Cuello* were always enriched by friendly and sympathetic colleagues who are unforgettable.

I am also grateful for Prof. Dr. Viacheslav Nikolaev who gave me the ability to work right from the beginning with his newly installed microscope. During the first months at the University Medical Center Hamburg-Eppendorf he even took the time to the explain the experimental set-up to me and was always willing to discuss the results with a great positive attitude. I also owe a lot to Hariharan Subramanian who helped me as well with troubleshooting at the FRET microscope and even came to the lab during cold winter nights.

I would like to express my deepest gratitude to Prof. Dr. Thomas Eschenhagen for offering me the possibility to do my thesis at the Department of Experimental Pharmacology and Toxicology at the University Medical Center Hamburg-Eppendorf. I highly value the scientific meetings we had, his input and his vision of experimental work, which will accompany my scientific work in the future.

For scientific inspiration and feedback as well as for their support I would like to thank Prof. Dr. Lucie Carrier, Dr. Justus Stenzig, Silke Reischmann and Dr. Sonia Singh.

During this thesis I particularly enjoyed the collaborative work with other groups, and I would like to thank Philip Eaton, Joseph Burgoyne, Alisa Kamynina, Kjestine Schmidt, Cor de Wit as well as Susanne Lutz and Sebastian Pasch for providing advice and for introducing me to new methods.

Looking forward, I would like to express my deepest appreciation to Prof. Dr. Heimo Ehmke, who will be a member of the examination board during my disputation.

I am grateful to the technical assistants and the warmth they extended to me during my time at the department and their help concerning the conductance of experiments and the search for materials and samples.

Finally, I would like to thank my loving parents and my brother Emanuel, who have been by my side, especially throughout the last years. I would like to thank them for listening to numerous versions of my presentations and for their honest feedback. I would like to thank them for the mutual exchange, for always believing in me and encouraging me. My deep appreciation belongs as well to my grandparents who always made sure I knew they were proud.

Taken together, I am more than grateful for the memories I had in the Department and the working group *Cuello*. It impacted my way of looking at medicine as well as people. The project meant a lot to me and today, I am very grateful for that.

12 Curriculum Vitae

Der Lebenslauf wurde aus datenschutzrechtlichen Gründen entfernt.

13 Congress contributions (selected)

11 / 2018	Scientific talk **„A novel oxidant sensor in the cGMP-binding pocket of PKGIα regulates second messenger-mediated kinase activity“** | Mara Goetz | 2nd Dutch-German Meeting, of the German Society for Microcirculation | Dutch Endothelial Biology Society and Dutch Society for Microcirculation | Amsterdam (NLD)
07 / 2017	Scientific talk **„A novel oxidant sensor in the cGMP-binding pocket of PKGIα regulates second messenger-mediated kinase activity“** | Mara Goetz | 34th Annual Meeting of the International society for heart research (ISHR) | Hamburg (GER)
04 / 2017	Scientific talk **„A novel oxidant sensor in the cGMP-binding pocket of PKGIα regulates second messenger-mediated kinase activity“** | Mara Goetz | DKG Jahrestagung | Mannheim (GER)
01 / 2017	Scientific talk **„A molecular mechanism of oxidant-induced vasorelaxation in vivo“**, Mara Goetz, Kjestine Schmidt | NCCR Retreat | Tremsbüttel (GER)
10 / 2016	Poster **“A potential molecular mechanism of Nitroxyl-mediated regulation of positive inotropy“** | „DGK Herztage“ | Berlin (GER)
11 / 2015	Poster **„Oxidative activation of cAMP-dependent protein kinase by nitroxyl modulates myofilament protein phosphorylation”** | SFRBM Meeting | Boston (USA)
09 / 2015	Scientific talk **„Role of HNO-dependent oxidation of PKGIα in the regulation of blood pressure“** | Young-DZHK-Retreat | Potsdam (GER)
03 / 2015	Poster **„PKGIα is a novel target of HNO and leads to kinase activation“** | Dutch-German Joint Meeting of the Molecular Cardiology Groups | Garmisch (GER)
02 / 2015	Scientific talk **„Role of HNO-dependent oxidation of PKGIα in the regulation of blood pressure“** | Meeting of the Cardiovascular Research Center | UKE | Hamburg (GER)
02 / 2015	Scientific talk **„Detection and functional impact of oxidative posttranslational modifications“** Sonia Donzelli, Mara Goetz; Cardiovascular Research Center | UKE | Hamburg (GER)

14 Eidesstattliche Versicherung

Ich versichere ausdrücklich, dass ich die Arbeit selbständig und ohne fremde Hilfe verfasst, andere als die von mir angegebenen Quellen und Hilfsmittel nicht benutzt und die aus den benutzten Werken wörtlich oder inhaltlich entnommenen Stellen einzeln nach Ausgabe (Auflage und Jahr des Erscheinens), Band und Seite des benutzten Werkes kenntlich gemacht habe.
Ferner versichere ich, dass ich die Dissertation bisher nicht einem Fachvertreter an einer anderen Hochschule zur Überprüfung vorgelegt oder mich anderweitig um Zulassung zur Promotion beworben habe.
Ich erkläre mich einverstanden, dass meine Dissertation vom Dekanat der Medizinischen Fakultät mit einer gängigen Software zur Erkennung von Plagiaten überprüft werden kann.

Unterschrift: .....